

AN ANALYSIS OF DELTA MODULATED INVERTERS WITH
APPLICATIONS TO SUBMERSIBLE MOTORS

CENTRE FOR NEWFOUNDLAND STUDIES

**TOTAL OF 10 PAGES ONLY
MAY BE XEROXED**

(Without Author's Permission)

MOHAMMAD ALI CHOUDHURY



**An Analysis of Delta Modulated Inverters with
Applications to Submersible Motors**

by

© **Mohammad All Choudhury**

A thesis submitted in partial fulfillment
of the requirements for the degree of
Doctor of Philosophy

Faculty of Engineering and Applied Science
Memorial University of Newfoundland
St. John's, Newfoundland

CANADA

December, 1988

Permission has been granted to the National Library of Canada to microfilm this thesis and to lend or sell copies of the film.

The author (copyright owner) has reserved other publication rights, and neither the thesis nor extensive extracts from it may be printed or otherwise reproduced without his/her written permission.

L'autorisation a été accordée à la Bibliothèque nationale du Canada de microfilmer cette thèse et de prêter ou de vendre des exemplaires du film.

L'auteur (titulaire du droit d'auteur) se réserve les autres droits de publication; ni la thèse ni de longs extraits de celle-ci ne doivent être imprimés ou autrement reproduits sans son autorisation écrite.

ISBN 0-315-50455-2

Abstract

This thesis presents an analysis of delta modulated inverters and their applications to submersible motors. Submersible motors are induction motors with unique constructional features. These motors are required to operate in one of the most harsh environmental conditions. The operating characteristics of the submersible motor pump system require soft starting facility and variable speed operation during production. To satisfy both requirements, a delta modulated inverter supply is proposed for the operation of the submersible motor. Several delta modulation schemes have been studied and the rectangular wave delta modulation technique is selected for the switching of the inverter. Rectangular wave delta modulation provides inherent constant voltage/frequency (V/f) characteristic of the supply voltage and current control of the motor. The constant V/f characteristic is provided by the low-pass filter in the feedback loop of the modulator and the current control is provided by the hysteresis window of the quantizing comparator in the feedforward path of the modulator.

The modulator and the inverter waveforms were studied using discrete Fourier transform (DFT). This is simpler than the conventional Fourier series analysis. It is suitable for on-line harmonic analysis of the modulated waveforms. It also gives the information about the sub-harmonics of the modulated waveforms. An on-line harmonic minimization technique using a tuned filter in the delta modulator has been implemented. This method uses the continuous tuning of the feedback filter in the modulator to minimize the low order harmonics

of the modulated wave for variable frequency operation of the inverter.

The steady state and starting characteristics of the submersible motor supplied from the rectangular wave delta modulated inverter have been studied using time-domain analysis. Time domain analysis of inverter-fed submersible motors was found to be more accurate and easier than the conventional frequency domain analysis. The motor was provided with ramp frequency and voltage (RFV) control to reduce its electrical and mechanical starting stresses. A semi-closed loop operation has been chosen to maintain constant slip operation of the motor. For the semi-closed loop operation, motor speed was estimated using the motor terminal voltage, current and the phase angle between them.

The characteristics of the modulator and the motor fed from the rectangular wave delta modulated inverter were experimentally verified.

Dedicated To My Parents



Acknowledgement

I express my sincerest appreciation to professors Dr.M.A Rahman, and Dr. J.E Quicoe for their encouragement throughout the preparation of this thesis. My sincerest thanks are due to Dr. M.A Rahman for his financial support all along this research. I take this opportunity to thank the School of Graduate Studies of the Memorial University of Newfoundland for their financial support through the university fellowship. I acknowledge the support and encouragement rendered, by Dr. T.R Chari, associate dean of the Faculty of Engineering and Applied Science. I thank Dr. Shelley-Quin, assistant professor of the Department of French and Spanish for her help in the preparation of the manuscript of this thesis.

The assistance received from the University computing services is gratefully acknowledged. Technical help of Mr. Richard Newman, Mr. Donald Guy and Mr. Thomas Pike of the Faculty of Engineering and Applied Science is gratefully acknowledged.

My special thanks and gratitude are due to Dr. M.A Rahman, his wife Mrs. Alta Rahman and their family for making my stay in St. John's a very enjoyable one.

Table of Contents

Abstract	ii
Acknowledgement	v
List of Symbols	xii
List of Abbreviation	xvii
List of Figures	xviii
List of tables	xxx1

Chapter-1

Introduction

1.1 Features of submersible drives	1
1.1.1 Review of submersible drives	2
1.1.2 Advantages of variable speed SMPs	4
1.2 Inverter fed variable speed induction motors	7
1.2.1 Review of PWM techniques for power converters	9
1.3 Delta modulated inverter control of submersible motors	12
1.4 The modulator and the inverter waveform synthesis	18
1.5 The on-line control strategy for a submersible drive system	23
1.6 The analysis of the delta modulated inverter and the submersible motor pump performance	27

1.7	Thesis objectives and outlines	28
-----	--------------------------------	----

Chapter 2

Delta Modulation Technique and The Selection Criteria For The Inverter Drives

2.1	Introduction	30
2.2	Delta modulation technique	30
2.3	A brief review of the delta modulation technique	34
	2.3.1 Typical applications of delta modulators outside communication field	37
2.4	Delta modulation scheme for inverter fed submersible motors	38
	2.4.1 Drive requirements	38
	2.4.2 Modulator requirements	43
	2.4.3 Characteristics of three simple delta modulators	46
	A. Characteristics of the linear delta modulator	48
	B. Characteristics of a sigma delta modulator	56
	C. Characteristics of rectangular wave delta modulators	61
2.5	Conclusions	71

Chapter-3

Analysis and Optimization of Rectangular Wave Delta Modulator

3.1	Introduction	72
3.2	The rectangular wave delta modulator	73
3.2.1	The simple rectangular wave delta modulator	73
3.2.2	Analysis of the rectangular wave delta modulator	74
3.2.3	The tuned rectangular wave delta modulator for optimized operation	86
3.3	Analysis of RWDM using DFT and windowed DFT	93
3.3.1	Necessity of DFT analysis of PWM waveforms	93
3.3.2	Methodology	94
3.3.3	Discrete Fourier transforms of RWDM waveforms	96
3.3.4	Spectral leakage	102
3.3.5	Window functions	104
3.3.6	DFT of windowed RWDM waveforms	107
3.4	Summary of analytical results	108
3.5	Practical Modulator Circuits	122
3.5.1	The rectangular wave delta modulator	127
3.5.2	The tuned RWDM	129
3.6	Experimental results	129

3.7	Limitations	150
3.8	Conclusions	151

Chapter -4

Analysis of Submersible Motor Fed From Three Phase

RWDM Inverter

4.1	Introduction	152
4.2	Synthesis of three phase rectangular wave delta modulated inverter waveforms	153
4.3	Choice of switching for three phase inverter	164
4.4	Harmonic Analysis of three phase RWDM inverter waveforms using DFT on windowed waveforms	166
4.5	Analytical modeling of inverter-fed submersible motors	171
	4.5.1 Inverter output waveforms	179
	4.5.2 Motor model	180
	4.5.3 Load model	183
4.6	Steady state performance of submersible motor fed from RWDM inverter	185
4.7	Start up response of submersible motor fed from RWDM inverter	190
4.8	Experimental results	199

Chapter -5**Variable speed operation of submersible motors**

5.1	Introduction	208
5.2	Submersible pump performance	209
5.3	Control strategy for variable speed submersible motor drive	213
5.4	Determination of operating condition of induction motors from terminal quantities	215
5.4.1	Speed measurement using a practical circuit	218
5.5	Semi-closed loop operation of submersible motor pump fed from DM inverter	221 221
5.6	Experimental results	228
5.7	Conclusions	228

Chapter - 8

Summary and conclusions	230
Reference	235
Appendix	252
I. Three phase delta modulator circuits and logic circuits	252
II. Design and construction of the speed sensor	259
III. A novel variable frequency three phase sine wave generator	269
IV. Motor ratings	276
V. Motor equations of d-q axis	278

List of Symbols

A_n = Fourier coefficients.

B_n = Fourier coefficients

C_n = Fourier coefficients

D_m = motor damping factor

D_p = pump damping factor

$e(t)$ = error signal

E_c = control voltage of the modulator

E_m = amplitude of the modulating sine wave

f = frequency in Hz

$F = L_r L_p - L_m^2$

f_p = clock frequency of the delta modulator

f_R = ripple frequency

f_{idle} = idling frequency

$\overline{G(j\omega)}$ = transfer function of the feed forward path of the modulator

$g(x)$ = gate function, $x = f(t, t_1, t_2)$

$\overline{H(j\omega)}$ = transfer function of the feedback path of the modulator

H = head lift in ft. or meter as appropriate

I_1 = fundamental motor current

i_d = direct axis current

i_q = quadrature axis current

J_m = motor inertia constant

J_p = pump inertia constant

$K_N(E_m, \omega)$

or $K_N(E_m)$ describing functions

K_s = spring constant

L_t = equivalent motor inductance

L_1 = stator leakage inductance

L_2 = rotor leakage inductance

L_m = mutual inductance of the motor

$L_{dt} = L_t - L_m$

$L_{dr} = L_r - L_m$

m_{dte} = slope of the triangular wave during idling

m_n = n th harmonic component of the modulator output waveform

m_1 = fundamental component of the modulator output waveform

$m(t)$ = modulated wave

M_1 = fundamental component of the modulated wave

$m_T(t)$ = modulated wave of one cycle

$m(t + nT)$ = modulated switching waveform shifted by nT

N_c = number of commutations

N_r = rotor speed in rpm or in radians/sec

N_s = synchronous speed in rpm or in radians/sec

N_p = number of pulses in one cycle

n = order of harmonics

p = differential operator

Q = flow rate in gallon/sec.

r_1 = stator resistance in ohms

r_2 = rotor resistance in ohms

R_e = equivalent resistance of the motor in ohms

r_i = core resistance in ohms

s = motor slip

S = slope of the estimated waveform in volts/seconds

T_e = developed torque in Nm.

T_L = load torque in Nm.

T_m = motor torque in Nm.

t_i = i -th pulse termination time in second

T = period of a periodic wave in second

$T_s =$ sampling frequency in Hz.

$u(x) =$ unit step function, $x = f(t, t_1)$

$V =$ Voltage in volts or in pu

$V_s =$ logic power supply voltage in volts.

$V_{fn} =$ nth harmonic voltage of the carrier waveform

$V_{ln} =$ nth harmonic voltage of the modulator output waveform

$V_{ab}, V_{bc}, V_{ca} =$ line to line voltages

$V_{an}, V_{bn}, V_{cn} =$ line to neutral voltages

$V_d =$ direct axis voltage in volts

$V_q =$ quadrature axis voltage in volts

$V_{ln-w} =$ windowed line to neutral voltage in volts

$V_s =$ Fourier voltage of inverter output in volts

$V_{dc} =$ dc input to the inverter in volts

$V_R =$ rms voltage of the reference sine wave in volts

$V_1 =$ fundamental component of the modulator output voltage in volts

$W(t) =$ window function

$$W_N = e^{j\frac{2\pi}{N}}$$

$\hat{x}(t) =$ estimated signal of the delta modulator

$x(t) =$ input signal to the modulator

$X(f)$ = frequency spectra of the signal $x(t)$

$x(n)$ = sampled version of continuous signal $x(t)$

$x(N)$ = n th sample value of $x(t)$

X_e = motor input reactance in ohms

y_n = n th harmonic of estimated wave

Z_e = motor input impedance in ohms

Δ_R = step size of rectangular wave delta modulator

Δ = window width

δ_i = i th pulse position in radians

ω_1 = fundamental frequency

ω_n = n -th harmonic frequency = $n\omega$ radians/sec

ω_e = synchronous speed in radians/sec

ω_r = rotor speed in radians/sec

ω_m = motor angular speed in radians/sec

ω_p = pump angular speed in rad./sec

ψ_d = direct axis flux

ψ_q = quadrature axis flux

τ = integrator time constant in volts/sec

θ_1 = fundamental power factor in radians

List of Abbreviations

CRT	Cathode ray tube
DFT	Discrete Fourier transforms
DPCM	Differential pulse code modulation
DM	Delta modulation
FFT	Fast Fourier transform
GTO	Gate turn off
LDM	Linear delta modulator
PWM	Pulse width modulation
PCM	Pulse code modulation
RWDM	Rectangular wave delta modulation
RFV	Ramp frequency and voltage
SM	Submersible motor
SCR	Silicon controlled rectifier
SMP	Submersible motor pump
SDM	Sigma delta modulation
SPWM	Sine pulse width modulation
UPS	Uninterruptible power supply
VLSI	Very large scale integration

LIST OF FIGURES

- 1.1 Voltage versus frequency characteristic
required for constant torque and constant
power operation of an induction motor. 13
- 1.2 The single phase inverter and the load current variation
required in a hysteresis current control. 13
- 1.3 The block diagram of a rectangular wave delta modulator. 15
- 1.4 The waveforms of a rectangular wave delta modulator. 15
- 1.5 The block diagram of a tuned rectangular wave delta modulator. 19
- 1.6 The simulated modulated waveform of a rectangular wave delta
modulator and its spectrum obtained by discrete
Fourier transform. 21
- 1.7 The simulated Hámning windowed modulated waveform of a
rectangular wave delta modulator and its spectrum obtained
by discrete Fôurier transform. 22
- 1.8 The block diagram of the open loop control of a submersible
motor fed from the rectangular wave delta modulated inverter. 24
- 1.9 Pump performance curves at variable speed operations. 25
- 1.10 The schematic diagram of the semi-automatic control of

submersible motor fed from rectangular wave delta modulated inverter.	26
2.1 The block diagram of a simple delta modulator.	32
2.2 Waveforms of the simple delta modulator.	
2.3 Block diagrams of the linear, the sigma and the rectangular wave delta modulators.	47
2.4 Idling waveforms of three delta modulators.	49
2.5 Fundamental voltage variation of three modulators with change in operating frequency.	52
2.6 Step responses of three modulators.	53
2.7 Root locus of the linear delta modulator.	57
2.8 Root locus of the sigma delta modulator.	57
2.9 Root locus of the rectangular wave delta modulator.	68
3.1 The block diagram of a rectangular wave delta modulator.	75
3.2 Expected waveforms of a rectangular wave delta modulator.	75
3.3 Fundamental voltage variation of rectangular wave delta modulated waves with change in operating frequency.	82
3.4 Harmonics of rectangular wave delta modulated waveform at various operating frequencies.	83

3.5	Variation of the number of commutation of output of waveforms of a rectangular wave delta modulator versus frequency.	85
3.6	A spectrum of the idling waveform of a rectangular wave delta modulator.	87
3.7	A rectangular wave delta modulator with two integrators in the feedback path.	89
3.8	The simple integrator and the tuned integrator circuits.	91
3.9	The block diagram of a rectangular wave tuned delta modulator.	91
3.10	Simulated modulated waveforms produced by a rectangular wave delta modulator for 10 - 75 Hz operations.	98
3.11	Simulated waveforms of the tuned rectangular wave delta modulator for control voltage variation of 1-7 volts at 60 Hz operation.	99
3.12	Spectra of the waveforms of figure 3-10 obtained by discrete Fourier transforms.	100
3.13	Spectra of the waveforms of figure 3-11 obtained by discrete Fourier transforms.	101
3.14	Illustration of spectral leakage.	103
3.15	Three windows, the Hamming window, the Hanning window and the Blackman window.	106

3.16 Side lobe characteristics of the three windows.	106
3.17 Hamming windowed waveforms of a rectangular wave delta modulator at 10-75 Hz operations.	109
3.18 Hanning windowed waveforms of a rectangular wave delta modulator at 10-75 Hz operations.	110
3.19 Blackman windowed waveforms of a rectangular wave delta modulator at 10-75 Hz operations.	111
3.20 Hamming windowed waveforms of a tuned rectangular wave delta modulator at 60 Hz operation for control voltage variation of 1 to 7 volts.	112
3.21 Hanning windowed waveforms of a tuned rectangular wave delta modulator at 60 Hz operation for control voltage variation of 1 to 7 volts.	113
3.22 Blackman windowed waveforms of a tuned rectangular wave delta modulator at 60 Hz operation for control voltage variation of 1 to 7 volts.	114
3.23 Spectra of Hamming windowed waveforms of rectangular wave delta modulator for 10-75 Hz operations.	115

- 3.24 Spectra of Hanning windowed waveforms of rectangular wave delta modulator for 10 - 75 Hz operations. 116
- 3.25 Spectra of Blackman windowed waveforms of rectangular wave delta modulator for 10 - 75 Hz operation. 117
- 3.26 Spectra of Hamming windowed waveforms of the tuned rectangular wave delta modulator at 60 Hz operation with control voltage variation of 1-7 volts. 118
- 3.27 Spectra of Hanning windowed waveforms of tuned rectangular wave delta modulator at 60 Hz operation with control voltage variation of 1-7 volts. 119
- 3.28 Spectra of Blackman windowed waveforms of tuned rectangular wave delta modulator at 60 Hz operation with control voltage variation of 1-7 volts. 120
- 3.29 Fundamental voltage variation of the rectangular wave delta modulated waveforms with frequency. 121
- 3.30 Fundamental voltage variation of the tuned rectangular wave delta modulated wave with change in frequency. 123
- 3.31 Fundamental voltage variation of the tuned rectangular wave delta modulated wave with variation of control voltage. 123

- 3.32 Variation of the number of commutation of rectangular wave delta modulator waveforms with change in operating frequency. 124
- 3.33 Variation of the number of commutations of the tuned rectangular wave delta modulator waveforms with change in operating frequency. 124
- 3.34 A practical rectangular wave delta modulator circuit. 130
- 3.35 Typical waveforms of the practical rectangular wave delta modulator circuit. 131
- 3.36 The tuned rectangular wave delta modulator circuit. 132
- 3.37 Waveforms of the rectangular wave delta modulator circuit for 10-75 Hz operations. 134
- 3.38 Waveforms of the practical tuned rectangular wave delta modulator at 60 Hz operation for control voltage variation of 1 to 7 volts. 137
- 3.39 Spectra of modulated waveforms of the rectangular wave delta modulator for 10-75 Hz operations. 139
- 3.40 Spectra of modulated waveforms of the tuned rectangular delta modulator at 60 Hz operation for control voltage variation of 1-7 volts. 141

3.41	Experimental fundamental voltage variation of rectangular wave delta modulated wave with change in operating frequency.	142
3.42	Experimental fundamental voltage variation of tuned rectangular wave delta modulated waves for various control voltages.	144
3.43	Experimental fundamental voltage variation of tuned rectangular wave delta modulator wave for various operating frequencies.	144
3.44	Experimental variation of number of commutations of rectangular wave delta modulated waves.	145
4.1	The single phase bridge inverter output. (type-A switching.)	154
4.2	The single phase bridge inverter output. (type-B switching.)	154
4.3	Switching waveforms of the three phase inverters.	156
4.4	The construction of type-B switching waveforms by gate functions.	157
4.5	The illustration of defining the three phase inverter output from the switching waveforms.	158

4.6	Typical line to line voltages of a three phase delta modulated inverter(type-B switching).	162
4.7	Typical line to neutral voltages of a three phase delta modulated inverter(type-B switching).	163
4.8	Typical d-q axis voltages of a three phase delta modulated inverter (type-B switching).	166
4.9	Fundamental voltage availability of a three phase rectangular wave delta modulated inverter.	167
4.10	Line to neutral voltage waveforms of a tuned rectangular wave delta modulated inverter.	169
4.11	Spectra of inverter waveforms with constant control voltage but variable frequency.	170
4.12	Hanning windowed waveforms of the three phase rectangular wave delta modulated inverter.	172
4.13	Hanning windowed waveforms of the three phase rectangular wave delta modulated inverter.	173
4.14	Blackman windowed waveforms of the three phase rectangular wave delta modulated inverter:	174

4.15 Spectra of Hamming windowed waveforms of a three phase delta modulated inverter.	175
4.16 Spectra of Hanning windowed waveforms of a three phase delta modulated inverter.	176
4.17 Spectra of Blackman windowed waveforms of a three phase delta modulated inverter.	177
4.18 The induction machine models in d-q axis.	181
4.19 The electrical analog model of a submersible pump.	184
4.20 The line current of the conventional induction motor with sinusoidal supply ($\frac{1}{4}$ full load).	188
4.21 The line current of the submersible induction motor with sinusoidal supply ($\frac{1}{4}$ full load).	188
4.22 The line current of the submersible motor with rectangular wave delta modulated inverter supply at 60 Hz ($\frac{1}{4}$ full load).	189
4.23 The spectrum of the line current obtained by discrete Fourier transform at 60 Hz ($\frac{1}{4}$ full load).	189
4.24 The computed developed torque of the submersible motor with the rectangular wave delta modulated inverter supply at 60 Hz.	192

- 4.25 The computed on-line starting current of the conventional induction motor with sinusoidal input. 192
- 4.26 Computed on-line developed torque characteristics of the conventional induction motor for a sinusoidal supply. 193
- 4.27 The starting speed of the conventional induction motor with sinusoidal supply. 194
- 4.28 The computed on-line starting current of the submersible induction motor with sinusoidal supply. 194
- 4.29 Computed on-line developed torque characteristics of the submersible induction motor with sinusoidal supply. 195
- 4.30 The starting speed of the submersible induction motor with sinusoidal supply. 196
- 4.31 The computed on-line starting current of the submersible induction motor with the rectangular wave delta modulated inverter supply without RFV. 196
- 4.32 Computed on-line developed torque characteristic of submersible induction motor for a rectangular wave delta inverter supply without RFV. 197

- 4.33 The starting speed of the submersible induction motor with the rectangular wave delta modulated inverter supply without RFV. 198
- 4.34 The computed on line starting current of the submersible induction motor with the rectangular wave delta modulated inverter supply with RFV. 200
- 4.35 Computed on-line developed torque characteristics of the submersible induction motor for a rectangular wave delta modulated inverter supply with RFV. 201
- 4.36 The starting speed of the submersible induction motor with the rectangular wave delta modulated inverter supply with RFV. 202
- 4.37 The experimental line current of the submersible motor fed from the three phase rectangular wave delta modulated inverter at 60 Hz. 204
- 4.38 The starting current of the submersible motor with sinusoidal supply (at no load). 205
- 4.39 The starting current of the submersible motor with the rectangular wave delta modulated inverter supply at no load. 205
- 4.40 The starting current of the submersible motor with the rectangular wave delta modulated inverter supply at no load (with RFV). 206

- 5.1 The performance curve of the submersible pump (J54). 210
- 5.2 Performance curves of the submersible pump at different operating frequencies. 211
- 5.3 Performance curves and the pump efficiency curve showing the range of maximum efficiency operation of the pump. 211
- 5.4 The schematic diagram of the open loop control of a submersible motor fed from the delta modulated inverter supply. 214
- 5.5 The schematic diagram of the semi-closed loop control of a submersible motor fed from delta modulated inverter supply. 214
- 5.6 The basic equivalent circuit of an induction motor. 216
- 5.7 The computed and the measured speed obtained by the proposed speed estimation method at 63 Hz operation of the motor. 219
- 5.8 The computed and the measured speed obtained by the proposed speed estimation method at 73 Hz operation of the motor. 219
- 5.9 The block diagram of the speed sensor. 220
- 5.10 The speed of the submersible motor at no load measured by the proposed speed sensor. 222
- 5.11 Variation of the slip, the frequency and the fundamental voltage of the motor for a sudden increase in load. 227

A1.1 Practical delta modulator.	253
A1.2 The logic circuit for generating the gating signals of two SCRs or transistors of a three phase inverter.	255
A1.3 The transistor inverter.	258
A2.1 The block diagram of the speed sensor.	263
A2.2 The voltage conditioning circuit used in the speed calculator.	264
A2.3 The current conditioning circuit used in the speed calculator.	264
A2.4 The frequency conditioning circuit used in the speed calculator.	264
A2.5 The phase angle measurement circuit of the speed calculator.	266
A2.6 The speed calculator.	268
A3.1 Phasor diagram of generating the three phase variable frequency sine wave.	271
A3.2 The output of a quadrature oscillator.	272
A3.3 Three phase sine wave generator and its output.	275

List of Tables

Table 2-1 Summary and comparison of LDM, SDM and RWDM.	70
Table 3-1 Table of harmonics of a RWDM.	125
Table 3-2 Table of harmonics of tuned RWDM.	126
Table 3-3 Table of harmonics of RWDM.	146

CHAPTER-1

INTRODUCTION

The submersible motor is a class of induction motors. For certain applications as in pumping sub-surface fluids; these motors have unique constructional features. The uniqueness lies in their long and narrow construction. The size and shape restrict their number of stator turns and number of poles to the minimum. Because of these restrictions submersible motors draw 8-12 times their full load current during line voltage starts. Also, they reach their steady state operating conditions quickly. Electro-mechanical problems associated with the high starting current and quick speed up result in frequent shaft breakdowns of these motors. The continuous on-line operation of submersible motors under variable load conditions result in their inefficient operations. Researchers engage in a constant effort to use the state-of-the-art static inverter controls for the soft start and the near maximum efficiency operation of these motors.

The closed-loop control of a submersible motor using pulse width modulated(PWM) inverter is difficult. One of the difficulties encountered involves obtaining the speed feedback from the shaft of completely sealed motors. As a solution to this problem a semi-closed loop operation of submersible motors fed from delta modulated inverters is proposed. One of the goals in this respect is to design and study the delta modulation technique for three phase inverter operations. A proper selection of the type of delta modulator for switching a three phase inverter is made on the basis of drive requirements. Three simple delta

modulators are considered for the selection. These modulators are the linear, the sigma and the rectangular wave delta modulators. The rectangular wave delta modulator is selected on the basis of its superiority over the other two modulators in this particular application. The harmonics of the modulator and the inverter waveforms are studied using discrete Fourier transforms (DFT). A novel way of optimizing the modulator and inverter waveforms using the tuned modulator is proposed and implemented. This method is suitable for continuous on-line harmonic minimization of the inverter waveforms. The delta modulation scheme is successfully used for the inverter operation to meet the starting and other operating requirements of submersible motors. A simple but elegant technique to estimate the speed of an induction motor is developed. This method is incorporated with the submersible motor in a semi-closed loop control with delta modulated inverter supply. The start up and operating performances of the delta modulated inverters are studied using the d-q axis model of the motor and the inverter voltages. Analyses are carried out using the time domain solution of the motor and inverter voltage equations. This involves the synthesis of inverter voltages in time domain which is done by using gate functions. This method is different from the conventional frequency domain analysis.

1.1 Features of Submersible Drives:

The electrical submersible drive consists of a submersible motor (SM) coupled to a load. The principal applications of these systems are in pumping ground water, drainage of mines, off-shore exploration and marine resource developments.

There are many applications of these motors related to marine environments. Some of these applications are in the field of hydro-carbon exploration and production, ocean mining, dredging, dynamic positioning of large ships and platforms, and in drilling equipment for sea floor rock sampling.

Submersible motors are usually sealed from the environments they work in. In some cases they have an imposed limitation on their radial dimensions. The limit of radial dimension also restricts the number of stator turns and the number of poles of these motors. The long and slim construction as well as the small number of poles and stator turns make submersible motors vulnerable to severe starting and operational stresses. During on-line start, submersible motors accelerate to their steady state speed very rapidly. The loads (i.e. the pumps) experience tremendous torsion on their shaft during starting periods and fail to respond to the fast speed of the motors. A survey of literature shows that the major failures in the form of broken shafts of these units are due to the electromechanical problems during start up periods.

The non-compatibility of load is another major problem of submersible motors. These systems are designed to run with certain loads at near optimum efficiency of operation. However, this operating condition cannot be maintained during the production cycle. The loads may change due to changes in economic or operating conditions. In such circumstances two scenarios may prevail. Either the total system has to be replaced by a new one or the system is run below the recommended operating range. Also, submersible motors frequently encounter

insulation failures due to thermal, mechanical, and environmental stresses [1-4]. Heating problems arise because of minimal insulations, delicate stator turns and quick magnetic saturation of motors. These motors are also sensitive to the operating voltage unbalance, overvoltage and the frequency of start/stop operations[5]. Variable speed operation of submersible motors supplied by static inverters may reduce most of these problems.

1.1.1 Review of Submersible Drives:

The main use of submersible drives is in the field of submersible motor pumps. Significant advances in the electrical submersible system design and manufacture have made it the most cost effective means of lift under most pumping conditions. The submersible pumps were in use in the United States as early as 1900 [6]. These pumps were used for artificial lift of ground water and were operated by motors at ground levels.

Consideration of cost, maintenance, and efficiency led to the development of motors directly attached to the submersible pumps[7]. The first subsurface centrifugal pump for oil well service in the United States was installed in Russel field, Kansas in 1926 [8]. Since then, these motors have been used extensively in inshore applications. The significant use of submersible motor pumps for artificial lift of oil at sea was introduced in 1965 at Long Beach Unit in the United States[9]. The next major use of submersible motor pumps for artificial lift of offshore oil was in the Montrose field in the North sea in 1976[10]. In 1981 the pro-

duction of Beatrice field in the North sea started relying exclusively on the artificial lift using electrical submersible pumps[11,12]. During relatively short period of experience these units showed short operating life and unreliable operations[13]. Subsequently many other uses of submersible motors were reported in off-shore and on-shore applications. Some of these applications are in trimming and ballast duties on drilling and production platforms, fire fighting duties and mining [14]. In 1978, a submersible motor pump was used to handle 1,000 tons of manganese nodules out of a depth of more than 5,000 meters below the sea. Prior to this, the submersible motor went into operation at a depth of 10,000 meter in a French submarine, the Archemedes[15]. The motors also have a wide range of uses in off-shore applications as, for example, in drilling and in propulsion [16]. The newer generation of dynamically positioned ships invariably use electrical submersible motors for driving their thrust propellers [17].

1.1.2 Advantages of Variable Speed SMPs :

There are three different types of submersible motors, namely the oil filled, the semi-wet, and the wet submersible motors [18]. Since the early days the ability to control the speed of a drive according to the load has been a desirable feature. Submersible drives also require this feature in order to meet the demands of start/stop stress and load variability. The start/stop stresses can be reduced substantially by using power supplies with soft start characteristics.

The various methods available for speed changing of a motor can be classified in three categories. These are the intermediate speed changer, the dc motor drive and the ac motor drive [19,20]. The first two types have very good speed variability. However, they are excluded from use in submersible motors because of their lack of ruggedness. The speed of an ac induction motor can be effectively changed by supplies having variable frequency. Variable frequency supply can be obtained from motor generator sets or static power converters [20]. Due to relatively low cost, weight, and controllability, static power converters are the most popular speed controllers of ac motors [21,22]. For artificial lift systems variable speed submersible motors are the most cost effective means for meeting various operating conditions[23-25]. Variable speed operation would allow the drive to adapt to well conditions and new requirements without replacing production equipments[26-30]. The advantages obtainable from variable speed operation of submersible motors are:

1. Continuous operation.
2. Elimination of frequent start/stop operation.
3. Matched loading at all operating conditions.
4. Reduced solid settling.
5. Reduced motor heating.
6. No need for additional soft starter.
7. Extended range of loading.

8. Easy maintenance.
9. Elimination of the need for frequent replacement.
10. Automatic monitoring of load conditions.
11. Improved efficiency.
12. Improved reliability.

1.2 Inverter Fed Variable Speed Induction Motors :

The speed of an induction motor is dominantly governed by the synchronous speed, the slip of the motor, and the voltage applied. The usual methods of speed control of induction motors are :

- a) Constant frequency stator voltage control.
- b) Variable voltage variable frequency control.
- c) Variable current variable frequency control.
- d) Slip power regulation.

AC voltage controllers are used in applications like single phase fractional horse power drives, speed control of induction motor driven pumps, fans, and in solid state start of medium to large horse power motors[30-32]. The controllers produce harmonics in the supply line and are characterized by poor power factors and inefficient performances[33-36]. Because of these disadvantages the use of ac voltage controllers for speed regulation of large motors is limited.

As the technology developed, static voltage source inverters were introduced for controlling the speed of induction motors. The inverters achieve the speed control by changing the frequency of the supply. There are basically two different types of voltage source inverters, the square wave and the pulse width modulated (PWM) inverters. Square wave inverters were introduced in the 1960s with the innovation of forced commutation techniques of the silicon controlled rectifier[37,38]. Technological advances made possible the use of power transistors, and gate turn off thyristors (GTOs) as power switches in inverters [39]. Besides voltage source inverters, induction motors can also be supplied from current source inverters[40-41].

Variable voltage and variable frequency control of induction motors can be achieved in several ways. Traditionally, solid state ac to ac frequency changers commonly known as cyclo-converters have been employed in a limited scale. These converters allow voltage and frequency changes in one power conversion stage without any energy storage elements. Applications of cyclo-converters are limited due to their operating frequency ranges. The main applications of cyclo-converters are for large and slow speed drives[30]. Square wave inverters are used for variable voltage, variable frequency control of ac motors. The disadvantages of using square wave inverters are high harmonic losses and torque pulsation in motors, poor line side power factors, harmonic interferences, and the requirement of dual power conversion for simultaneous voltage and frequency change. Various techniques have been introduced to improve the waveforms of inverters in the

past. One such technique is the pulse width modulation (PWM) scheme for switching inverters. In this method, the switching devices of the inverter are switched ON and OFF many times within a half cycle in order to generate a variable voltage variable frequency supply. The output waveforms of pulse width modulated inverters are low in harmonics. The pulse width modulated inverter drives are considered as the most versatile ac drives presently available. Side by side with innovations of new schemes, the analysis of solid state drives also drew attention in the recent past[41-47]. These analyses constitute a significant part in understanding the solid state drives.

1.2.1 Review of PWM Techniques For Power Converters:

The disadvantages of normal square wave voltage source and current source inverters have led to the developments of pulse width modulated converters. In the pulse width modulation technique the switches of the power converters are operated at higher frequencies according to a particular modulation technique so as to produce pulses of varying widths at the output of the inverter.

The earliest modulation techniques applied to inverter operation are single pulse modulation and the multiple pulse modulation [48-52]. These techniques are capable of providing inverter output voltages with low harmonic contents. These modulation techniques were eventually replaced by the sine pulse width modulation (SPWM)[52,53]. At the beginning two different types, namely the asynchronous and synchronous sine pulse width modulation schemes were used for

switching power converters[54]. In sine pulse width modulation technique a sine wave is compared with a high frequency triangular wave to determine the switching points of the modulated waves. For drive applications the fixed frequency modulation was found to be problematic at different operating frequencies. In order to overcome the drawbacks of ordinary sine pulse width modulation variable ratio PWM schemes were introduced. Presently, three distinct sinusoidal pulse width modulation schemes are in use for inverters[54-57]. They are the 1) natural sampling method, 2) regular sampling method, and 3) the optimal switching strategy. The first method is similar to the method described in the previous paragraph. In the regular sampling technique, the sine wave is replaced by a sampled or a stepped sine wave. This method is very popular in microcomputer implementation [58,59]. The third approach uses optimized switching strategies based on certain performance criteria[60]. As a result of the developments in microprocessor technology in recent years, the implementation of optimized pulse width modulation for switching inverters has become feasible[61,62,63]. Two types of PWM strategies have been reported recently for inverter operation. They are the bang-bang sampled PWM technique and the delta modulation (DM) technique. The principle of bang-bang sampling is based on the motor output current hysteresis comparison with a reference waveform, to generate the modulated waveforms[64-68]. In recent years delta modulation has been finding its way for generating switching waveforms of inverters[68]. Several types of delta modulation have been investigated so far for various power converter operations.

including inverters and rectifier-inverters[69,70]. The analysis and the applications of the PWM inverters in drives are also important areas of research[71-76]. However, due to the complexity of modulation processes, a general approach for such studies has not yet been developed.

The control of ac machines, especially an induction motor is quite involved. The complexity increases if rigid performance specifications are prescribed. Basic control schemes reported so far can be placed mainly in two categories: a) the scalar control method, and b) the vector control method[77,78]. The scalar control method includes V/f control, torque and flux control, and current control. The V/f control can either open-loop or closed-loop. The other scalar control methods are implemented invariably in closed-loop control. So as to improve the sluggish response of induction motor in scalar control the vector control technique was introduced. The vector control method is a closed-loop operation in which the input currents of the motors are self controlled so that the machine behaves like a dc motor[79]. Apart from scalar and vector control methods, adaptive and sliding mode controls of PWM inverter fed induction motor have also been proposed. However, these techniques are yet to become popular in industrial applications. Due to certain limitations, such as the need for an individually designed controller, vector control has not been widely accepted in industrial applications until recently[79].

1.3 Delta Modulated Inverter Control of Submersible Motors:

The operating conditions of submersible motors virtually preclude the use of closed-loop control schemes. Therefore, it is necessary to formulate an open loop control scheme for such drives. The basic requirements of submersible drives are :

- a) Well defined constant torque and constant power operation over a wide load range with variable frequency operation.
- b) Quick response to load changes.
- c) Soft start.
- d) Current control.

With proper design, the first and the third requirements can be met with a V/f characteristic of the inverter fundamental output voltage as shown in fig. 1-1. Quick response to load changes is usually achieved in conventional pulse width modulated drives through closed-loop hysteresis current and speed controls. Figure 1-2 shows the waveforms of a current controlled single phase inverter drive. In such a closed-loop control the excursion of the current within a window is obtained by the hysteresis comparison of the load current and a reference sine wave. Whenever the current reaches the upper or lower limit of the window, the switching of the inverter is reversed. Conventionally, this type of control is achieved by comparing the load current with a reference sine wave to produce a difference signal. This difference signal is fed into a hysteresis comparator which produces the modulated wave required for switching the power devices in an

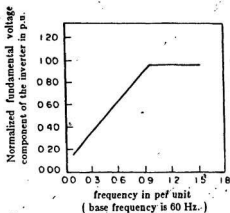


Fig. 1.1 Voltage versus frequency characteristic required for constant torque and constant power operation of an induction motor.

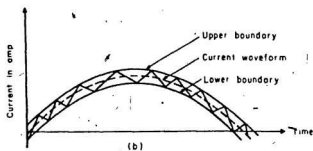
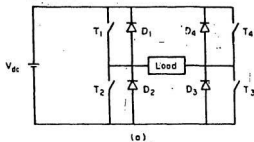


Fig. 1.2 The single phase inverter and the load current variation required in a hysteresis current control.
 (a) The bridge inverter. (b) Load current variation in a hysteresis current control

inverter. Since the load current changes as the load varies, it is necessary to scale either the current or the reference sine wave to facilitate the comparison. The current limit is determined by the window width of the hysteresis comparator. A reduction in the window width or in the hysteresis band would result in reduction of low order harmonics of the motor current.

The basic requirements of submersible drive with pulse width modulated inverter can mostly be met with a closed loop controller if the conventional sine pulse width modulation schemes are employed. In submersible motors the control requirements are difficult to implement with the conventional open loop control techniques. The adoption of delta modulation technique for the control of inverter to drive submersible motor would allow such control to become a reality[80]. The added advantage of using delta modulation in drives lies in its ability for on-line optimization of the inverter operation. The combination of using delta modulation technique, the on-line optimization, and on-line monitoring of motor operating conditions would improve the performances of the drives in open-loop control.

The delta modulation scheme shown in fig 1.3 (a), is a simple and effective modulation technique. For inverter switching a variable frequency sine wave is compared with the estimated waveform of the modulator. The difference signal produced by this comparison is known as the error signal. The error signal is quantized by the quantizer in the feed-forward path of the modulator to produce the modulated waveform. There are many types of delta modulators available.

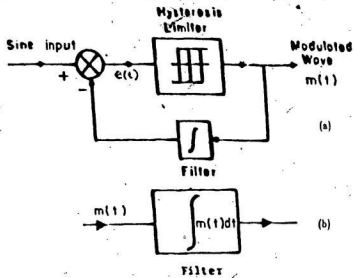


Fig. 1.3 The block diagram of a rectangular wave delta modulator.
(a) The modulator. (b) The demodulator.

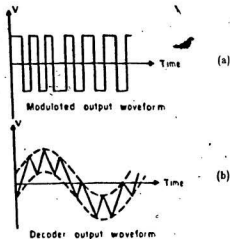


Fig. 1.4 The waveforms of a rectangular wave delta modulator.
(a) The modulated wave. (b) The demodulated wave.

This thesis shows that the rectangular wave delta modulators exhibit characteristics that meet the control requirements of submersible motor drives. The rectangular wave delta modulator [fig. 1-3 (a)] is composed of a hysteresis quantizer instead of a simple ON/OFF controller. This modulator has an inherent characteristic which ensures the ramp voltage to frequency variation of the fundamental voltage during pulse width modulated mode of operation. This fundamental voltage vs. frequency relationship of the rectangular wave delta modulator output is almost similar to the V/f characteristic shown in fig. 1-1. Due to this characteristic of rectangular wave delta modulator, the drive requirements of soft start, and distinct constant torque and constant power modes of operation at variable frequency can be obtained in open loop control. The current control of this modulation process can be explained from the expected waveforms of the modulator (coder) and the demodulator (decoder). The expected waveforms of the coder and the decoder for a sinusoidal input to the modulator are shown in fig. 1-4. The output waveform of the modulator is a pulse width modulated wave. The decoder is a linear filter which decodes this waveform as shown in fig. 1-4(b). Since the modulator contains its own decoder in the feedback circuit, a waveform similar to the demodulated signal but known as the estimated wave, is obtained at the output of the feedback filter. The oscillation of the estimated wave is bounded by windows of the hysteresis quantizer. The same oscillation boundary is, therefore, imposed on the decoded signal at the output of the decoder. In drives, the modulator generates the switching signal for the inverter and the

motor acts as a low pass filter in the same way as the decoder. Thus the excursion of the current of rectangular delta modulated inverter fed motor is also bounded between certain windows. It is important to note that the harmonic currents in a motor are determined primarily by the leakage inductances and the frequency of the supply. At higher operating frequency, the leakage reactances due to harmonics are higher. As a result, the filtering effect of the motor is smoother during high frequency operation of the inverter. Under this circumstance the current waveform of the motor is not only bounded by upper and lower window limits but also smoothed by the filtering effect of the motor. This current control process due to delta modulation is obtained without any feedback from the motor. Therefore, the process is an open-loop control. The rectangular wave delta modulated waveforms are well defined and they can easily be studied analytically. On the other hand, in the ordinary feedback current hysteresis control technique the output of the modulator is dependent on so many factors that the analytical study of the modulated waveform is often tedious.

Another benefit of rectangular wave delta modulation is the on-line optimization of the modulator waveforms. This is evident from the fact that the harmonic contents of the modulated waveforms can be controlled through the variation of several parameters in the modulator. Two of these parameters are the window width and the feedback filter characteristic. One of the easiest ways to achieve optimization is through the use of a tuned filter, the cutoff frequency of which can be varied via the command signal of the

modulator (fig. 1-5) [81,82]. This allows the reduction of low order harmonics. Low order harmonics start appearing otherwise in the modulated waveform as the operating frequency of the input sine reference wave is increased. Researchers have been trying to selectively reduce the harmonics in the inverter output waveforms. In the past, success has been achieved in this regard for constant frequency inverter waveforms through various harmonic minimization techniques and microcomputer waveform synthesis. However, such techniques had little success in the operation of variable frequency inverters. The delta modulation technique is, thus, a promising application in this area.

1.4 The Modulator and The Inverter Waveform Synthesis:

The studies of the performances of the modulator, the inverter and their applications require a knowledge of harmonics of the modulated waveforms. In the past, inverter waveforms generated by different pulse width modulation schemes have been studied by Fourier series analysis. In the present study discrete Fourier transform is used to determine the harmonics of the modulator and inverter waveforms. It is a well known fact that pulse width modulated waveforms contain subharmonics due to the concurrent presence of the modulating and the carrier wave frequencies in the modulated waves. The conventional Fourier series analyses on such waveforms determine only the frequency components which are multiples of the modulating frequency and ignore the presence of subharmonics. Also, in the past no comprehensive method has been reported on the possible calculation of harmonics on-line. To overcome the above

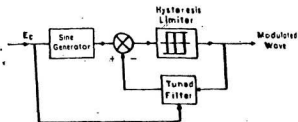


Fig. 1.5 The block diagram of a tuned rectangular wave delta modulator.

drawbacks of Fourier series analysis, discrete Fourier transform method (DFT) is proposed in this study[83,84]. In this approach, the pulse width modulated waveforms are defined and simulated by gate functions, and the switching points of the waveforms. The switching points are obtained from the solution of a set of equations defining the rectangular wave delta modulated waveforms. The simulated waveforms are then sampled for discrete Fourier transform analysis.

The rectangular data windowing of ordinary discrete Fourier transform gives rise to leakage spectra and Gibbs phenomenon[85]. In order to reduce the effect of these phenomena and obtain smooth spectra of modulated waveforms, tapered windowing of sampled modulated waveforms has been suggested. Windowing of sampled waveforms is a common practice of waveform synthesis in communications. The effects of three common windows were investigated. These are the Hamming, the Hanning and the Blackman window. The windows have been chosen for their simplicity of application. A typical modulated waveform of a single phase inverter and the spectrum obtained by discrete Fourier transform is shown in fig. 1-6. The Hanning windowed waveform of the same and its spectrum obtained by DFT is shown in fig. 1-7 as an illustration of the windowing process.

The main advantage of the DFT approach of analysis is that it is simple and may be adapted for on-line harmonic determination of the modulated waveforms of the inverter. It enables the investigators to determine the subharmonics present in the waveforms. The determination of subharmonics has been neglected so far in power converter waveform analysis.

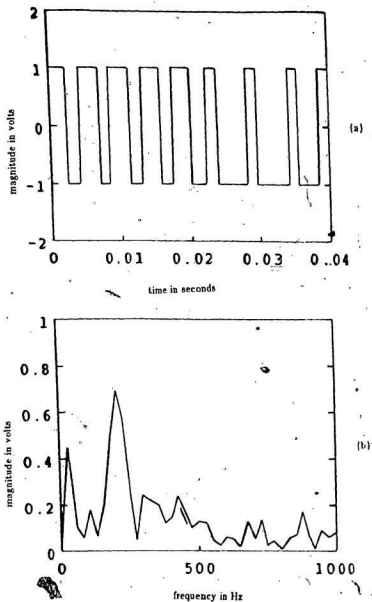


Fig. 1.6 The simulated modulated waveform of a rectangular wave delta modulator and its spectrum obtained by discrete Fourier transform.
(a) The simulated modulated wave.
(b) The spectrum of the modulated wave.

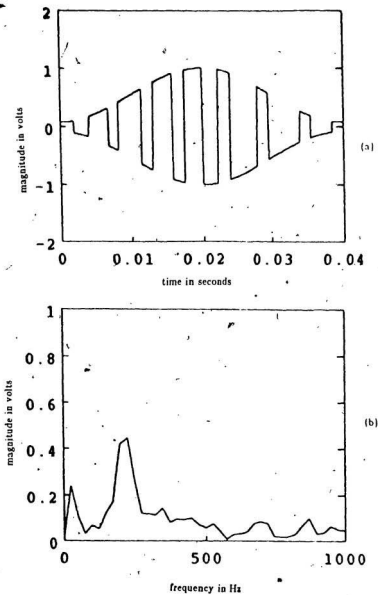


Fig. 1.7 The simulated Hamming windowed modulated waveform of a rectangular wave delta modulator and its spectrum obtained by discrete Fourier transform.
(a) The simulated Hamming windowed waveform.
(b) The spectrum of the Hamming windowed waveform.

1.5 The On-Line Control Strategy for a Submersible Drive System:

Fig. 1-8 illustrates the schematic of an open-loop control scheme. For automatic speed variation in response to sudden changes in load, it is necessary that the inverter responds by changing the operating frequency. The necessity of such a speed change in a submersible pump drive applications is illustrated in fig. 1-9. To match the pump production curves and operate at near maximum efficiency, the speed of the motor must be changed. It is, therefore, necessary for the control scheme to have a provision to monitor the speed of the motor and adjust the frequency of the inverter accordingly. This is also required for constant slip operation of the motor at all operating frequencies. The constant slip ensures that the motor operates in the recommended efficiency range. In practical applications the speed is not obtainable from the submersible motor by conventional speed feedback methods. As a result, it is necessary to estimate the speed, torque and other operating conditions from the voltage, current and the input power of the motor. In this research a simple method based on input impedance measurement technique was developed for an on-line prediction of required operating conditions. It was successfully used for the control of the motor in the linear range. The schematic of the automatic control of such inverter operation with variation of load is shown in fig. 1-10

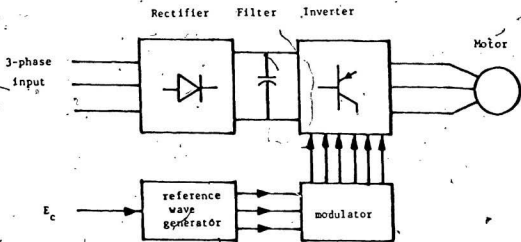


Fig. 1.8 The block diagram of the open-loop control of a submersible motor fed from the rectangular wave Delta modulated inverter.

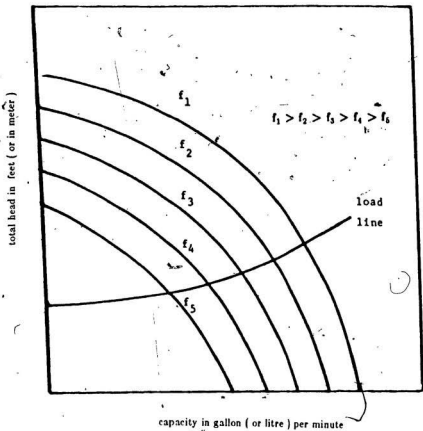


Fig. 1.9 Pump performance curves at variable speed operations.

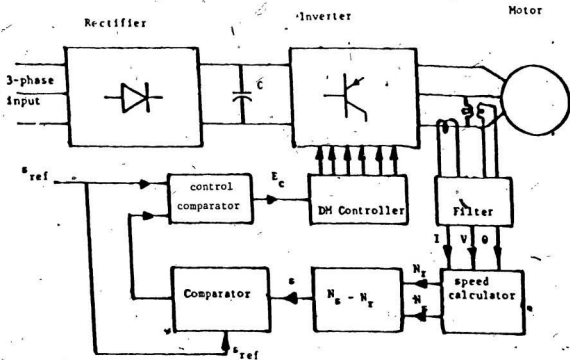


Fig. 1.10 The schematic diagram of the semi-automatic control of submersible motor fed from a rectangular wave delta modulated inverter.

1.6 The Analysis of the Delta-Modulated Inverter and the Submersible Motor Pump Performance:

Most analyses of inverter fed ac drive systems reported in the literature are based on the Fourier series of the inverter output voltages and on the d-q axis transformation of the machine models. In this study the three phase inverter output voltages were studied with DFT on windowed sampled waveforms. However, for the drive analysis an unconventional approach was followed. Instead of finding the Fourier voltage responses and super-imposing them, the unit step response of the motor for each pulse of a modulated waveform was found and super-imposed. The d-q axis model of the motor was used to formulate the motor equations. This type of analysis eliminates the errors usually encountered in the Fourier series analysis. In the frequency domain, a finite number of harmonics of the Fourier series are usually considered for the performance analysis of the motor. The dominant harmonics of pulse width modulated waveforms occur at very high frequencies and their inappropriate truncation may result in the loss of information of the effects of these dominant harmonics.

Steady state and transient analyses were performed on the d-q axis model of the motor. The steady state response does not change over time and it remains the same over successive cycles. Therefore, in steady state analysis the response for each single pulse is calculated. The individual responses are then superimposed to find the total response for one cycle of the supply. For transient analysis however, the responses due to pulses ranging over several cycles of the

supply are calculated and superimposed.

1.7 Thesis Objectives and Outlines:

The objective of this study is the application of the delta modulated inverter for submersible motor operation. Many of the control demands of submersible motors can be satisfied through the use of delta modulated inverters. The choice of the modulator for the submersible motor is made on the basis of submersible motor requirements. The operational characteristics of different delta modulators were studied to facilitate the choice of the type of modulator. The study of the selection criteria was concentrated mainly on the three simplest delta modulators and the results of the study are presented in chapter 2. The rectangular wave delta modulation technique was selected for inverter switching. The characteristics of the rectangular wave delta modulated waveforms were analyzed to find the performances of the modulator and the inverter. One of the main objectives of this thesis was to develop a method to optimize inverter waveforms on-line. A novel method of optimization of inverter waveforms using tuned rectangular wave delta modulator was proposed and successfully implemented during this research. The proposed method is described and analyzed in chapter 3. Chapter 3 also includes the analyses of RWDM and tuned RWDM modulator output waveforms. For the waveform analysis the discrete Fourier transforms were used on the sampled and windowed sampled waveforms. This type of waveform analysis is also suitable for on-line spectral estimation and

sub-harmonic detection of PWM waveforms. Chapters 4 and 5 are concerned with studying the performances of submersible motors fed from delta modulated inverters. The inverter fed submersible motor performance was studied using time domain solution of the motor and inverter voltage equations. The semi-automatic operation of a submersible motor was achieved by motor speed estimation from the current, voltage and power measurement of the motor and is described in chapter 5. Finally the claims and conclusions of this research are summarized in chapter 6 together with recommendations for future works.

CHAPTER-2

Delta Modulation Technique and The Selection Criteria For Inverter Drives

2.1 Introduction:

The objectives of this chapter are to describe the delta modulation systems, their important characteristics as well as their limitations with regard to inverter operation. At present, there are different types of delta modulators available. The variations stemmed from the need for and requirements of different applications and the necessity to improve the modulator performance. For inverter switching the modulation schemes adapted are restricted to the simpler ones. A brief review of the delta modulation technique is presented in this chapter. Selection criteria of the modulator for inverter switching are discussed. The criteria are based on the requirements of the drive and the modulator. Characteristics of three modulators are studied. These are the linear, the sigma and the rectangular wave delta modulator. Based on this study, the rectangular wave delta modulator (RWDM) has been chosen for the inverter switching for submersible motor drives.

2.2 Delta Modulation Technique:

Different forms of delta modulation (DM) have recently been used in inverters and other power converters. It has the advantage of retaining many of the features of currently used pulse width modulation (PWM) techniques. Delta modulation is known as the simplest method for modulating an analog signal to

its digital form [86], without significant redundancy in encoding the signal. The basic delta modulator consists of a comparator quantizer and a filter (fig. 2-1). The comparator at the input of this block compares the input signal with the stepwise approximation of the input signal. The difference signal produced by the comparison is known as the error signal. The quantizer quantizes the error signal according to the sign of the error signal to produce the positive and negative pulses of the modulated wave. The function of the integrator in the modulator is to reconstruct the input signal from the output modulated signal. The input to the integrator is the modulated waveform. The integrator acts as a low pass filter and estimates the modulating signal. For digital conversion the digitized waveform is obtained by a sampler in the modulator block. Depending on the use of sampler, the estimated waveform may be a stepped estimation or a triangular estimation (fig. 2-2). The estimated waveform is also called the carrier waveform in delta modulation. The estimated waveform or the carrier waveform in delta modulation is a self-generated signal. If $x(t)$, $\bar{x}(t)$, $m(t)$ and $e(t)$ are the input, the estimated, the modulated and the error signal respectively, the DM technique described above can be expressed as follows

For the modulator without sampler:

$$e(t) = x(t) - \bar{x}(t) \quad (2-1)$$

$$m(t) = \text{sgn}\{e(t)\} \quad (2-2)$$

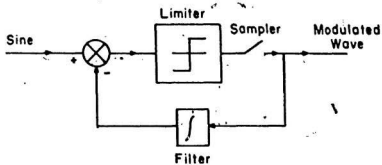


Fig. 2.1 The block diagram of a simple delta modulator.

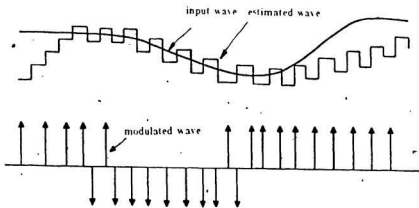


Fig. 2.2 Waveforms of the simple delta modulator.

$$\tilde{x}(t) = \int m(t) dt \quad (2-3)$$

For modulator with sampler:

$$e(KT_s) = x(KT_s) - \tilde{x}(KT_s) \quad (2-4)$$

$$m(t) = \sum V_D \operatorname{sgn}[x(KT_s) - \tilde{x}(KT_s)] \delta(t - KT_s) \quad (2-5)$$

$$\tilde{x}(t) = \int m(t) dt. \quad (2-6)$$

where,

V_D is the level of quantization

sgn is the sign function

T_s is the sampling frequency

In encoding a signal, delta modulation has two distinct restrictions. When the predicted signal $\tilde{x}(t)$ is smaller than the actual signal $x(t)$ at the beginning, the first impulse has the weight $+V_D$. When fed-back and integrated, that impulse produces a step wise change in $e(t)$ and causes a negative impulse. If $x(t)$ remains constant $\tilde{x}(t)$ follows it in steps until the rate of change is too rapid. If the rate of change is too fast slope overload takes place. This occurs when the window width Δ is too small to track a rapidly changing signal. Slope overload occurs due to the modulator's inability to track large changes of the input

signal $x(t)$ in a small time interval. Slope overload is considered to be a basic limitation in delta modulation schemes for communication systems. However, the same characteristic may be used to an advantage in switching power converters.

A variation of DM is the differential pulse code modulation (DPCM) with a multilevel quantizer instead of two level quantization. Functionally, DPCM signal is a pulse code modulated (PCM) representation of the difference signal $[x(t) - \bar{x}(t)]$, where $\bar{x}(t)$ has a variable step size ranging from V_D to $QV_d/2$. Q is the number of quantization level. Signal $\bar{x}(t)$ follows signal $x(t)$ more accurately when companding is used. This results in lower idling, fast start up and less chance of slope overload. The following section gives a brief review of the DM technique as it evolved for digital communications.

2.3 A Brief Review of Delta Modulation Technique:

The linear delta modulation was first reported in 1946 and its early description emerged in the 1950s [87,88]. In linear delta modulation the modulator receives a band limited analog signal at the input and produces a binary output signal. The output of the modulator is also locally decoded by the integrator in the feed-back path and subtracted from the input signal to form an error which is quantized to one of two possible levels depending on the polarity of the error signal. The closed loop arrangement of the DM encoder ensures that the polarity of the pulses is adjusted by the sign of the error signal. This ensures that the locally decoded waveform will track the input signal. This type of delta

modulator is known as a linear modulator because the decoder at the receiving end is a linear network. Despite the attractive simplicity of the delta modulation coders, initial drawbacks had prevented their wide-scale use at the start [89]. Delta modulation remained an interesting field for theoretical studies in communication systems for decades. This situation began to change when more refinements were suggested [90] and today development of delta modulation is in full progress. At present, many communication research institutions are engaged in in-depth exploration of the technique and its applications [91,92,93]. The simplicity of delta modulation has inspired numerous refinements and variations since its basic invention in 1948 by De Loraine and Derjavgotch [89]. Most of these DM systems have received impetus from the applications of digitization of audio and video signals. The initial DM coder consisted of a single integrator (analog) or a first order predictor (digital) in its feedback path. Subsequently, the DM coder with double integrator and multiple integrator (or their substitutes, the predictors in the digital domain) were used in the feedback path for more precise signal tracking [94]. Some investigators replaced the integrator of the feedback loop with RC network by introducing the concept of exponential delta modulators [95]. In order to suit the technique for uncorrelated signals, sigma delta modulation was introduced in 1962 [96,97]. In the initial sigma delta modulators, the input signal was passed through an integrator prior to coding. Subsequent modification replaced the feedback integrator and the integrator at the front with a single integrator at the feed-forward path. This pre-emphasizes the

low frequency input signal thereby increasing the sample correlation. To keep pace with pulse code modulation several researchers suggested an adaptive delta modulation (ADM) scheme [97,98]. In adaptive delta modulation the value of the signal at each sample time is predicted to be a non-linear function of the past value of the quantized signal. In literature, two other DM schemes frequently encountered are the companded and the asynchronous delta modulation schemes [99,100]. The companded DM technique uses compression of large signal levels as compared to the smaller ones. Compression is done prior to encoding using compressor circuits, and expansion of the signal is done at the decoder side to recover the signal. The asynchronous delta modulation system has digital output quantized in amplitude but not in time. The rectangular wave delta modulation (RWDM) is one of the asynchronous delta modulation techniques. In rectangular wave delta modulation, the memory-less quantizer of the modulator circuit is replaced by a non-linear element whose characteristics are that of a hysteresis loop or a bang-bang controller. Also, samplers of ordinary modulators are permanently closed. This form of delta modulation was first reported by Sharma [101,102].

In addition to the modulators already mentioned, there are various other delta modulators which have been sporadically suggested by different researchers [89]. Nonetheless, their operations are basically similar to the modulators already discussed.

2.3.1 Typical Use of Delta Modulators Outside Communication Field:

Since delta modulation is the simplest of all the available modulation techniques it is being used extensively in communication applications. However, it has applications in other fields as well. At the present time instrumentation techniques rely increasingly on digital techniques. Delta modulators offer attractive applications in such areas. Due to very large scale integration (VLSI), the cost of implementation is no longer a reason for choosing delta modulation over other modulation techniques. It is the simple encoding process and the requirements of a simple decoder which are the most advantageous features of the DM techniques. Some of the important uses of delta modulation technique in instrumentations are measurement of noise, time scaler (transient) display of cathode ray tubes (CRTs) and recorders, peripherals for hybrid computers, and in power measurements by delta sigma wattmeters [103,104]. Also, delta modulation strategy plays an important role in the design and fabrication of digital filters [105,106,86]. In addition, speed control of a small ac motor using delta modulated class D low power amplifier was suggested during early days of DM developments [107,86]. This idea of speed control of small motors can be extended and adopted for high power three phase voltage source ac drive scheme.

2.4 Delta Modulation Scheme For Inverter Fed Submersible Motors:

Inverters are, functionally, power amplifiers used for the frequency and voltage control of the supply to a device. Inverters are also used in inverters for high frequency links between utilities and in high frequency induction heating. In induction motor drives modulation is used for the translation of sinusoidal reference voltage to a stream of positive and negative pulses. The pulses of unequal widths, carry the voltage and frequency information from the low power control side to the high power load side through the inverter. It is desirable that the low power control sinusoidal wave be conveyed to the load without much distortion. In applications such as the uninterruptible power supplies (UPS) and in high frequency link inverters, the output waveforms of the inverters are filtered to obtain sine waves at the load side. For ac drives, the motors themselves work as the low pass filters, thus additional filters are not required. The choice of a modulation scheme and the control system for the ac drives are however, dictated by the type of drives, their requirements and applications.

2.4.1 Drive Requirements:

The requirements for solid state drives for induction motors are well established [108]. Some of the basic requirements are:

1. Solid state ac drive has to be energy efficient.
2. AC to variable frequency ac conversion with a dc link to meet the variable

motor load.

3. Voltage variation with frequency to keep motor flux constant (the requirement for V/f constant).
4. Formidable range of speed variation from .2 to 2 pu of rated speed.
5. Fast torque response.
6. Good starting torque.
7. Lower torque pulsation and lower harmonic losses of the motor.
8. Adequate speed regulation.
9. Rapid protections against overload and loss of power.

To meet most of the above requirements closed loop control of the motor is necessary. The most versatile control method is the field oriented vector control or the decoupled field theory control [108]. For high performance drives the concept of vector control is the prime choice. Independent flux and torque control is possible through this method. However, since the input/output relationships between stator currents and input voltages of induction machines are non-linear, open loop constant V/f control is still the most widely used scheme [79]. In the vector control method, if the values used in the calculator deviate from correct ones (which may easily happen due to multiple changes in motor operating conditions) both the steady state and the transient responses of the motor would deteriorate substantially. Off-line parameter identification has been used extensively for fast and high performance motors. However, in such cases the whole

system cannot be built as a package module ready for industrial use. With a vector controller each motor requires an independently designed controller, and the controller tuning is necessary at the beginning of installation as well as during operation [109]. To avoid the difficulties inherent in the decoupled vector control method, many researchers have been trying to obtain comparable performances of motors using scalar control techniques. In a scalar control the voltage and the current are varied to maintain the constant slip operation of the machine. These types of controllers are used for robust drives. They are not optimized and are slow in response [110,111]. To obtain quick response in the scalar control methods, limit cycle or hysteresis (bang-bang) control of the flux and the current has been reported [112,110]. But such instantaneous current controls are problematic because of the necessity of three independent hysteresis comparators.

Submersible drives are mostly squirrel cage ac induction motors. Therefore, the selection criteria for solid state converters for these drives are the same as discussed previously. In addition to the requirements mentioned, the submersible motors require some additional features in the controllers. Submersible motors are an unique type of squirrel cage induction motors. Their starting characteristics and continuous operating conditions are unique due to the following reasons:

Submersible motors are long and narrow in shape. They have high rotor resistances and stator inductances. The geometry of the motor requires that the number of poles be kept to the minimum. When these motors are started from

the supplies of fixed voltage and frequency they start very quickly. The inertia of the motors help them start faster. As the motors start and attain their full speed the loads coupled with them (like pumps) experience tremendous torsion on their shaft. In some cases it has been observed that when the lower part of a pump moves a full revolution the upper part remains in stationary position. This results in broken shafts in drive systems. Experiences have shown that most of the failures resulting in submersible motor pump installations are due to this starting characteristic. This problem can be solved by proper voltage and frequency control of the supply during the start-up. Usually for induction motors it is an accepted practice to start the motors with low voltages in order to limit the starting currents. In applications involving submersible motors it is necessary to provide a soft start method which will simultaneously limit the starting current, the speed, and the torque. This can be achieved by designing a PWM controller which would allow the voltage and frequency of the supply to be low during start and reach the rated voltage and frequency in a ramp fashion.

Another related problem of submersible motors is the continuous changes in load conditions. During installation a motor is selected to match the load so that it runs at near maximum efficiency. But during operation the load may vary. Also due to many operational factors, after a certain time period, the load to the motor may change. In such a case, the motor may operate at lower efficiency or it may have to be replaced altogether incurring capital expenditures. The solid state PWM controller, with its ability to change frequency of the supply to the motor

can meet the load variability without replacement.

In many of the applications of submersible motors it is not possible to monitor the speed, torque and rotor position from the motor shaft continuously. This is because majority of these motors are sealed. This gives rise to the choice of only open-loop control with the facility to obtain motor operating quantities from the input voltage, current and power to the motor.

The above discussion highlights the following constraints on the PWM controllers to be used for submersible motors:

- a. For soft start of the motor, the controller has to provide a low voltage and low frequency supply which will gradually reach its operating voltage and speed.
- b. Variability of speed with load change to meet the criterion of operation at maximum efficiency condition.
- c. Open-loop controller is the choice with additional requirements of predicting motor speed and torque from the motor terminal quantities like voltage and current.

To obtain these characteristics, an open loop delta PWM inverter control method has been chosen. For on-line parameter estimation, a simple technique based on motor constants and the measurement of terminal voltage, and current has been developed.

To minimize both harmonic losses and pulsating torque in ac drives, the PWM techniques of harmonic reductions are commonly used. The harmonic minimization in PWM strategies are aimed at removing the low order torques so as to avoid low frequency mechanical resonances. When these strategies are implemented, rotor motions of motors improve. However, such techniques introduce higher order torque harmonics to the extent that they may excite additional resonance at higher frequencies in the motor and in the load [112]. Such high frequency resonances are unacceptable in applications like submersible motors. As a result, such optimized modulation techniques cannot be used in converters supplying submersible drives. In order to reduce the harmonic losses and pulsating torques a harmonic minimization method is developed based on the tuned filter concept of delta modulators for the submersible drives.

2.4.2 Modulator Requirements:

Modulation schemes are used in inverter operations for obtaining variable frequency supplies with low distortions of the output waveforms. Induction motor drives require such modulators to produce smooth V/f control of the output waveform upto the base frequency. The inverter requires low switching at higher operating frequencies. To achieve this in a normal sine PWM inverter it is necessary to vary the carrier triangular wave's frequency over a wide range. However, in drive applications this is not practical. The reason for this is that at higher carrier frequency, the commutation hazard increases and at low carrier fre-

frequency the motor constants are insufficient for adequate smoothing of current waveform. In sine PWM modulators such a dilemma is solved by using variable ratio schemes [113,114]. In delta modulation this property is obtained as an inherent characteristic of the modulator.

One basic disadvantage of using sine PWM modulators in inverters is the low dc voltage utilization, usually in the order of 45-50 percent. Researchers are constantly attempting to improve this percentage. Voltage utilization of 85 % has been achieved by careful selection of the delta modulator[115].

Smaller low order harmonics at the inverter output are functions of modulators' switching waveforms. It is, thus, necessary for the delta modulators used in inverter switching to have low order harmonics. In the delta modulation technique this is usually ensured by the waveform tracking principle of the modulators. The integrators used in the delta modulators are basically low pass filters. Also, the window width keeps the estimated wave within a certain limit. These two characteristics provide a kind of current control in the open loop operation of the motor. Similar current control is usually obtained in other PWM control of inverters by hysteresis current comparison in a closed-loop operation.

To reduce the pulsating torques and harmonic losses in the motor it is necessary for the modulators to incorporate optimization techniques. In delta modulators such improvement in modulator performance can be attained by on-line variation of the modulator parameters like filter characteristic or the window width. In section (3.2.3), an improved delta modulator with tuned filter is described.

The stable operation of motors requires higher voltage availability at a higher operating frequency. This requirement of the drive can be satisfied to a large extent by the V/f variation inherent in the delta modulated inverters. In open loop control of submersible drives, a gradual increase of voltage and frequency for the soft start purpose is also met by the switching characteristic of the modulator.

The two main criteria for the choice of delta modulators are the stability of the modulators during variable frequency operation and the speed of their response to a changing input signal. Some applications also necessitate frequency independence of the output of the modulator. Delta modulators are non-linear device with or without hysteresis quantizer within the feed-forward loop. Therefore, an analytical method of finding their step responses and the stability is difficult. Usually, the step responses of such modulators are found by the system simulation technique and also from experimental observations. The stability criteria reported in this study are obtained by the describing function method [116-110]

The criteria for the modulators described above, cannot be fulfilled by any single modulator. This is especially true when different linear delta modulators (LDM) have different characteristics. In choosing the modulator for switching the inverter for drive applications, the operating characteristics of three modulators were examined. These three modulators are the linear, the sigma and the rectangular wave delta modulators.

2.4.3 Characteristics of Three Simple Delta Modulators:

Three simple delta modulators which have been used in the past for generating inverter switching waveforms are shown in fig. 2-3. The linear delta modulator (LDM) consists of a quantizer-comparator in the feed-forward path and an integrator in the feedback path. In addition it has a sampler to digitize the output waveform. In the sigma delta modulator (SDM) the integrator is placed in the feed-forward path before the quantizer block. The rectangular wave delta modulator (RWDM) has a hysteresis quantizer. The sampler in the rectangular wave delta modulator is permanently closed. The output of the linear and the sigma delta modulators are digitized and appear in the form of pulses. In contrast, the output of the rectangular wave delta modulator is in pulse width modulated form. The tracking signals of the linear and the rectangular wave delta modulators are the integrated output (stepped in the LDM and triangular in the RWDM). For the sigma delta modulator (SDM) the tracking signal is the output waveform itself.

The characteristics of these three modulators are examined with respect to the drive requirements. The modulator performance in ac drives depends on many factors. The basic characteristics examined for each modulator are:

1. The idling characteristics.
2. The overload characteristics.
3. The availability of fundamental voltage with change in operating frequency.

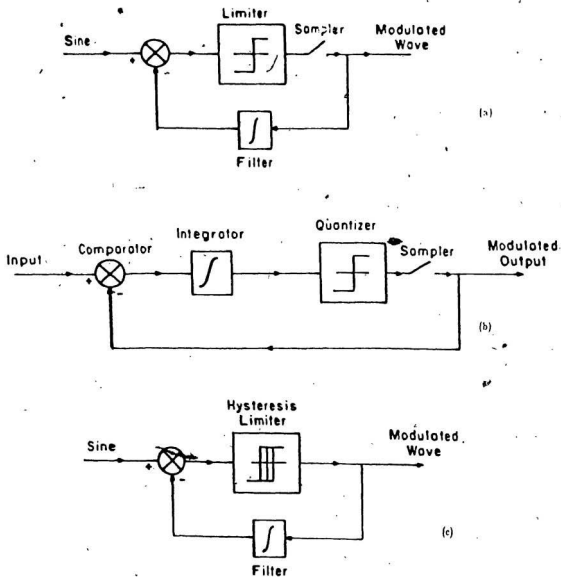


Fig. 2.3 Block diagrams of the linear, the sigma, and the rectangular wave delta modulators.

(a) The linear delta modulator.

(b) The sigma delta modulator.

(c) The rectangular wave delta modulator.

4. Stability of the modulator.
5. Step response of the modulator.
6. Current tracking capability in the open loop control of drives.

A. Characteristics of The Linear Delta Modulator:

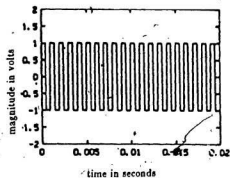
The linear delta modulator (LDM) is the simplest of all delta modulators. The input signal to the linear delta modulator is compared with the estimated signal. The error signal produced by this comparison is quantized to two levels. The output of the quantizer is then digitized by the sampler.

1. Idling Characteristics[86]:

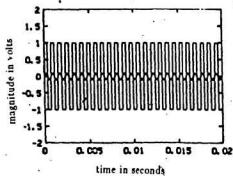
A linear delta modulator with no signal at the input produces an output of equally spaced positive and negative pulses. This property of delta modulators is known as the idling phenomenon. The sequence of output represents a high frequency square wave. Fig. 2-4(a) shows the idling pattern of LDM. If an inverter is ON during the idling, either the load or the filter before the load attenuates the idling waveform. Nevertheless, it constitutes a loss in the overall system.

2. Overload Characteristic:

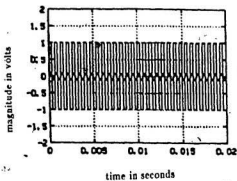
In the delta modulation technique a situation may prevail during the encoding process when the slope of the input signal may become greater than the slope of the estimated signal. In such a situation the feedback signal fails to track the input signal. This is known as the slope overload condition of the modulator. Slope overload of a linear delta modulator depends on many factors such as the



(a)



(b)



(c)

Fig. 2.4 Idling waveforms of three delta modulators.

- (a) Idling waveform of the linear delta modulator.
 (b) Idling waveform of the sigma delta modulator.
 (c) Idling waveform of the rectangular wave delta modulator.

frequency of the input signal, the magnitude of the input signal, the clock rate and the step size of the estimated wave etc. In a linear delta modulator, when slope overload takes place, a sequence of identical polarity pulses occur at the output of the modulator. For a sinusoidal input to the modulator the condition for preventing slope overload condition is [86]

$$E_m 2 \pi f_m \leq \Delta f_p \quad (2-7)$$

where,

$$\text{input signal} = E_m \sin 2 \pi f_m t,$$

Δ is the step size, and

f_p is the clock frequency of the sampler.

and the maximum amplitude E_m which does not overload the modulator is given by [86]

$$E_m = \frac{\Delta f_p}{2 \pi f_m} \quad (2-8)$$

The slope overload in linear delta modulator is dependent on the amplitude and the frequency of the input sine wave. Since there is no other waveform tracking mechanism involved in an LDM, the slope overload takes place quickly. This characteristic is disadvantageous for the inverter operation.

3. Fundamental Voltage Availability:

The fundamental voltage of an inverter shows a similar trend to the fundamental voltage of the switching waveform. It is, therefore, necessary that the fundamental voltage variation of the switching waveform provides a trend of ramp increase from the low starting frequency to the operating frequency. In addition, voltage should remain constant after the transition of inverter waveform from the PWM mode to the square wave mode of the operation.

It has been found that the fundamental voltage availability of the linear delta modulator varies slowly with increasing frequency. Once the slope overload takes place, the voltage availability does not change with frequency. The variation of voltage in the low frequency operation in pulse width modulation mode is not a significant one. The fundamental voltage availability of a linear delta modulator is shown in fig. 2-5.

4. Step Response:

The initial settling times of delta modulators are usually investigated by step responses of the modulator. Analytical determination of such step responses of the delta modulators is restricted due to the nonlinear quantizer in the feed-forward path. However, computer simulation approach or an experimental determination allows us to find their response time to step changes. The simulated step response of a linear delta modulator with linearized approximation of the modulator is shown in fig. 2-6(a). It is apparent from fig. 2-6(a) that the linear delta modulator requires a certain settling time after application of a step

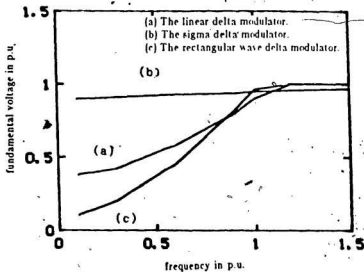


Fig. 2.5 Fundamental voltage variation of three modulators with the change in operating frequency.

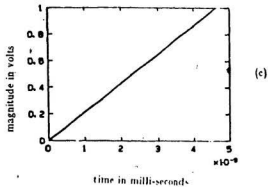
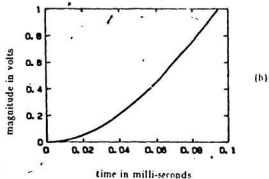
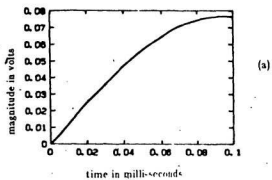


Fig. 2.0 Step responses of three delta modulators.
 (a) Step response of a linear delta modulator.
 (b) Step response of a sigma delta modulator.
 (c) Step response of a rectangular wave delta modulator.

to track the input signal. The responses of these modulators are not rapid enough for sudden changes and thus may not be suitable for operation of inverters to supply motors.

5. Stability:

The delta modulators, being closed-loop systems, are subject to an investigation of their stable operating conditions. Some of these modulators encounter unstable operation with the increase in operating frequencies. Due to the presence of the quantizer in the feed-forward path all delta modulators are non-linear devices. For the stability study of these modulators several methods of nonlinear control techniques can be used. The most common method in the preliminary study of such non-linearities is the describing function method [116-119]. The method assumes that the non-linearity does not generate sub-harmonics and all harmonics are filtered out or reduced before the input stage of the nonlinearity. By definition, the describing function is the ratio of the fundamental of the output voltage to the peak value of sinusoidal input voltage of the the non-linear element.

$$K_N(E_m, \omega) = \frac{Y_1}{E_m} / \phi_1 \quad (2-9)$$

where,

$K_N(E_m, \omega)$ is the describing function,

Y_1 is the fundamental of the output wave, and

E_m is the amplitude of the input sine wave $E_m \sin \omega t$.

In stability studies using describing function, the nonlinear elements in the systems are replaced by their describing functions. The Nyquist stability criteria for closed loop systems are then applied. The characteristic equation for a closed loop system representing the delta modulators is formulated. The limit cycle operation of a modulator is then determined from the root locus of characteristic equation.

For the linear delta modulator, the describing function $K_N(E_m, \omega)$ is given by [120]

$$K_N(E_m) = \frac{4V}{\pi E_m} \quad (2-10)$$

and the characteristic equation for this system for the block diagram shown in fig. 2-4 (a) can be formulated as follows:

The input /output relationship is given as

$$\frac{c}{r} = \frac{K_N(E_m)}{1 + K_N(E_m)H(j\omega)} \quad (2-11)$$

where, $H(j\omega)$ is the transfer function of the feed-forward path.

The characteristic equation is given as

$$1 + K_N(E_m)H(j\omega) = 0 \quad (2-12)$$

From relation (2-12), the limit cycle condition can be deduced as

The sigma delta modulation (SDM) is a variation of linear delta modulation. The sigma delta modulator is basically a linear delta modulator preceded by an integrator. The integrator at the front, and the integrator of the feedback path can be replaced by a single integrator placed in the feed-forward path of the modulator. In the sigma delta modulator the integrated error signal is quantized to produce the modulated signal. In this type of modulator the slope overload characteristic is independent of the frequency of the input signal.

B. Characteristics of a Sigma Delta Modulator:

In the linear delta modulator the estimated waveform at the output of the integrator is stepped in nature and there is no upper or lower bound of its excursion. As a result, it does not have a current tracking capability when used for inverter switching.

6. Current Tracking Ability in Open Loop Operation of Drives:

The describing function in this case is frequency independent. The root locus for the varying gain of $H(j\omega)$ and the inverse describing function $\frac{K_N(E_m)}{1}$ is shown in Fig. 2-7. It is evident from Fig. 2-7 that linear delta modulators are stable and no limit cycle condition prevails in them.

$$H(j\omega) = \frac{K_N(E_m)}{1} \quad (2-13)$$

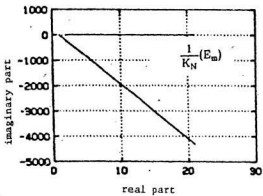


Fig. 2.7 Root locus of the linear delta modulator

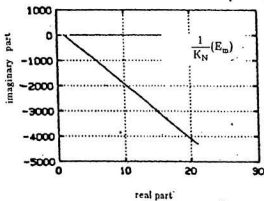


Fig. 2.8 Root locus of the sigma delta modulator.

1. Idling Characteristic:

The idling characteristic of a sigma delta modulator is the same as the idling characteristic of a linear delta modulator. The idling characteristic of a sigma delta modulator is shown in fig. 2-4(b).

2. Overload Characteristic:

The performance change in a sigma delta modulator from that of an ordinary linear delta modulator is in the slope overload characteristic due to the repositioning of the integrator. In linear delta modulators, it was found that slope overload condition is dependent on the frequency of the input signal. For a sinusoidal input in a sigma delta modulator, the condition of slope overload prevails only when amplitude of the input sine wave is equal to the product of the window width and the sampling frequency[86]. This slope overload condition is independent of operating frequency of the modulating wave. The condition of slope overload of a sigma delta modulator is given by

$$E_m = \Delta f_p \quad (2-14)$$

As a result of frequency independence, in variable frequency operation of inverter, slope overload condition will not be encountered if a sigma delta modulator is used. These modulators are, therefore, suitable for applications in inverters where slope overload cannot be tolerated over a wide range of frequency.

3. Fundamental Voltage Availability:

The fundamental output voltage of a sigma delta modulator shows little variation with the change of operating frequency. Due to frequency independence of slope overload it remains in pulse width modulation mode of operation for a wide range of frequency. As a consequence, the necessary fundamental voltage variation for ac motor operation is not available from a normal sigma delta modulator. The fundamental voltage availability of a sigma delta modulator is shown in fig. 2-5.

4. Step Response:

The computer simulation of the step response of a sigma delta modulator is shown in fig. 2-6(b). From this step response it is apparent that the sigma delta modulator is faster in response than the linear delta modulator. This would ensure a faster response to sudden load changes of the inverters.

5. Stability:

The stability criterion for a sigma delta modulator is the same as that for the linear delta modulator. The describing function method of analysis shows that sigma delta modulators are inherently stable and they do not show any limit cycle condition. Similar to a linear delta modulator, the describing function of a sigma delta modulator can be expressed as [120]

$$K_N(E_m) = \frac{4V}{\pi E_m} \quad (2-15)$$

The output/ input relationship for the block diagram shown in fig. 2-3(b) is given as:

$$\frac{c}{r} = \frac{G(j\omega) K_N(E_m)}{1 + G(j\omega) K_N(E_m)} \quad (2-16)$$

Where, the $G(j\omega)$ is the feed forward transfer function of the integrator.

The characteristic equation is

$$1 + G(j\omega) K_N(E_m) = 0 \quad (2-17)$$

and the condition for limit cycle occurrence is

$$G(j\omega) = -\frac{1}{K_N(E_m)} \quad (2-18)$$

The root locus plots with varying gain of $G(j\omega)$ and the inverse describing function $\frac{1}{K_N}(E_m)$ for a sigma delta modulator are shown in fig. 2-8. From the plot it is evident that the limit cycle condition does not prevail in a sigma delta modulator.

6. The Current Tracking Capability in Open-loop Operation of Drives:

The estimated waveform at the output of a sigma delta modulator is a pulsed waveform. The integrated error signal is quantized to produce the modulated waveform. As a result, there is no current waveform tracking situation in open-loop sigma delta modulated inverter drive.

7. Optimisation Criterion:

The sigma delta modulator offers many advantageous features over the linear delta modulator. The fundamental voltage availability of the modulator and its inability to restrict the current oscillation within certain boundaries makes it an un-attractive choice for drive applications. Also, when implemented in hardware, the sigma delta modulators do not allow any on-line optimization of modulated waveform. This inability is due to the positioning of the integrator in the feed-forward path. The tuning of the integrator is possible, but since the error signal has a very low amplitude, tuning the integrator with an aim to reduce harmonics would result in complete loss of operation of the modulator.

C. Characteristics of Rectangular Wave Delta Modulators:

The rectangular wave delta modulator (RWDM) is similar to the linear delta modulator. The difference between the two is in the quantizer comparator. In rectangular wave delta modulator, the quantizer is a hysteresis quantizer rather than a normal ON-OFF controller. Also, the sampler after the quantizer is permanently closed in rectangular wave delta modulator. The modulated waveform in this type of modulator is also generated by the quantization of the error signal. Due to the hysteresis comparator-quantizer, the estimated signal is bounded by the hysteresis limits.

1. Idling Characteristic:

The idling characteristics of the asynchronous delta modulators are different from those of the linear and the sigma delta modulators. During idling the rectangular wave delta modulator oscillates at very high frequency, limited only by the propagation delay. The output of the modulator is either +V or -V. The output signal is fed back into the input comparator after integration in the form of a rising or falling ramp. In the absence of an input signal, the error signal is the same as the ramp signal. When the ramp hits the upper or lower hysteresis limit, the output of the modulator changes the polarity of the pulse. Therefore, the process continues as long as no input signal is present. The frequency of the idling waveform is dependent on the hysteresis band and the integrator's time constant. The idling frequency of the rectangular wave delta modulator can be expressed as:

$$f_{idle} = \frac{m_{idle}}{4\Delta} \quad (2-19)$$

Where,

m_{idle} is the slope of the triangular wave and Δ is the window width.

The output of a rectangular wave delta modulator during idling as obtained by computer simulation is shown in fig. 2-4(c).

2. Overload Characteristic:

Overload characteristic of a rectangular wave delta modulator (RWDM) depends on several factors. These factors are, the amplitude of the input signal, the slope of the estimated waveform, the frequency of operation, and the window width of the hysteresis band.

The slope overload of the rectangular wave delta modulator is dependent on the frequency of operation of the modulator. With all other parameters remaining constant, the slope overload takes place at a certain operating frequency and the modulator remains in the slope overload beyond this frequency. The frequency where the slope overload takes place can be varied by changing the window width of the hysteresis comparator. The larger the window width, the quicker the slope overload condition takes place in the rectangular wave delta modulation. If the modulator is required to run without slope overload, the window width can be selected to provide such operation. With constant window width, the slope overload occurs approximately when the slope of the estimated wave becomes equal to the slope of the input sine wave. The slope overload condition of the rectangular wave delta modulator can be obtained as

$$r = \frac{E_m \sin 2\pi f \frac{T}{2} + 2 \Delta_R}{\frac{T}{2}} \quad (2-20)$$

where, Δ_R = window width of rectangular wave delta modulator.

Equation (2-20) can also be expressed as

$$r = 2f (E_m \sin 2\pi + 2 \Delta_R) \quad (2-21)$$

$$r = 4f \Delta_R \text{ or } f = \frac{r}{4 \Delta_R} \quad (2-22)$$

3. Fundamental Voltage Availability:

The nature of bounded estimated waveform of the rectangular wave delta modulator between the window widths $\pm \Delta_R$, assures a ramp fundamental voltage variation with frequency of operation in PWM mode. This fact can be established from the following:

If y and m are estimated and the modulated waveforms of a rectangular wave delta modulator respectively, then for a simple integrator circuit in the modulator having transfer function $\frac{1}{(1 + jr\omega)}$, the input/output relationship is given by

$$\frac{y_n}{m_n} = \frac{1}{1 + jr\omega_n} \quad (2-23)$$

where,

y_n and m_n are the n -th harmonic of the estimated and the modulated waveforms of RWDM respectively, and $\omega_n = 2\pi n f$. For the fundamental voltage, the following relationship holds

$$\frac{y_1}{m_1} = \left| \frac{1}{r\omega_1} \right| = \left| \frac{1}{r\omega} \right| \quad (2-24)$$

Since the estimated waveform oscillates within a window width of $\pm \Delta_R$ about the input sine wave, it can be assumed that the fundamental voltage of the estimated wave is equal to the voltage of the input sinusoid E_m . The equation (2-24) can therefore be written as

$$\frac{E_m}{M_1} = \left| \frac{1}{r\omega} \right| \quad (2-25)$$

Equation (2-25) can be re-written as

$$\frac{M_1}{E_m} = |r\omega| \quad (2-26)$$

Since E_m is kept at a constant value in the modulator for inverter switching, it is apparent that fundamental voltage variation is linearly dependent on the frequency of operation.

$$M_1 = rE_m\omega = rE_m 2\pi f = Kf \quad (2-27)$$

where,

$$K = rE_m 2\pi$$

This linear dependency of the fundamental voltage of the modulator output with frequency is valid until the modulator reaches its slope overload condition.

During slope overload condition the modulator output is the square wave having the same frequency as that of the input sine wave. As a result, the fundamental of the output waveform remains constant as long as the slope overload condition prevails. The fundamental voltage variation of RWDM with frequency is shown in fig. 2-5. The characteristic obtained meets the drive requirements already discussed.

4. Step Response:

The rectangular wave delta modulators are inherently quick in response. This is due to the presence of the hysteresis limiter in the feed forward path of the modulator. The simulated step response of RWDM is shown in fig. 2-6.

5. Stability:

The describing function analysis of the rectangular wave delta modulator shows that with single integrator in the feedback loop the modulator is stable, and does not show any limit cycle condition. However, this situation changes with the use of two or more integrators in the feedback loop[101]. With a single integrator in the feedback path, the describing function analysis is as follows:

The describing function of a hysteresis comparator is given as

$$K_N(E_m) = \frac{4V}{\pi E_m} \sin^{-1} \frac{\Delta_R}{2E_m} \quad (2-28)$$

E_m is the amplitude of the input sine wave.

The input/output relationship of the modulator is given as

$$\frac{c}{r} = \frac{K_N(E_m)}{1 + K_N(E_m)H(j\omega)} \quad (2-29)$$

$H(j\omega)$ is the transfer function of the integrator in the feedback path. The characteristic equation can be written as

$$1 + K_N(E_m)H(j\omega) = 0 \quad (2-30)$$

and the limit cycle condition will prevail if

$$H(j\omega) = -\frac{1}{K_N(E_m)} \quad (2-31)$$

The root locus plots with varying gain of $H(j\omega)$ and $\frac{1}{K_N(E_m)}$ are shown in fig. 2-9. It is evident from fig. 2-9 that the rectangular wave delta modulator with single integrator does not exhibit any limit cycle condition during its operation.

6. Current Tracking Capability in Open Loop Operation:

The use of rectangular wave delta modulation offers a major advantage in inverter fed drives. If an inverter is switched by the waveform of rectangular wave delta modulator, the hysteresis current control of inductive loads is obtained without any feedback from the load. In motor controls, usually, the current tracking is done by closed loop control. The use of a rectangular wave

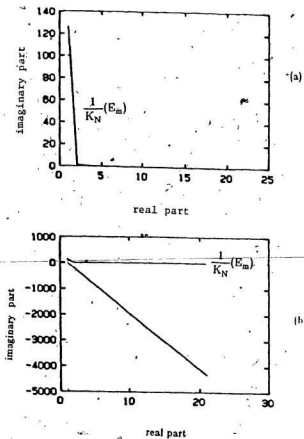


Fig. 2.9 Root locus of the rectangular wave delta modulator.

(a) The root locus of $\frac{1}{K_N}(E_m)$

(b) The root locus of $\frac{1}{K_N}(E_m)$ and $H(jw)$.

delta modulated inverter would allow one to obtain hysteresis current control in open loop operation of the motor. Due to the presence of the hysteresis band in RWDM, the modulator sets the switching frequency of the inverter in such a manner that the current waveform of the load is bound within certain envelope. This criterion of the modulator is particularly needed in inverter operation for the motor in situation where the required feedback signals for closed loop operation is difficult to obtain.

Table 2-1 contains both a summary and a comparison of features of the three delta modulators discussed. The comparison shows that the RWDM should be the choice of the modulator for inverter switching for submersible drives. Besides the advantageous features already mentioned the rectangular wave delta modulator was considered to be the best among the simple delta modulators because of its lowest signal to noise ratio, and low quantization error[86]. It was also suggested for industrial uses particularly in transmitting signals over short distances for instrumentations.

The other significant reason for choosing rectangular wave delta modulator for inverter switching is the ability of on-line optimization of the inverter output waveform by the tuned filter. A unique method of optimizing the modulator waveform using a tuned filter is discussed in section 3.2.3.

Table 2-1

Summary and Comparison of LDM, SDM and RWDM

	LDM	SDM	RWDM
Idling output	Square wave output of high frequency	square wave output of high frequency	square wave of high frequency
Overload	Depend on step size and frequency of input	depend on step size only.	Depends on step size and frequency of input
Fundamental voltage availability	moderate ramp characteristics in PWM mode	moderate ramp characteristics	ramp in PWM mode and constant voltage in square wave mode
Step response	slower response than the SDM and RWDM	response is fast	response is inherently faster due to hysteresis quantizer
Stability	Inherently stable	Inherently stable	Stability depends on the frequency and the gain of overall modulator
Current limiting capability	Absent	Absent	Present
On-line optimization	Possible with tuned filter	Possible but difficult	Possible with tuned filter

2.5 Conclusions:

The delta modulation technique is proposed for the switching of inverters in drive applications. The criteria for the modulator and the drive requirements of submersible motors have been established. On the basis of the requirements for drive applications, the characteristics of three simple delta modulators have been examined to find the best suitable delta modulator for switching an inverter. The three modulators examined for possible use in inverters to run submersible motors are the linear, the sigma and the rectangular wave delta modulators. It has been established that the rectangular wave delta modulator is the most suitable of the three which can advantageously be used for the operation of submersible motors.

Chapter-3

Analysis and Optimization of The Rectangular Wave Delta Modulator**3.1 Introduction:**

A novel waveform synthesis and an on-line harmonics minimization of the inverter output voltage using delta modulation technique are described in this chapter. The proposed on-line harmonic reduction method uses a tuned filter in the feedback path of the delta modulator. The analysis of switching waveforms generated by a rectangular wave delta modulator is described. An investigation into the conventional way of defining the switching points and their analytical determination for harmonics using the Fourier series has been conducted. However, it was found that the discrete Fourier transform (DFT) technique would be more appropriate to study PWM waveforms, particularly in detecting sub-harmonics and for the on-line calculation of spectra of modulated waveforms [83,84]. Emphasis is given to the windowing process of sampled waveforms in order to reduce spectral leakage and the effects of Gibb's phenomenon encountered in discrete Fourier transforms (DFT).

Based on the analysis, the features of the delta modulation technique as applied to the operation of inverter are summarized. Realization of a practical modulator circuit, its operation, and the performance are also discussed. The details of the practical modulator circuit are included in the appendix. The operational limitations of inverters using DM switching are briefly discussed.

3.2 Rectangular Wave Delta Modulator:

Based on the selection criteria discussed in Chapter 2, the rectangular wave delta modulation (RWDM) has been selected for switching of an inverter to drive submersible motors. The intrinsic features of rectangular wave delta modulators are proved and verified. A novel method of optimization of inverter waveforms using the tuned modulator is suggested in this section.

3.2.1 The Simple Rectangular Wave Delta Modulator:

The following are the intrinsic features of rectangular wave delta modulators:

1. Upto the base frequency the fundamental voltage to frequency ratio remains constant.
2. Beyond the base frequency, the modulator operates in the square wave mode of operation. The available fundamental component of the voltage is constant in this region.
3. Low order harmonics in the carrier and the modulated waves are small in magnitudes.
4. For fixed window width the number of commutations of the modulated wave decreases with increase in operating frequency.
5. Modulator performance can be changed by changing the window width or the filter characteristic.
6. The modulator is stable, and it has a fast response to any step change

in its input.

The basic rectangular wave delta modulator is shown in fig. 3-1. With a sinusoidal input to this block, the output waveform is a modulated waveform as shown in fig. 3-2(b). The integrator in the feed-back path of this modulator is a low pass filter having an approximate transfer function of $\frac{1}{r.s}$. The output of this integrator is, therefore, a high frequency triangular wave having an average shape of a sine wave. This waveform is also known as the estimated waveform. The comparator at the front of the modulator compares the input sine wave with the estimated wave. An error signal e , is generated from the difference. The hysteresis comparator quantizes the error signal to give the modulated signal. Due to the presence of the hysteresis comparator, the error signal is bounded between $\pm \Delta V$ of the reference signal. As a result, whenever the error signal reaches any of the hysteresis boundaries the modulated signal is forced to change its polarity. This in turn changes the direction of the the excursion of carrier triangular wave. The excursion of the carrier triangular wave is also bounded above and below the input sine wave by a window $\pm \Delta V$. The various waveforms of the rectangular wave delta modulator are shown in fig. 3-2.

3.2.2 Analysis of The Rectangular Wave Delta Modulator:

The analysis of the rectangular wave delta modulator requires the knowledge of switching points of the modulated waveforms. To find the switching points of typical output waveforms of a rectangular wave delta modulator of

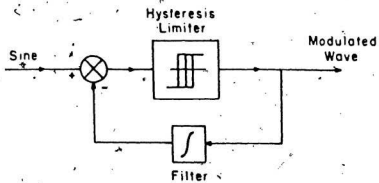


Fig. 3.1 The block diagram of a rectangular wave delta modulator.

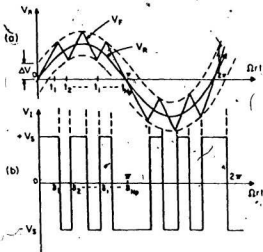


Fig. 3.2 Expected waveforms of a rectangular wave delta modulator.

- (a) The input sine wave and the estimated triangular wave.
 (b) The modulated wave.

fig. 3-2, the following basic equations are used.

Termination of the first pulse position is governed by the relationship

$$\frac{\Delta V}{S} + \frac{V_R}{S} \sin \omega_R t_1 = \omega_R t_1 \quad (3-1)$$

Where,

ΔV = half the window width as shown in fig. 3-2

S = Slope of the triangular carrier wave

t_1 = first pulse termination time

$V_R \sin \omega_R t$ = input sine reference wave

ω_R = the frequency of the input sine wave in radians/sec.

With the knowledge of the first pulse termination time, the successive switching points of the modulated wave can be obtained by numerical solution of the output equation(3-2) [121]

$$t_i = \frac{2 \Delta V + S t_{i-1}}{S} + \frac{V_R \sin \omega_R t_{i-1} - V_R \sin \omega_R t_i}{(-1)^i S} \quad (3-2)$$

In the PWM mode of operation a knowledge of the switching points of the modulated wave allows one to write the equation of the modulated wave in terms of gate function as

$$m(t) = \sum_{\Lambda=0, T, 2T, \dots}^{2T} \sum_{i=0}^{N_p} (-1)^{i+1} [g(t, \Lambda + t_i, \Lambda + t_{i+1})] \quad (3-3)$$

where,

N_p is the number of pulses in one cycle

T is the period of one cycle

$(Z-1)$ is the number of cycle of the input signal simulated

t_i is the i th pulse termination time

t_{i+1} is the $(i+1)$ th pulse position

$m(t)$ is the modulated wave

$g(t, v, w)$ is the gate function and defined as

$$g(t, v, w) = u(t-v) - u(t-w) \quad (3-4)$$

$u(t-v)$ and $u(t-w)$ are the unit step functions which are given as

$$u(t-v) = 1 \text{ for } t > v$$

$$= 0 \text{ for } t \leq v$$

(3-5)

$$u(t-w) = 1 \text{ for } t > w$$

$$= 0 \text{ for } t \leq w$$

(3-6)

The waveforms of the rectangular wave delta modulator were defined using the switching points obtained from solution of equations (3-1) to (3-6). The ordinary Fourier series technique was initially carried out. The modulated wave can be expressed in terms of Fourier series. The Fourier coefficients of modulated waveforms in terms of switching points can be written as

$$A_n = \frac{2 V_{dc}}{n \pi} \sum_{i=1,2}^{N_p} (-1)^{i+1} (\sin n \delta_i - \sin n \delta_{i-1}) \quad (3-7)$$

$$B_n = \frac{2 V_{dc}}{n \pi} \sum_{i=1,2}^{N_p} (-1)^{i+1} (\cos n \delta_{i-1} - \cos n \delta_i) \quad (3-8)$$

where,

$\delta_i = \omega_R t_i$ is the i th pulse position in radians.

V_{dc} is the dc supply voltage

n is the order of harmonics

A_n and B_n are the n th order Fourier coefficients.

For the pulse width modulated mode of operation, the fundamental voltage of the switching waveform can be obtained from equations (3-7) and (3-8) as

$$A_1 = \frac{2 V_s}{\pi} \sum_{i=1,2}^{N_p} (-1)^{i+1} (\sin \delta_i - \sin \delta_{i-1}) \quad (3-9)$$

$$B_1 = \frac{2 V_s}{\pi} \sum_{i=1,2}^{N_p} (-1)^{i+1} (\cos \delta_{i-1} - \cos \delta_i) \quad (3-10)$$

Fundamental voltage is given as

$$V_1 = \sqrt{(A_1^2 + B_1^2)} \quad (3-11)$$

The fundamental voltage variation of the modulated wave can also be obtained from the modulator's characteristics as follows:

If y and m are the estimated and the modulated waveform of rectangular wave delta modulator respectively, then for a simple integrator circuit with transfer function $\frac{1}{sr}$, the input/output relationship of the integrator is

$$\left| \frac{y_n}{m_n} \right| = \left| \frac{1}{r\omega_n} \right| \quad (3-12)$$

Where y_n and the m_n are the n th harmonics of the two waveforms and $\omega_n = 2\pi f_R n$. For fundamental of the voltage, equation (3-12) can be expressed as

$$\left| \frac{Y_1}{M_1} \right| = \left| \frac{1}{r\omega_1} \right| = \left| \frac{1}{r\omega} \right| \quad (3-13)$$

Assuming the fundamental voltage of the estimated wave to be equal to the magnitude of the input sine wave V_R , equation (3-13) can be written as

$$\left| \frac{V_R}{m_1} \right| = \left| \frac{1}{r\omega} \right| \quad (3-14)$$

$$\left| \frac{m_1}{V_R} \right| = |r\omega| \quad (3-15)$$

Since V_R remains constant, the fundamental component of voltage varies almost linearly with frequency. When the modulator operates in the square wave mode of operation, its voltage variation can be obtained from the slope overload condition.

The modulator reaches its slope overload condition when the following condition prevails:

$$r = \frac{V_R \sin 2\pi f_R \frac{T}{2} + 2\Delta_R}{\frac{T}{2}} \quad (3-16)$$

where, $\Delta_R =$ is the window width of the hysteresis limits.

Equation (3-16) can be simplified to

$$f_R = \frac{r}{4\Delta_R} \quad (3-17)$$

In the square mode of operation during the slope overload the harmonics of the modulator output waveform are given as

$$V_n = \frac{4V}{n\pi} \quad (3-18)$$

The fundamental voltage variation is given as

$$V_1 = \frac{4V_n}{\pi} \quad (3-19)$$

A typical fundamental voltage relationship of rectangular wave delta modulated waveform with variation of operating frequency is shown in fig. 3-3. Figure 3-3 shows that, for pulse width modulation mode of operation of the modulator, the fundamental voltage increases linearly with frequency, and in the square wave mode of operation the fundamental voltage remains constant over an increased range of the frequency.

The theoretical harmonic analysis is carried out using the expressions obtained in this section and the results are shown in fig. 3-4. The theoretical result shows that during low frequency operation of the modulator the significant harmonics of the output waveforms are of higher orders. As the operating frequency of the modulator is increased the lower order harmonics start appearing. Once the modulator reaches the square wave mode of operation the magnitudes of the harmonics remain constant. The study revealed that the harmonic contents of a delta modulator can be changed by variation of different parameters like the window width ΔV , the integrator time constant τ and the amplitude V_m of modulating wave.

Variation of Number of Switching in RWDM waveform:

The number of commutations in any inverter is an important feature. The increase in commutation results in increased commutation losses in the inverter. Some applications require that this loss be kept at a minimum level. The amount of switching has to be kept at a minimum for perfect commutation of the

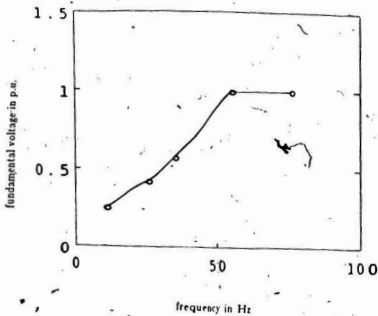


Fig. 3.3 Fundamental voltage variation of rectangular wave delta modulated waves with change in operating frequency. (p.u. value of the output voltage is the ratio of the output voltage to the fundamental voltage of a square wave of the same frequency)

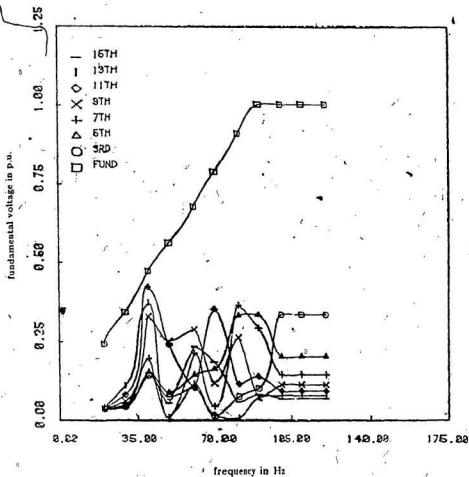


Fig. 3.4 Harmonics of rectangular wave delta modulated waveforms at various operating frequencies.

switching devices of the inverter as well. The number of pulses/half cycle of the modulator output waveform can be determined by using the analysis for determination of switching points.

The i -th pulse termination of the modulator output voltage in RWDM mode of operation is given by

$$\delta_i = \omega_R t_i \quad (3-20)$$

where t_i is the i -th pulse termination time. Solution of the equation (3-20) for δ_i at $\delta_i = \pi$, gives the number of pulses per half cycle of the modulating wave as

$$i = N_p \quad (3-21)$$

The number of switching per cycle is given as

$$N_c / \text{cycle} = 2 N_p \quad (3-22)$$

The number of commutation /sec can be obtained as

$$N_c / \text{sec} = 2 N_p f_R \quad (3-23)$$

Equations (3-20) to (3-22) are solved for different-frequencies of operations. The results are shown in fig. 3-5 for various values of modulating signal level V_R . The results show that without any other change, the number of switching of modulated wave decreases with the increase in operating frequency. This is a desired characteristic for the safe operation of inverters.

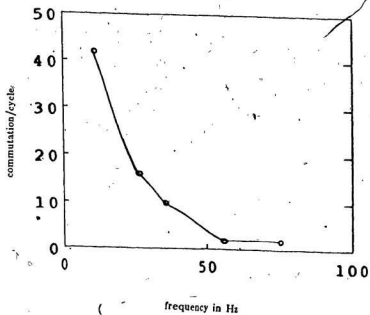


Fig. 3.5 Variation of the number of commutation of output waveforms of a rectangular wave delta modulator versus frequency.

Idling Characteristic:

The idling characteristic of RWDM is mentioned in relation to the selection criteria in section 2.4.3. The idling frequency of RWDM is given by

$$f_{idle} = \frac{r}{4 \Delta} \quad (3-24)$$

The output of the modulator during idling is a square wave. The harmonics of this idling output waveform are given by

$$V_n = \frac{4 V_s}{n \pi} \quad (3-25)$$

Since the fundamental frequency of the idling wave is very high, other harmonics which are the odd multiples of the fundamental frequency are high also. A typical spectrum of an idling waveform of the rectangular wave delta modulator is shown in fig. 3-6.

3.2.3 The Tuned Rectangular Wave Delta Modulator for Optimized Operation:

Delta modulation offers the possibility of on-line harmonic minimization of pulse width modulated inverter output without resorting to conventional optimization processes. Conventional harmonic minimization includes selective harmonic elimination and harmonic weighting techniques [122,123]. They attempt to modify the harmonic contents of the inverter output voltage in a desired fashion.

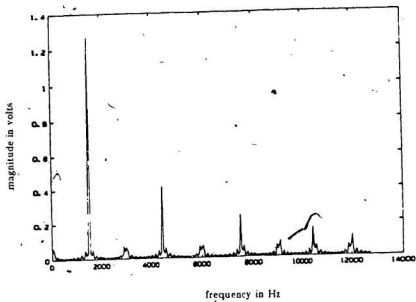


Fig. 3.6 A spectrum of the idling waveform of a rectangular wave delta modulator.

These are normally achieved by waveform synthesis methods. Harmonic minimization through waveform synthesis are computationally intensive because they require the solution of sets of transcendental equations. The preferred technique has been to determine the switching instances by off-line computation with a main-frame computer. The switching points are stored in the erasable programmable read only memory (EPROM) of a micro-computer for use during the inverter operation. For fixed frequency inverter operations this works well. However, for continuously variable frequency operation of an inverter it requires numerous look-up tables in EPROMs. These techniques of PWM inverter waveform synthesis for optimization have been identified and reported as spectral manipulation similar to the filtering process [124]. It has been shown that harmonic contents of a sine pulse width modulated inverter waveform can be altered as desired by a filter. Nonetheless, reconstruction of filtered waveforms to generate actual switching waveforms of an inverter is very involved. As an alternative, the use of digital delta filter [124] or a multi-stage delta modulator was suggested [81]. Fig.3-7. shows a double integrator rectangular wave delta modulator. The second integrator in the modulator performs additional low pass filtering to the estimated signal to reduce the magnitude of harmonics at a particular range of frequency set by the filter characteristic. However, at very high frequency operation, the double integrator modulators become unstable [101]. This instability restricts the application of double integrator delta modulator in inverter operations.

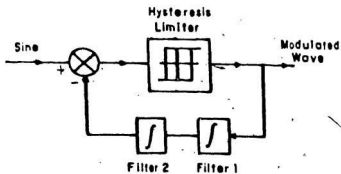


Fig. 3.7 A rectangular wave delta modulator with two integrators in the feedback path.

In this research, an easy but versatile method of improving the harmonic contents of the inverter by using a tuned delta modulator is developed [82]. This method allows the use of a single integrator in the delta modulator, yet it is used to perform the harmonic minimization in the desired fashion without limiting its performance.

Tuned Delta Modulator:

The integrator circuit generally used in the feedback path of the delta modulator is shown in fig. 3-8(a). The integrator acts as a low pass filter having a fixed cutoff frequency as determined by the following transfer function

$$\frac{e_o(s)}{e_i(s)} = \frac{k}{rs + 1} \quad (3-26)$$

where k is the gain of the filter and r is the time constant of the integrator. In the modulator, $e_o(s)$ is the output signal and $e_i(s)$ is the input signal. The filter has a fixed cutoff frequency f_c . The harmonic contents of the estimated and that of the modulated waves can be changed by varying the time constant of the integrator.

In the tuned delta modulator the fixed cut-off frequency integrator is replaced by a tuned filter as shown in fig. 3-8(b). The tuned filter is a combination of a linear analog multiplier and an integrator [125]. The tuned integrator has a transfer function as

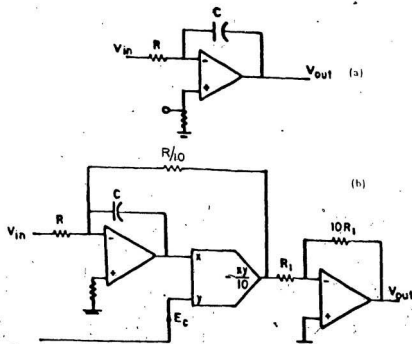


Fig. 3.8 The simple integrator and the tuned integrator circuits.

(a) The simple integrator circuit.

(b) The tuned integrator circuit.

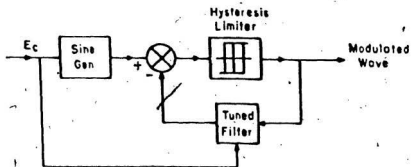


Fig. 3.9 The block diagram of a tuned rectangular wave delta modulator.

$$\frac{e_o(s)}{e_i(s)} = \frac{k}{\frac{10r}{E_c} s + 1} \quad (3-27)$$

In this filter, the input to the multiplier is a command signal E_c . Equation (3-27) shows that the incorporation of the multiplier with the integrator makes the integrator's time constant variable with E_c . This ability to change the time constant makes the cut-off frequency of the filter a variable parameter. The variation of E_c is made in such a way that, as the frequency of operation of the modulator is increased, the cut-off frequency is lowered. This, in turn, reduces the appearance of lower order harmonics from the modulator's output waveform. This criterion is selected because it has been found that in the ordinary rectangular wave delta modulator the modulated waveform approaches a square wave with the increase of operating frequency. This causes the low order harmonics to be dominant. The modified block diagram of the delta modulator with the tuned filter is shown in fig. 3-9.

The performance of a tuned delta modulator was studied theoretically and experimentally. The theoretical study was carried with the help of discrete Fourier transform (DFT).

3.3 Analysis of RWDM Using DFT and Windowed DFT:

3.3.1 Necessity of DFT Analysis of PWM Waveforms:

Previous theoretical works on pulse width modulated inverter waveform synthesis are based on the ordinary Fourier series method [126]. Spectral information of these converter waveforms is necessary for their design and performance study. Very few papers, however, dealt with computer processing of actual waveforms for validation of simulated waveforms. Also, harmonic analysis by the Fourier series does not account for the subharmonics present in the pulse width modulated waveforms. These subharmonics are inherent in all pulse width modulated waveforms because they have components of modulating waveform and the carrier waveform [126]. In the case of delta modulated waveforms, this is true as well. Most of the delta modulation schemes, being nonsynchronous process usually do not have the symmetrical properties of the Fourier series analysis. Therefore in order to study the nature of the modulated waveforms of the delta modulated inverters, an approach is taken towards the development of an efficient method of spectral analysis based on discrete Fourier transform (DFT). Emphasis is placed on the problem of spectral leakage minimization introduced by truncation of sampled waveforms. The long and short range spectral leakages are caused by non-synchronous sampling [127] and the abrupt data truncation.

The method of spectral analysis reported in this section includes the simulation of delta modulated waveforms from the switching points obtained by

solving equations (3-1) and (3-2). The waveforms are sampled and then the discrete Fourier transform is carried out on the sampled waveforms. To minimize spectral leakages in the magnitude spectra, the sampled waveforms are studied with three different window functions as well. These windows are the Hamming, the Hanning and the Blackman windows.

3.3.2 Methodology:

Discrete Fourier transform has been carried out on the sampled simulated waveforms of the rectangular and the tuned rectangular wave delta modulator. The discrete Fourier transform pair representing the continuous Fourier transform has been used in this analysis. This was done to facilitate the detection of all frequency components including the subharmonics of the modulated signal.



Discrete Fourier Transform (DFT):

The Fourier transform pair for continuous signals can be written as:

$$X(f) = \int_{-\infty}^{\infty} x(t) e^{-j2\pi ft} dt. \quad (3-28)$$

$$x(t) = \int_{-\infty}^{\infty} X(f) e^{j2\pi ft} df. \quad (3-29)$$

for $-\infty < f < \infty$ and $-\infty < t < \infty$, $j = \sqrt{-1}$.

The analogous discrete Fourier transform pair that apply to the sampled versions of these functions can be written as [85]

$$X(m) = \frac{1}{N} \sum_{n=0}^{N-1} x(n) e^{-j \frac{2\pi m n}{N}} \quad (3-30)$$

$$x(n) = \sum_{m=0}^{N-1} X(m) e^{j \frac{2\pi m n}{N}} \quad (3-31)$$

Both $X(m)$ and $x(n)$ are in complex series.

When the expression $e^{j \frac{2\pi m n}{N}}$ is replaced by the term W_N , the DFT transform pairs take the form

$$X(m) = \frac{1}{N} \sum_{k=0}^{N-1} x(k) W_N^{-m k} \quad (3-32)$$

$$x(n) = \sum_{j=0}^{N-1} X(j) W_N^{j n} \quad (3-33)$$

Equations (3-32) and (3-33) can be denoted by the transform pair as

$$X(m) = D[x(n)] \quad (3-34)$$

$$x(n) = D^{-1}[X(m)] \quad (3-35)$$

With the subscripts omitted from W_N , the equation (3-32) can be written as

$$X(0) = x(0) W^0 + x(1) W^0 + x(2) W^0 + \dots + x(N-1) W^0 \quad (3-36)$$

$$X(1) = x(0) W^0 + x(1) W^1 + x(2) W^2 + \dots + x(N-1) W^{N-1}$$

$$X(N-1) = x(0) W^0 + x(1) W^{N-1} + \dots + x(N-1) W^{N-1}$$

In matrix form, equation (3-36) can be written as

$$\begin{bmatrix} X(0) \\ X(1) \\ X(2) \\ \vdots \\ X(N-1) \end{bmatrix} = \begin{bmatrix} W^0 & W^0 & W^0 & \dots & W^0 \\ W^0 & W^1 & W^2 & \dots & W^{N-1} \\ W^0 & W^2 & W^3 & \dots & W^{2(N-1)} \\ \vdots & \vdots & \vdots & \ddots & \vdots \\ W^0 & W^{N-1} & \dots & \dots & W^{N-1} \end{bmatrix} \begin{bmatrix} x(0) \\ x(1) \\ x(2) \\ \vdots \\ x(N-1) \end{bmatrix} \quad (3-37)$$

Where $x(0), x(1), \dots, x(N-1)$ are the sample values of signal $x(t)$ at sampling instances. The evaluation of the above form of DFT can be done either by a direct method which is computationally time consuming or by various fast Fourier transform (FFT) algorithms available to evaluate DFT [128,85].

3.3.3 Discrete Fourier Transform of RWDM Waveforms:

The first step in evaluating spectral content of the modulated waveforms is

to simulate the waveforms at different frequencies of operation using the switching points obtained by solving equations (3-1) and (3-2). The waveforms thus obtained for the RWDM modulator for 10 Hz-75 Hz operation are shown in figs. 3-10(a) - 3-10(c). Similar waveforms have been obtained for the tuned rectangular wave delta modulator. Simulated waveforms at 60 Hz operation with E_c varying from 1 - 7 volts are shown in figs. 3-11(a) - 3-11(c). The magnitude spectra obtained for waveforms of figs. 3-10 and 3-11 are shown in figs. 3-12, and 3-13 respectively. The mentioned properties of the rectangular and the tuned rectangular wave delta modulators are evident from these spectra. In fig. 3-10, it is clear that the waveforms are in pulse width modulation mode at lower frequencies of operations. At higher frequencies of operations, the waveforms are square waves. In tuned rectangular wave delta modulators the same feature is available, but at higher operating frequencies the waveforms remain in modulated form due to the tuning of the filter. From the spectra of fig. 3-12 for RWDM the linear variation of fundamental voltage of the RWDM with frequency is observed. From the spectra of fig. 3-13, the improvement of the lower harmonic contents of the modulated waveform from those of fig. 3-12 is observed. Also, it is evident that the spectra obtained by this DFT technique are virtually continuous, giving all frequency components.

Usually, the spectra obtained by DFT operation on sampled waveforms are corrupted by spectral leakage [85]. Errors are introduced due to rectangular data windowing and sampling of the actual waveforms. Similar errors are encountered

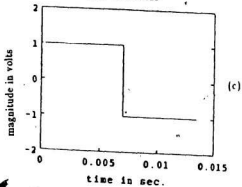
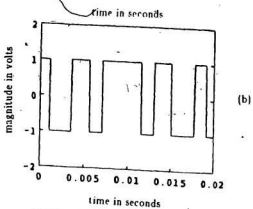
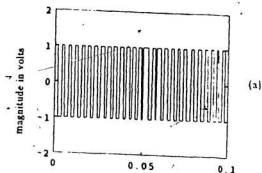


Fig. 3.10 Simulated modulated waveforms produced by a rectangular wave delta modulator for 10-75 Hz operations.
(a) The waveform of 10 Hz, (b) the waveform of 55 Hz and (c) the waveform of 75 Hz operations.

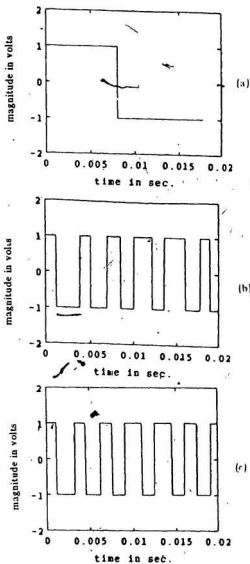


Fig. 3.11 Simulated modulated waveforms of a tuned rectangular wave delta modulator for control voltage variation of 1 to 7 volts at 60 Hz operations.

(a) The waveform at control voltage = 1 volt.
 (b) The waveform at control voltage = 4 volts.
 (c) The waveform at control voltage = 7 volts.

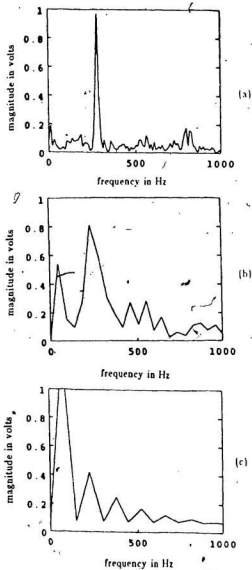


Fig. 3.12 Spectra of waveforms of figure 3.10, obtained by discrete Fourier transforms.
 (a) Spectrum of the waveform at 10 Hz operation.
 (b) Spectrum of the waveform at 55 Hz operation.
 (c) Spectrum of the waveform at 75 Hz operation.

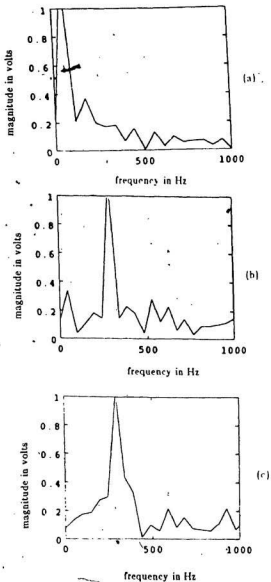


Fig. 3.13 Spectra of waveforms of figure 3.11 obtained by discrete Fourier transforms.

- (a) Spectrum of the waveform at control voltage = 1 volt.
- (b) Spectrum of the waveform at control voltage = 4 volts.
- (c) Spectrum of the waveform at control voltage = 7 volts.

in the spectra obtained for rectangular wave delta modulator waveforms analyzed in this section. The spectral leakage is explained with an illustration in section 3.3.4. The conventional method to reduce the effects of spectral leakage in DFT analysis is to window the waveforms to be analyzed with proper windows. The data windows truncate the sampled waveforms gradually at the front and the trailing end. Discrete Fourier transforms are then carried out on windowed modulated waveforms.

3.3.4 SPECTRAL LEAKAGE:

Spectral leakage is explained in fig. 3-14 by an illustration of discrete Fourier transform of a cosine waveform [85]. Fig. 3-14(a) shows that the continuous Fourier transform of a cosine wave consists of two impulses, symmetrical about zero frequency. The data window $w(t)$ through which the signal $s(t)$ is analyzed has a continuous Fourier transform of a sinc function as shown in fig. 3-14(b). When the cosine wave of fig. 3-14 (a) is windowed by the rectangular window of 3-14(b), it results in a truncated waveform which has a Fourier spectra as shown in fig. 3-14(c). Thus, the spectrum consists of two sinc functions and is corrupted by a blurred spectrum around actual spectra. When sampling is performed, the resulting frequency domain function gives rise to further error in the spectra as shown in figs. 3-14(d) - 3-14(f). The problems of leakage are associated with the variations from ideal conditions. The multiplication by the data window in the time domain is equivalent to convolution in frequency domain. Thus,

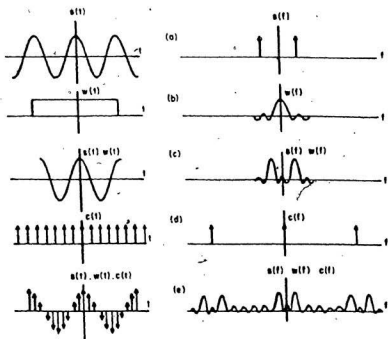


Fig. 3.14 Illustration of the spectral leakage. [85]

the result of the impulse structure of a cosine wave's frequency response when convolved with the Fourier transform of a square data window, is a function of $\frac{\sin x}{x}$ form. This sinc function is not localized on the frequency axis. In fact it has a series of spurious peaks called side lobes. The objectives of spectral analysis of windowed waveforms are to localize the contribution of given frequencies by reducing the amount of leakage through the side lobes. This consists of applying the data window to the time series of the signal to be analyzed which has lower side lobes in the frequency domain than the rectangular window.

3.3.5 Window Functions:

Windowing of sampled waveforms is analogous to the weighting of modulated waves to reduce the side lobe patterns of waveforms in order to minimize leakage through the side lobes. In this study, three windows are considered for data windowing of delta modulated waveforms. These are the Hamming, the Hanning and the Blackman windows. These three window functions are chosen for their convenient application to the sampled data. An extensive review of these and other window functions are given in reference [129]. The three windows considered in this study have the following expressions [129]:

Hamming Window:

$$w(t) = .54 - .46 \cos \frac{2\pi t}{NT} \quad (3-38)$$

Hanning Window:

$$w(t) = .5 \left(1 - \cos \frac{2\pi t}{NT} \right) \quad (3-39)$$

Blackman Window:

$$w(t) = .42 - .5 \cos \frac{2\pi t}{NT} + .08 \cos \frac{4\pi t}{NT} \quad (3-40)$$

The three windows represented by equations (3-38)-(3-40) are shown in fig. 3-15. The sharpest rising characteristic is that of Blackman window and the flattest is that of Hamming window. The Hanning window occupies a position in between. The side lobe characteristics of these three windows when used as a filter, are obtained by the discrete Fourier transforms on the sampled windows using equations (3-38) through (3-39). The side lobe characteristics of the three windows are shown in fig. 3-16. Fig. 3-16 shows that the Hamming window has a smaller main lobe with the first side lobe located at 0 db. The Hanning window has wider main lobe and the first side lobe is located at -40db. The Blackman window has almost similar main lobe as Hamming window but the first side lobe is located at -70 db. It is, therefore, expected that the DFT of the windowed sampled modulated waveforms will have order of performance as the Blackman, the Hanning and the Hamming window respectively.

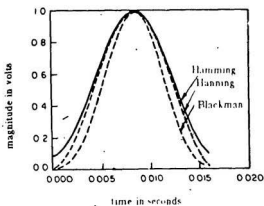


Fig. 3.15 Three windows, the Hamming window, the Hanning window, and the Blackman window.

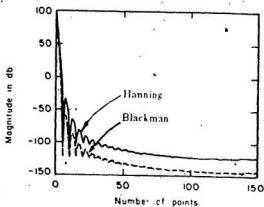
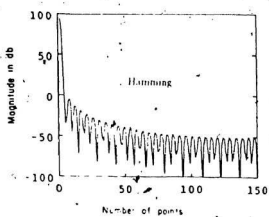


Fig. 3.16 Side-lobe characteristics of three windows.
 (a) Side-lobe characteristic of the Hamming window.
 (b) Side-lobe characteristics of the Hanning and the Blackman windows.

3.3.6 DFT of Windowed RWDM Waveforms:

To perform the discrete Fourier transform on windowed modulated waveforms, the waveforms obtained as described in section 3.3.3 and shown in figs. 3-10 and 3-11 were sampled. The sampled waveforms were windowed by sampled version of the Hamming, the Hanning and the Blackman windows. The sampled windows are expressed as:

Hamming:

$$w(n) = .54 - .46 \cos \frac{2\pi n}{N-1} \quad (3-41)$$

for $0 < n < N-1$

Hanning:

$$w(n) = .5 \left(1 - \cos \left(\frac{2\pi n}{N-1} \right) \right) \quad (3-42)$$

for $0 < n < N-1$

Blackman :

$$w(n) = .42 - .5 \cos \frac{2\pi n}{N-1} + .08 \cos \frac{4\pi n}{N-1} \quad (3-43)$$

for $0 < n < N-1$

The windowed rectangular wave delta modulated waveforms of figs. 3-10

and 3-11 are shown in figs. 3-17 through 3-19. The windowed waveforms of the tuned modulator with a control voltage range of 1 - 7 volts are shown in figs. 3-20 to 3-22. The typical spectra for windowed modulated waveforms obtained by discrete Fourier transforms are shown in figs. 3-23 to 3-25. Typical spectra for windowed waveforms of a tuned modulator are shown in figs. 3-26 to 3-28. The results of these windowed harmonic analysis show that the spectra obtained by this method have less leakage compared to those obtained for rectangular windowing of the waveforms.

3.4 Summary of Analytical Results:

The fundamental voltage variation obtained by spectral analysis shows the following trend:

1. For ordinary RWDM waveforms, the fundamental voltage increases linearly with the frequency. The linearity remains in the modulated mode of operation. Beyond the base frequency, the modulator goes into the square wave mode of operation and remains there for higher operating frequencies. The fundamental component of this square wave is constant and is given by $\frac{4V}{\pi}$ (fig. 3-29).
2. In the tuned modulator the fundamental voltage variation is linear with frequency. However, the rate of linear variation is less in the tuned modulator than the variation obtained for ordinary modulator. Tuning of the modulator causes the fundamental component of the voltage to increase at a slower

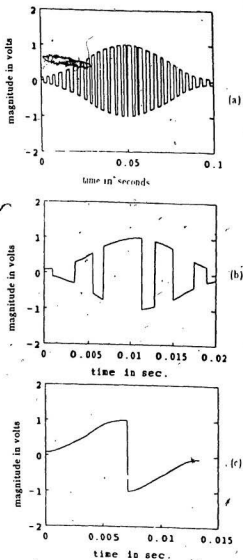


Fig. 3.17 Hamming windowed waveforms of a rectangular wave delta modulator at 10-75 Hz operations.

(a) Hamming windowed waveform at 10 Hz operation.

(b) Hamming windowed waveform at 55 Hz operation.

(c) Hamming windowed waveform at 75 Hz operation.

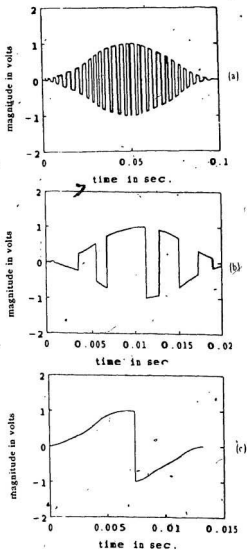


Fig. 3.18 Hanning windowed waveforms of a rectangular wave delta modulator at 10-75 Hz operations.

(a) Hanning windowed waveform at 10 Hz operation.

(b) Hanning windowed waveform at 55 Hz operation.

(c) Hanning windowed waveform at 75 Hz operation.

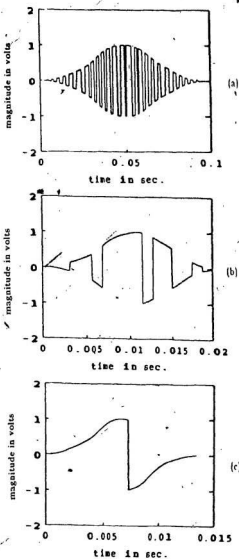


Fig. 3.19 Blackman windowed waveforms of a rectangular wave delta modulator at 10-75 Hz operations.

- (a) Blackman windowed waveform at 10 Hz operation.
- (b) Blackman windowed waveform at 55 Hz operation.
- (c) Blackman windowed waveform at 75 Hz operation.

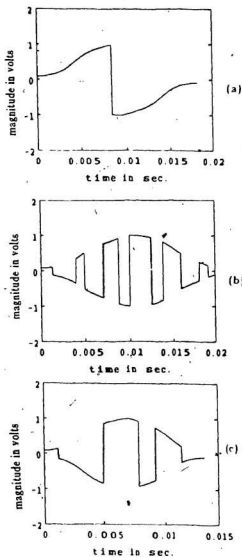


Fig. 3.20 Hamming windowed waveforms of the tuned rectangular wave delta modulator at 60 Hz operation for control voltage variation of 1 to 7 volts.

- (a) Hamming windowed waveform, control voltage = 1 volt.
- (b) Hamming windowed waveform, control voltage = 4 volts.
- (c) Hamming windowed waveform, control voltage = 7 volts.

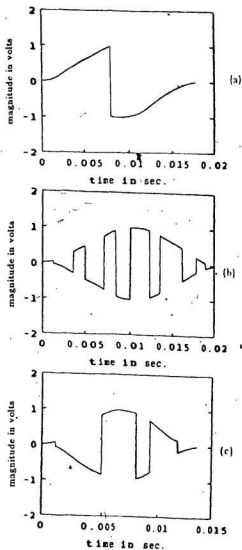


Fig. 3.21 Hanning windowed waveforms of the tuned rectangular wave delta modulator at 60 Hz operation for control voltage variation of 1 to 7 volts.

- (a) Hanning windowed waveform, control voltage = 1 volt.
- (b) Hanning windowed waveform, control voltage = 4 volts.
- (c) Hanning windowed waveform, control voltage = 7 volts.

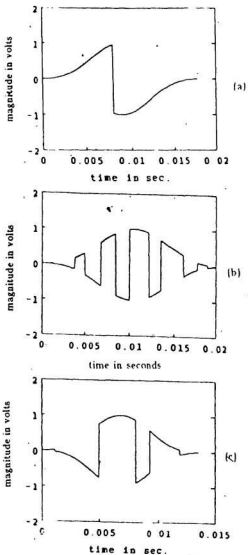


Fig. 3.22 Blackman windowed waveforms of the tuned rectangular wave delta modulator at 60 Hz. operation for control voltage variation of 1 to 7 volts.

- (a) Blackman windowed waveform, control voltage= 1 volt.
- (b) Blackman windowed waveform, control voltage= 4 volts.
- (c) Blackman windowed waveform, control voltage= 7 volts.

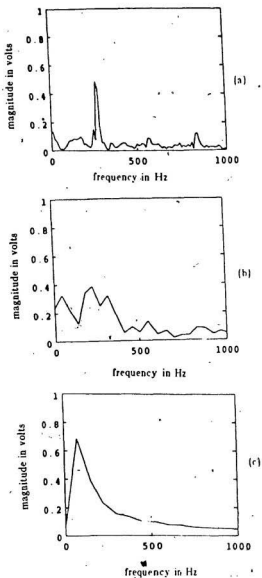


Fig. 3.23 Spectra of Hamming windowed waveforms of rectangular wave delta modulator for 10-75 Hz operation.

- (a) Spectrum of Hamming windowed waveform at 10 Hz operation.
 (b) Spectrum of Hamming windowed waveform at 55 Hz operation.
 (c) Spectrum of Hamming windowed waveform at 75 Hz operation.

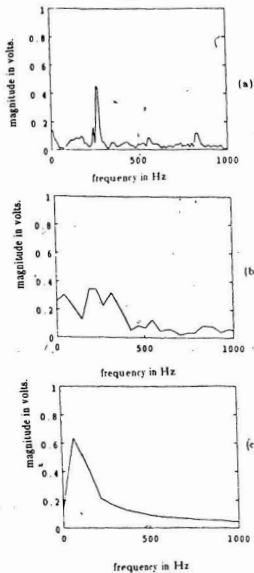


Fig. 3.24 Spectra of Hanning windowed waveforms of rectangular wave delta modulator for 10-75 Hz operation.
 (a) Spectrum of Hanning windowed waveform at 10 Hz operation.
 (b) Spectrum of Hanning windowed waveform at 55 Hz operation.
 (c) Spectrum of Hanning windowed waveform at 75 Hz operation.

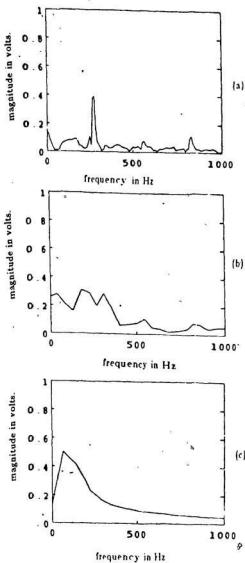


Fig. 3.25 Spectra of Blackman windowed waveforms of rectangular wave delta modulator for 10-75 Hz operation.

(a) Spectrum of Blackman windowed waveform at 10 Hz operation.
 (b) Spectrum of Blackman windowed waveform at 55 Hz operation.
 (c) Spectrum of Blackman windowed waveform at 75 Hz operation.

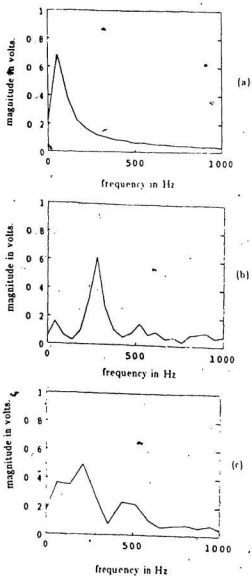


Fig. 3.26 Spectra of Hamming windowed waveforms of the tuned rectangular wave delta modulator at 60 Hz operation with control voltage variation of 1-7 volts.

- (a) Spectrum of Hamming windowed waveform, control voltage=1 volt.
- (b) Spectrum of Hamming windowed waveform, control voltage=4 volts.
- (c) Spectrum of Hamming windowed waveform, control voltage=7 volts.

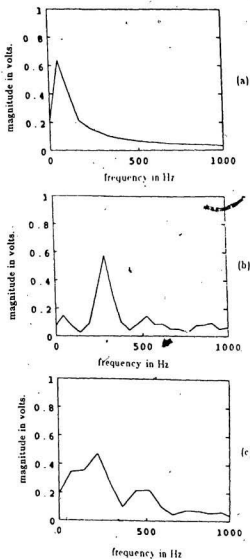


Fig. 3.27 Spectra of Hanning windowed waveforms of the tuned rectangular wave delta modulator at 60 Hz operation with control voltage variation of 1-7 volts.

- (a) Spectrum of Hanning windowed waveform, control voltage = 1 volt.
 (b) Spectrum of Hanning windowed waveform, control voltage = 4 volts.
 (c) Spectrum of Hanning windowed waveform, control voltage = 7 volts.

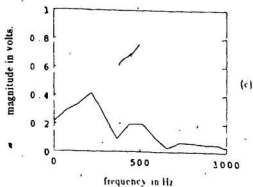
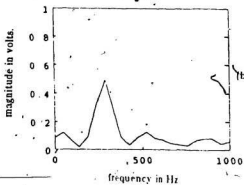
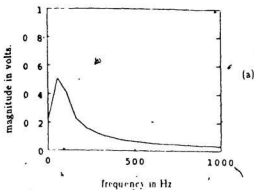


Fig. 3.28 Spectra of Blackman windowed waveforms of the tuned rectangular wave delta modulator at 60 Hz operation with control voltage variation of 1-7 volts.

- (a) Spectrum of Blackman windowed waveform, control voltage=1 volt.
 (b) Spectrum of Blackman windowed waveform, control voltage=4 volts.
 (c) Spectrum of Blackman windowed waveform, control voltage=7 volts.

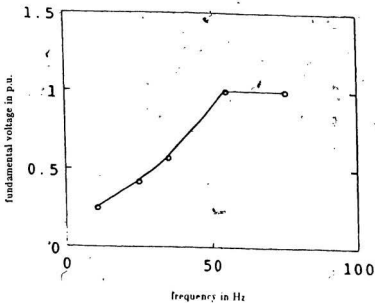


Fig. 3.29 Fundamental voltage variation of the rectangular wave delta modulated waveforms with frequency.

rate. The control voltage E_c moves the base frequency to a higher value.

These trends are shown in figs. 3-30 and 3-31.

3. The switching number of a rectangular wave delta modulated waveform decreases with the increase in the operating frequency of the modulator as shown in fig. 3-32.
4. With constant control voltage E_c (fig. 3-33), the number of switching of a tuned modulator waveform decreases with the increase of operating frequency. It was observed that the simultaneous increase in frequency and the control voltage keep the number of switching points nearly constant. As a result, for a longer range of frequency of operation the tuned modulator's output waveform remains in the pulse width modulation mode.

The spectral analysis of rectangular wave delta modulated waveforms are summarized in table 3-1. The results of the analysis of the tuned modulator waveforms are summarized in table 3-2. The comparison of the results of two tables shows significant improvement of lower order harmonic contents in tuned RWDM waveforms over those of ordinary RWDM waveforms.

3.5 Practical Modulator Circuits:

The block representation of RWDM shown in fig. 3-1 was realized in a practical circuit. The integrator of the rectangular wave delta modulator was replaced by a tuned integrator to realize the tuned modulator.

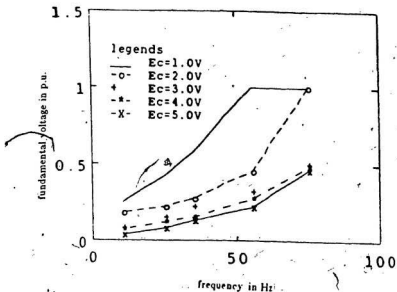


Fig. 3.30 Fundamental voltage variation of the tuned rectangular delta modulated waves with change in frequency.

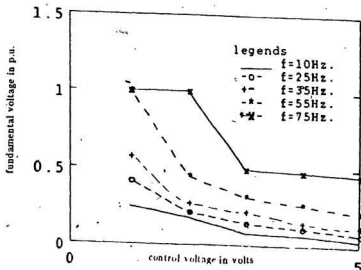


Fig. 3.31 Fundamental voltage variation of the tuned rectangular wave delta modulated wave with variation of control voltage.

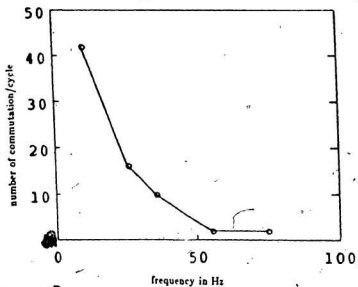


Fig. 3.32 Variation of number of commutation of rectangular wave delta modulated waveforms with change in operating frequency.

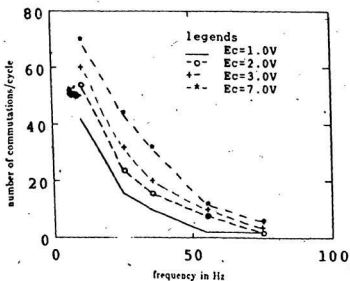


Fig. 3.33 Variation of number of commutations of the tuned rectangular wave delta modulated waveforms with change in operating frequency.

Table 3-1

Table of Harmonics
of RWDM

(Harmonics are in p.u. value, which is the ratio of actual magnitude of the harmonic to the magnitude of fundamental of the square wave)

order of harmonics	1	2	3	4	5	6	7	8	9	10
frequency in Hz.	pu	pu	pu	pu	pu	pu	pu	pu	pu	pu
10	.16									
25	.20				.15					.55
35	.27			.04			.90		.59	.15
55	.45		.05	.25	.66		.16	.16	.25	
75	1.00	.08	.87		.15	.25	.166	.15	.15	
order of Harmonics	11	12	13	14	15	16	17	18	19	20
freq. in Hz.	pu	pu	pu	pu	pu	pu	pu	pu	pu	pu
10		.08								
25	.75	.3		.15					.25	
35	.11				.25	.3				

Table 3-2
Table of Harmonics
of Tuned RWDM

(Harmonics are in p.u. value, which are
the ratio of actual magnitude of the
Harmonic to the magnitude of fundamental
of the square wave)

order of Harmonics	1	2	3	4	5	6	7	8	9	10
Ec in volts	pu									
2	1.00	.166	.316	.20	.166	.166	.066	.15		.125
4	.31	.04	.125	1.00		.12	.15	.04	.04	.166
5	.25		.125	.125	.125	.91	.16	.12		.10
6	.25	.125	.125	.91	.16	.166	.08	.08	.166	.08
7	.08	.08	.15	.15	.166	.166	.20	.833	.383	.25
order of harmonics	11	12	13	14	15	16	17	18	19	20
Ec in volts	pu									
2	.04	.04	.15	.125	.25					
4	.15	.04	.125	.15	.183					
5	.066	.04	.04	.15	.166					
6	.066	.04	.04	.15	.08					
7		.04	.008	.166	.09					

3.5.1 The Rectangular Wave Delta Modulator:

The analog circuit implementation of a RWDM is shown in fig. 3-34. The operation of the circuit can be described as follows: Sine reference or modulating wave $V_R \sin \omega_R t$ is applied to the input of the comparator A_1 . Whenever the output voltage of A_2 exceeds the upper or lower boundary (preset by $\frac{R_2}{R_3}$), the comparator A_1 reverses the polarity of modulated wave V_1 at the input of A_2 . This reverses the slope of V_F at the output of A_2 . It forces carrier wave V_F to oscillate around the reference waveform $V_R \sin \omega_R t$ at ripple frequency ω_r . Once the switching waveform is obtained, the signals for switching inverter can be generated by proper logic circuit design. Some basic waveforms of the circuit are shown in fig. 3-35.

In the circuit, the window width ΔV is determined by the circuit constants and the logic power supply. Dependence of ΔV on parameters like R_2 , R_3 and V_S is given by the following expression

$$\Delta V = \frac{R_2}{R_3} V_S \quad (3-44)$$

The slope of the carrier waveform is determined by the time constant of the integrator of the modulator. Since A_2 acts as a low pass filter, the actual output of the filter has the following relationship

$$V_{Fa} = \frac{V_{1a}}{n (R_1 C) \omega_R} \quad (3-45)$$

where,

V_{F_n} is the n th order harmonic of the carrier,

V_{I_n} is the n th order harmonic of the modulated wave,

ω_R is the frequency of the input sine wave,

$V_{F1} = V_R$ is the rms voltage of the input sine wave.

From the circuit analysis perspective, the fundamental voltage variation of rectangular wave delta modulator with frequency is given by



$$V_R = V_{F1} = \frac{V_{I1}}{(R_1 C)\omega_R} \quad (3-46)$$

or

$$\frac{V_{I1}}{\omega_R} = (R_1 C) V_R \quad (3-47)$$

Since the amplitude of V_R is maintained constant, the ratio $\left(\frac{V_{I1}}{\omega_R} \right)$ remains constant. Therefore, it is evident from the circuit analysis that the fundamental voltage variation follows the linear trend with increase in frequency.

3.5.2 The Tuned RWDM:

The practical modulator circuit described in the section 3.5.1 is modified according to the requirements for a tuned modulator. The ordinary integrator of the circuit of fig. 3-34 is replaced by a tuned integrator as shown in fig. 3-8 (b). When the tuned integrator is incorporated, the modified circuit takes the form shown in fig. 3-36. The principle of operation of this circuit is the same as described in, subsection 3.5.1. The only exception from the circuit described before is that the time constant of the integrator used in the tuned delta modulator can be controlled by an external control signal. This feature allows adjustment of the filter to a certain cut-off frequency to limit the harmonic contents of the output waveforms.

3.6 Experimental Results:

The harmonic contents of the rectangular wave delta modulator and the tuned modulator were studied using a spectrum analyzer. The results obtained theoretically were thus verified. The analyzer used in the experiments had the provision for Hanning windowing of the waveforms prior to the discrete Fourier transform. The waveforms of the experimental RWDM circuit (fig.3-34) are shown in fig.3-37 for a frequency range of 10 Hz to 75 Hz. It is evident that with the increase in frequency, the modulated waveform gradually goes through a transition from PWM mode to square wave mode. In the case of ordinary RWDM circuit the waveforms indicate that this transition takes place at 75 Hz. The

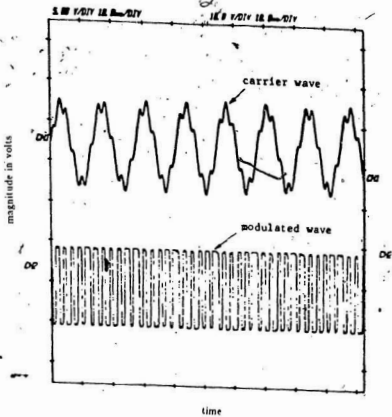


Fig. 3.35 Typical waveforms of the practical rectangular wave delta modulator.

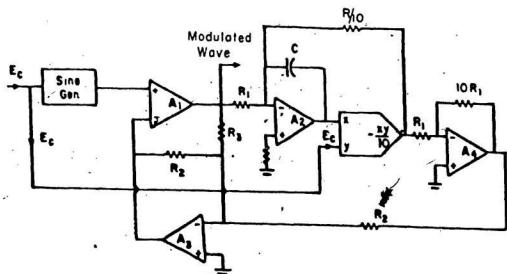


Fig. 3.36 The tuned rectangular wave delta modulator circuit.

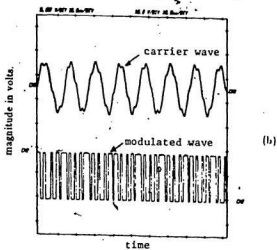
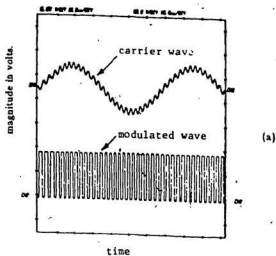


Fig. 3.37 Waveforms of the rectangular wave delta modulator circuit for 10-75 Hz operations. (continued)

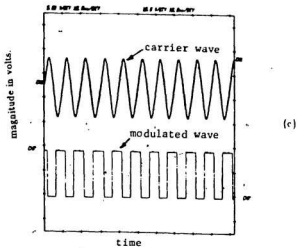


Fig. 3.37 Waveforms of the rectangular wave delta modulator circuit for 10-75 Hz operations.
(a) Waveforms at 10 Hz operation.
(b) Waveforms at 55 Hz operation.
(c) Waveforms at 75 Hz operation.

transition frequency can, however, be changed by varying the modulator's parameters. During the change of operating frequency it is apparent that the number of switching points also decrease with increased frequency.

Experimental waveforms of tuned RWDM are shown in fig. 3-38 for the 60 Hz operation with control voltage variation from 1 to 7 volts. It is evident that the carrier triangular wave's slope varies with control signal E_c . The number of commutation of tuned RWDM varies with a change in frequency of the reference wave. However, the variation is at a slower rate than that observed in the ordinary modulator waveforms.

The experimental waveforms were analyzed by a spectrum analyzer and the results for the regular and tuned rectangular wave delta modulator are shown in figs. 3-39 and 3-40 respectively. In fig. 3-39, the linear variation of the fundamental voltage of the modulator output is obvious. At 10 Hz the fundamental power component detected was 8.3 db. At 75 Hz the fundamental component of the power was 20 db. The fundamental power component remained constant for modulator operation beyond 75 Hz. The fundamental components of the modulator obtained from these experiments are shown in fig. 3-41. Fig. 3-41 shows that the voltage increases with the increase in frequency and remains constant beyond the base frequency of the modulator. Spectra for the tuned modulator waveform at 60 Hz with control voltage variation of 1 to 7 volts are shown in figs. 3-40. From fig. 3-40, the fundamental power component of the modulator wave is found to be 15.8 db with dominant harmonic frequencies at 240, 300, 330, 360,

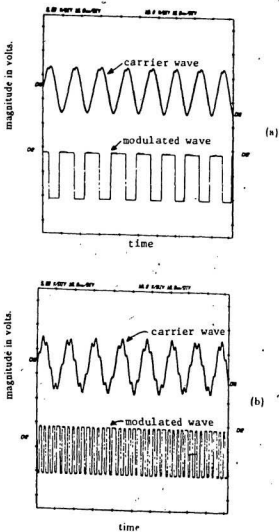


Fig. 3.38 Waveforms of the practical tuned rectangular wave delta modulator at 60 Hz operation for control voltage variation of 1-7 volts. (continued)

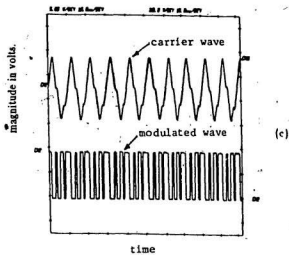
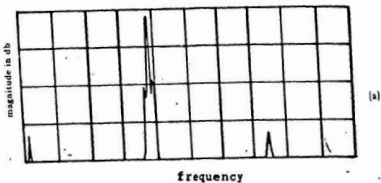


Fig. 3.38 Waveforms of the practical tuned rectangular wave delta modulator at 60 Hz operation for control voltage variation of 1-7 volts.

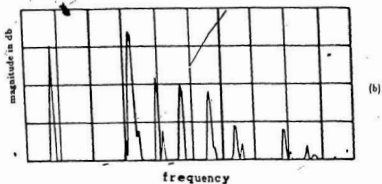
(a) Waveforms for control voltage = 1 volt.

(b) Waveforms for control voltage = 4 volts.

(c) Waveforms for control voltage = 7 volts.



PWR SPECT B : 2.048V No PEAK P: 5Hz
 SPAN: 0.000Hz -1.000000Hz SW: 20.0Hz FS: 20.000Hz 5dB/



PWR SPECT B : 13.948V No PEAK P: 5Hz
 SPAN: 0.000Hz -1.000000Hz SW: 20.0Hz FS: 20.000Hz 5dB/

Fig. 3.30 Spectra of modulated waveforms of rectangular wave
 delta modulator for 10 - 75 Hz operations. (continued)

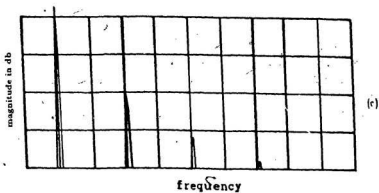
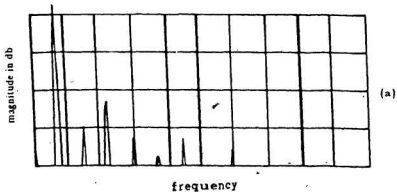
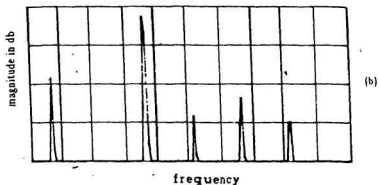


Fig. 3.39 Spectra of modulated waveforms of rectangular wave delta modulator for 10 - 75 Hz. operations.

- (a) Spectrum of modulated wave at 10 Hz operation.
- (b) Spectrum of modulated wave at 55 Hz operation.
- (c) Spectrum of modulated wave at 75 Hz operation.



PKR SPECT B : 20.14BV N: NONE P: 5HZ
 SPAN: 0.00072 -1.00007HZ SW: 20.14BV FS: 20.001BV 5dB/



PKR SPECT B : 0.64B N: NONE P: 5HZ
 SPAN: 0.00072 -1.00007HZ SW: 20.14B FS: 20.001B 5dB/

Fig. 3.10 Spectra of modulated waveforms of the tuned rectangular wave
 delta modulator at 60 Hz operation for control voltage
 variation of 1 - 7 volts. (continued)

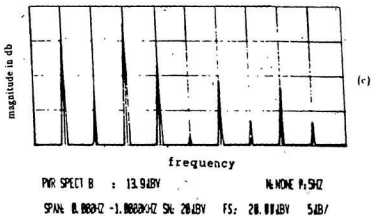


Fig. 3.40 Spectra of modulated waveforms of the tuned rectangular wave delta modulator at 60 Hz operation for control voltage variation of 1 - 7 volts.

- (a) Spectrum of modulated wave for control voltage = 1 volt.
- (b) Spectrum of modulated wave for control voltage = 4 volts
- (c) Spectrum of modulated wave for control voltage = 7 volts

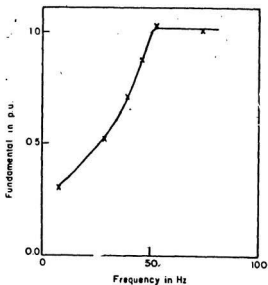


Fig. 3.41 Experimental fundamental voltage variation of rectangular wave delta modulated waves with change in operating frequency.

420, 520, 540 Hz and above. As the control voltage E_c was increased to 4 volts, the harmonic frequency components below 420 Hz were eliminated. The most dominant harmonics at $E_c = 4$ volt appear at 420 and 780 Hz. All other harmonics were reduced to negligible values. Increase in E_c at 60 Hz beyond 4 volts had little effect on the harmonic reduction as shown in the illustrations. The other factor observed during these harmonic reductions was that the fundamental voltage components reduced as the control voltage was increased. The fundamental voltage variations of the tuned modulator, with constant frequency operation at various control voltage and with constant control voltage operation at variable frequency, are shown in figs. 3-42 and 3-43 respectively.

The variation of the commutation number with the change in operating frequency for ordinary RWDM is shown in figs. 3-44. The variation was found to be as predicted. With an increased frequency in the operation of the modulator the number of commutation/cycle decreased and remained constant after the modulator reached its square wave mode. In the tuned modulator the number of commutations increased with the increase in the control voltage E_c . At a constant E_c , the pattern was the same as that of the ordinary modulator.

The experimental results of the harmonic analysis of the rectangular wave delta modulator and tuned rectangular wave delta modulator are summarized in table 3-3.

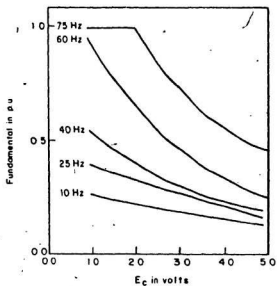


Fig 3.42 Experimental fundamental voltage variation of the tuned rectangular wave delta modulated waves for various control voltage.

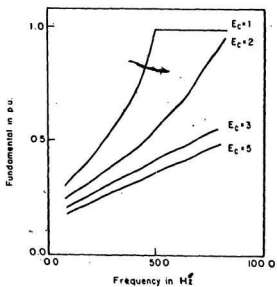


Fig 3.43 Experimental fundamental voltage variation of tuned rectangular wave delta modulated waves for various operating frequencies.

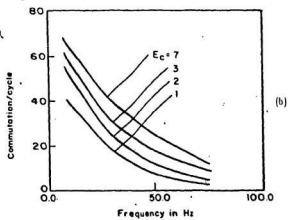
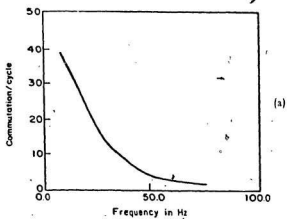


Fig. 3.44 Experimental variation of number of commutations of rectangular wave delta modulated waves.

(a) rectangular wave delta modulator.

(b) tuned rectangular wave delta modulator.

Table 3-3

Table of Harmonics
of RWDM
(Harmonics are in p.u. value, which is the
ratio of actual magnitude of the harmonic
to the magnitude of fundamental of the
square wave)

Experimental Results

order of harmonics	1	2	3	4	5	6	7
frequency in Hz.	pu						
10							
15	.216						
25	.257						
35	.331						.105
45	.394			.06	.08	.442	.313
55	.50				.372	.11	.148
65	.833	.221	.176	.186		.118	
75	.883	.148	.209	.125	.09	.125	
85	.883	.11	.263	.104	.125	.095	
100	.88	.105	.234	.09	.118	.09	

Table 3-3
(continued)

Table of Harmonics
of Tuned RWDM
(Harmonics are in p.u. value, which are
the ratio of actual magnitude of the
Harmonic to the magnitude of fundamental
of the square wave)

Experimental Results.

order of Harmonics	1	2	3	4	5	6	7	8	9	10
Ec in volts	pu	pu	pu	pu	pu	pu	pu	pu	pu	pu
1	.5				.37	.11	.15		.18	
2	.313				.09	.66	.19	.18		.124
3	.167							.118		
4	.139									
5	.12						.093	.788	.122	
6	.102						.09	.78	.105	
7	.095						.105	.742	.14	

order of harmonics	11	12	13	14	15	16	17	18	19	20
Ec in volts	pu	pu	pu	pu	pu	pu	pu	pu	pu	pu
1										
2	.248	.248	.09	.109						
3				.176						
4				.156	.095					
5				.124						
6										
7					.09					

3.7 Limitations:

Delta modulators when used in inverter applications, have three basic limitations. These limitations are:

1. Voltage limitations,
2. Commutation limitations, and
3. Synchronization limitation

In the pulse width modulation mode of the modulator output the fundamental voltage variation has shown linear dependency with the frequency. The voltage availabilities at lower frequencies are about 15-25 percent higher than those available from conventional sine PWM techniques. However, as the harmonic reduction technique is used in the tuned RWDM, this voltage availability is reduced. This reduction in the available voltage imposes limits on the harmonic reduction beyond a certain extent. Proper operation of the inverter switches and reduction in commutation losses require that the commutation number of the modulated waveform be limited. In the tuned modulator, the number of commutation increases with the increase of control voltage E_c . The modulator tune-up is, therefore, limited by the permissible number of switching of the inverter switches. The third limitation of the delta modulation arises from the free running characteristics of the modulators. The modulators in the delta modulation technique track the input reference signal continuously and the estimation process runs into successive cycles of the reference signal. As a result, the output waveform of ordinary RWDM is not symmetrical. In the inverter operation,

especially for three phase inverter operation, such non-symmetrical operation of the modulator would result in a dc level at the output of the inverter. This is not desirable. To make the modulated waves symmetrical in each half-cycle of the reference signal, in the practical implementations the modulator is forced to start the estimation process at the beginning of each half cycle of the reference signal. This has been achieved in the practical modulator circuit of fig. 3-34 by setting the capacitor voltage to zero at the instant of the beginning of each half cycle of the reference sine wave.

3.8 Conclusions:

A novel method of on-line inverter output waveform optimization using tuned rectangular wave delta modulator circuit has been described. This method eliminates the necessity of pre-programmed waveform synthesis and use of micro-computers for optimized waveform generation. The waveforms of ordinary RWDM and tuned RWDM have been analyzed using discrete Fourier transform and windowed discrete Fourier transform. The conventional time-frequency domain analysis of modulated waveforms was found unsuitable for on-line computations. It also fails to detect the non-integer harmonics present in the modulated wave. Discrete Fourier transform was found to be a better approach in this respect. Discrete Fourier transform was carried out on the windowed sampled waves to overcome the limitations of spectral leakages encountered in an ordinary discrete Fourier series analysis.

Chapter-4

Analysis of Submersible Motor Fed From Three Phase RWDM Inverter

4.1 Introduction :

In this chapter the synthesis of three phase RWDM inverter waveforms is outlined. Two different types of switching are analyzed. The type-A switching is one in which the switches of the inverter may be turned ON and OFF in each successive pulse of the modulated wave. In type-B switching each inverter switch is turned ON and OFF during one half-cycle by the switching pulses. Depending on the type of switching the inverter output waveforms are of different nature. These waveforms are analyzed to find their fundamental voltage availability and the harmonics of the output voltages. The waveforms are defined using switching points of the modulated waves generated by delta modulators. The harmonic analysis of inverter waveforms is done by the discrete Fourier transform on sampled waves. The analytical study proves that the type-B switching performs better than the type-A switching in the operation of three phase inverters. Therefore, the implementation part involves only the type-B switched inverter. The results of the three phase inverter waveform synthesis are used with the motor d-q axis model to find the steady state and the start up response of the submersible motor. The analytical results obtained are substantiated by experimental results. For experimental purposes a tuned rectangular wave delta modulated transistorized inverter was designed and built. The inverter was tested for the

steady state and the start up operations of the submersible motor.

4.2 Synthesis of Three Phase Rectangular Wave Delta Modulated Inverter Waveforms :

In single phase bridge inverters the inverter switches can be operated in two different schemes. In the first scheme (type-A), the inverter switching devices can be turned ON and OFF by the successive positive and negative pulses of the modulated wave to obtain the inverter output as shown in fig. 4-1. In the second scheme the inverter switches are operated in such a manner (type - B) that the output waveform appears like a modulated square wave as shown in fig. 4-2. Both the switching schemes are common in a single phase inverter operation. The type-A switching of three phase inverters allows the inverter to have very low harmonic contents but with low fundamental voltage availability. Whereas type-B switching allows greater fundamental voltage availability. Type-B switched inverter output voltages have dominant low frequency harmonics higher than those of type-A switched inverter.

In type-A scheme, the switching waveform of the inverter is the same as the modulated waveform obtained from the modulator. It has been shown that this switching waveform can be represented by following expressions:

For one cycle

$$m_T(t) = \sum_{i=0,1}^{N_s} (-1)^{i+1} [g(t, t_i, t_{i+1})] \quad (4-1)$$

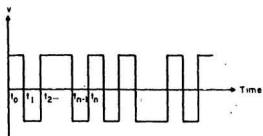


Fig. 4.1 The single phase bridge inverter output.
(type-A switching)

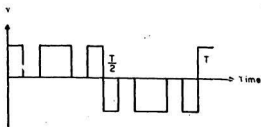


Fig. 4.2 The single phase bridge inverter output.
(type-B switching)

For multiple cycle

$$m(t) = \sum_{A=0, T, 2T, \dots}^{2T} \sum_{i=0, 1, \dots}^{N_p} (-1)^{i+1} \left[g(t, A+t_i, A+t_{i+1}) \right] \quad (4-2)$$

In type-B scheme, however, the switching waveform is the processed modulator output waveform and appears like the waveform shown in fig. 4-3(b). This switching waveform of fig. 4-3(b) can be represented by the following expressions as obtained from the illustration of fig. 4-4:

For one cycle

$$m_T(t) = \sum_{i=0, 1, \dots}^{N_p} \left[g(t, t_{2i}, t_{2i+1}) - g\left(t, t_{2i} + \frac{T}{2}, t_{2i+1} + \frac{T}{2}\right) \right] \quad (4-3)$$

For multiple cycle

$$m(t) = \sum_{A=0, T, 2T}^{2T} \sum_{i=0, 1, \dots}^{N_p} \left[g(t, t_{2i} + A, t_{2i+1} + A) - g\left(t, t_{2i} + \frac{T}{2} + A, t_{2i+1} + \frac{T}{2} + A\right) \right] \quad (4-4)$$

Knowing the representation of switching waveforms of both the schemes and by proper phase staggering (120° , -120° , etc.) and addition of scaled waves, the inverter output voltages can be obtained. The method for obtaining inverter output voltages is illustrated in fig. 4-5 for the square wave mode operation of the modulator. In fig. 4-5, the line to line voltages of three phase inverter are obtained by the addition of scaled modulator waves with the phase shifted scaled modulated wave. For obtaining three phase PWM inverter waveforms, the

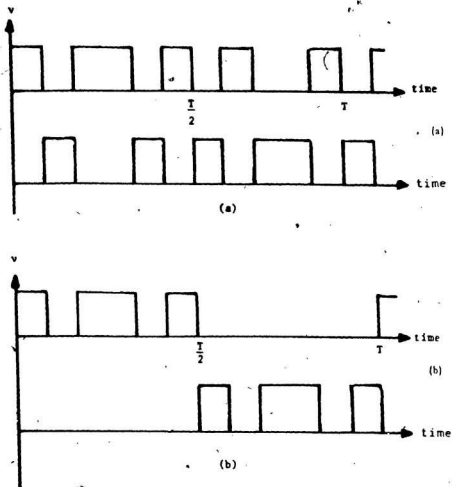


Fig. 4.3 Switching waveforms of the three phase inverter.
 (a) Switching waveforms, type-A.
 (b) Switching waveforms, type-B.

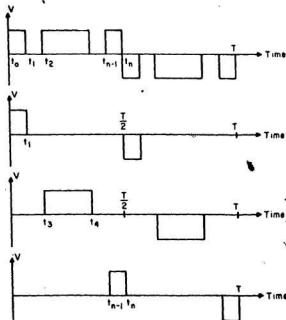


Fig. 4.4 The construction of type-B switching waveforms by gate functions.

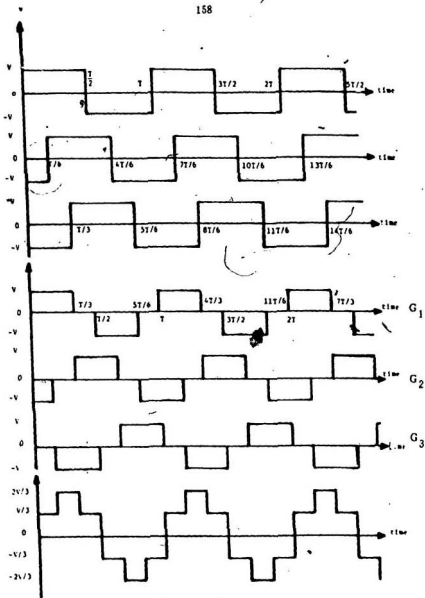


Fig. 4.5 The illustration of defining the three phase inverter output from the switching waveforms.

resultant waves are gated by the line to line voltage waveform of unity magnitude, and then the modulated pulses are shaped to $+V$ or $-V$. This is necessary because inverter line voltages cannot be more than V in either direction. The analytical expressions for the line to line voltages in terms of switching waveforms of type-A and type-B are obtained as

$$V_{ab} = \frac{1}{2}V_{dc} \left[m(t) + m\left(t + \frac{T}{6}\right) \right] u(t) G_1 \quad (4-5)$$

$$V_{bc} = \frac{1}{2}V_{dc} \left[m\left(t - \frac{T}{6}\right) + m\left(t - \frac{T}{3}\right) \right] u(t) G_2 \quad (4-6)$$

$$V_{ca} = \frac{1}{2}V_{dc} \left[m\left(t - \frac{T}{2}\right) + m\left(t + \frac{T}{3}\right) \right] u(t) G_3 \quad (4-7)$$

Since,

$$m\left(t - \frac{T}{2}\right) = -m(t) \quad (4-8)$$

$$m\left(t - \frac{T}{3}\right) = -m\left(t + \frac{T}{6}\right) \text{ and} \quad (4-9)$$

$$m\left(t + \frac{T}{3}\right) = -m\left(t - \frac{T}{6}\right) \quad (4-10)$$

Equations (4-5) to (4-7) can be re-written as:

$$V_{ab} = \frac{1}{2}V_{dc} \left[m(t) + m\left(t + \frac{T}{6}\right) \right] u(t) G_1 \quad (4-11)$$

$$V_{bc} = \frac{1}{2} V_{dc} \left[m \left(t - \frac{T}{6} \right) - m \left(t + \frac{T}{6} \right) \right] u(t) G_2 \quad (4-12)$$

$$V_{ca} = \frac{1}{2} V_{dc} \left[-m(t) - m \left(t - \frac{T}{6} \right) \right] u(t) G_2 \quad (4-13)$$

In equations (4-5) to (4-13), G_1 , G_2 , and G_3 are line-to-line voltage waveforms of unity magnitude in the square mode of operation. The line-to-neutral voltages of the inverter are given by the following expressions

$$V_{aa} = \frac{1}{3} (V_{ca} - V_{ab}) \quad (4-14)$$

$$V_{ba} = \frac{1}{3} (V_{ab} - V_{bc}) \quad (4-15)$$

$$V_{ca} = \frac{1}{3} (V_{bc} - V_{ca}) \quad (4-16)$$

The expressions for line-to-neutral voltages of the inverter can be written in terms of switching waveform as

$$V_{aa} = \frac{V_{dc}}{6} \left[\left\{ m(t) - m \left(t - \frac{T}{6} \right) \right\} G_3 - \left\{ m_1(t) + m \left(t + \frac{T}{6} \right) \right\} G_1 \right] u(t) \quad (4-17)$$

$$V_{ba} = \frac{V_{dc}}{6} \left[\left\{ -m(t) + m \left(t + \frac{T}{6} \right) \right\} G_1 - \left\{ m \left(t - \frac{T}{6} \right) - m \left(t + \frac{T}{6} \right) \right\} G_2 \right] u(t) \quad (4-18)$$

$$V_{ca} = \frac{V_{dc}}{6} \left[\left\{ -m \left(t - \frac{T}{6} \right) - m \left(t + \frac{T}{6} \right) \right\} G_2 - \left\{ -m(t) - m \left(t - \frac{T}{6} \right) \right\} G_3 \right] u(t) \quad (4-19)$$

In equations (4-1) to (4-19), the following terms apply:

$g(t, t_i, t_{i+1})$ is the gate function starting at time t_i and ending at time t_{i+1} ,

$u(t)$ is the unit step function,

$m(t)$ is the modulated switching waveform for type-A or type-B,

N_p is the number of pulses in half cycle,

$A = 0, T, 2T, \dots$ etc, where T is the period of the inverter wave,

m_T is the modulated switching waveform for one cycle only,

$m(t + nT)$ is the modulated switching waveform shifted by $+nT$

V_{ab}, V_{bc}, V_{ca} are the line to line voltages of the inverter,

V_{an}, V_{bn}, V_{cn} are the line to neutral voltages of the inverter.

Typical waveforms obtained by the above expressions for type-B switched inverters are shown in figs. 4-6 and 4-7 respectively. Using this method it is also possible to predict the theoretical waveforms of d-q axis voltages for the motor analysis. The d-q axis voltages V_d and V_q are obtained by the following transformation

$$\begin{bmatrix} V_q \\ V_d \end{bmatrix} = \frac{2}{3} \begin{bmatrix} 0 & \frac{\sqrt{3}}{2} & -\frac{\sqrt{3}}{2} \\ 1 & -\frac{1}{2} & -\frac{1}{2} \end{bmatrix} \begin{bmatrix} V_{ab} \\ V_{bc} \\ V_{ca} \end{bmatrix} \quad (4-20)$$

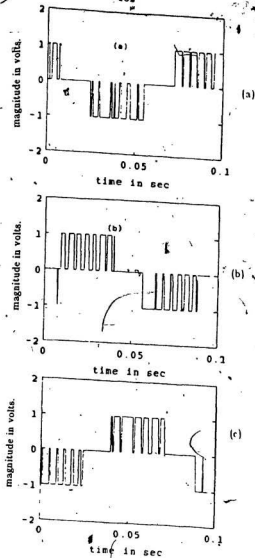


Fig. 4.6 Typical line to line voltages of a three phase delta modulated inverter. (type-B switching)

- (a) waveform of phase a,
- (b) waveform of phase b,
- (c) waveform of phase c.

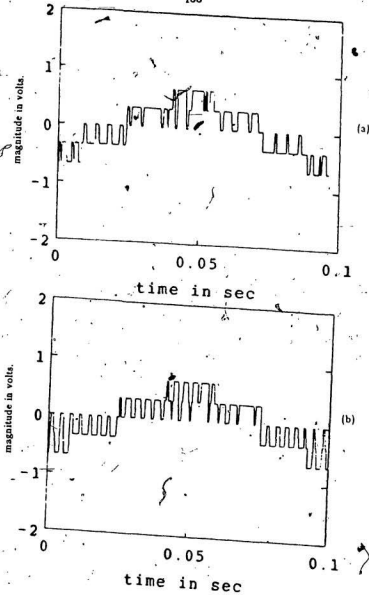


Fig 4.7 Typical line to neutral voltages of a three phase delta modulated inverter. (type-B switching)
(a) V_{an} , with control voltage = 2.0 volts.
(b) V_{an} , with control voltage = 3.0 volts.

or

$$V_q = \frac{1}{\sqrt{3}} [V_{bc} - V_{ca}] \quad (4-21)$$

$$V_d = \frac{1}{3} [2V_{ab} - V_{bc} - V_{ca}] \quad (4-22)$$

Substituting equations (4-5) to (4-7) in equations (4-21) and (4-22), V_d and V_q can be obtained as

$$V_q = \frac{1}{2\sqrt{3}} V_{dc} \left[\left(m \left(t - \frac{T}{6} \right) - m \left(t + \frac{T}{6} \right) \right) G_1 + \left(m \left(t \right) + m \left(t - \frac{T}{6} \right) \right) G_3 \right] \quad (4-23)$$

$$V_d = \frac{1}{6} V_{dc} \left[2 \left(m \left(t \right) + m \left(t + \frac{T}{6} \right) \right) G_1 - \left(m \left(t - \frac{T}{6} \right) - m \left(t + \frac{T}{6} \right) \right) G_2 - \left(-m \left(t \right) - m \left(t - \frac{T}{6} \right) \right) G_3 \right] \quad (4-24)$$

Typical axis voltages of a three phase type-B switched inverter waveforms obtained by equations (4-23) and (4-24) are shown in fig. 4-8.

4.3 Choice of Switching For Three Phase Inverter :

For a three phase inverter type-B switching is the preferable option. In single phase inverters, type-B switching gives rise to 3rd, 5th and other low order harmonics at the output of the inverter. However, in a three phase inverter due to inverter and load connections, some of these low order harmonics disappear or

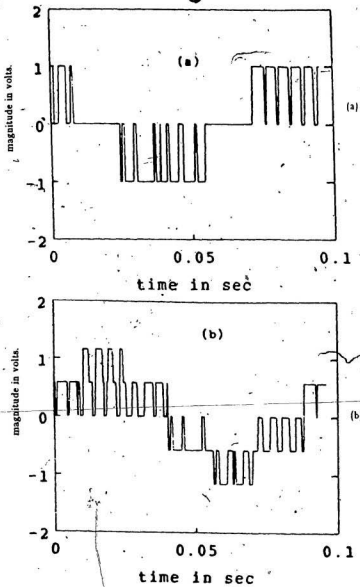


Fig. 4.8 Typical d-q axis voltages of a three phase delta modulated inverter.

(a) d - axis voltage. (b) q - axis voltage

are substantially reduced in their magnitudes. The choice of type-B switching is also due to the higher fundamental voltage availability of the inverter. Typical voltage availability of a three phase RWDM inverter switched in scheme-B is shown in fig. 4-9.

4.4 Harmonic Analysis of Three Phase RWDM Inverter Waveforms Using DFT on Windowed Waveforms

Harmonic analysis of a three phase rectangular wave delta modulated inverter waveforms by discrete Fourier transform is described in this section. The line to line, and the line to neutral voltages of the inverter were defined by equations (4-1) to (4-19). The line to neutral voltages thus obtained for a tuned delta modulated inverter are shown in fig. 4-10. The discrete Fourier transform (DFT) has been performed on the sampled waveforms. The spectra obtained for the ordinary DFT operation on the waveforms of fig. 4-10(b) are shown in fig. 4-11. The inverter waveforms were also studied with the Hamming, the Hanning and the Blackman windows. The windowed waveforms were obtained from the equations of three phase inverter output voltages and the window functions.

The windowed waveforms are obtained by the following

$$V_{ll-w}(t) = V_{ll} w(t) \quad (4-25)$$

where,

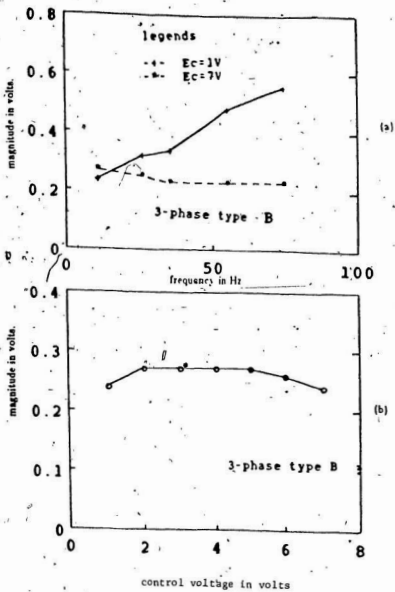


Fig. 4.9 Fundamental voltage availability of a three phase delta modulated inverter
 (a) with varying frequency
 (b) with varying control voltage

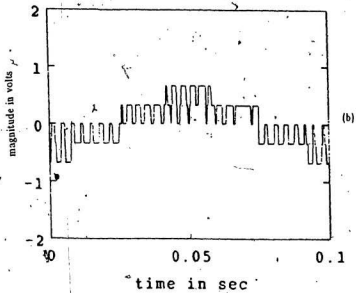
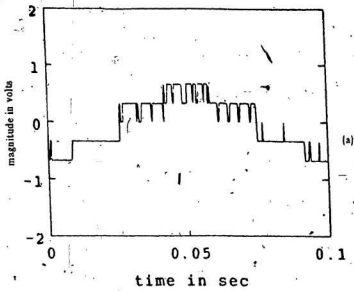


Fig. 4.10 Line to neutral voltage waveforms of a tuned rectangular wave delta modulated inverter. (continued)

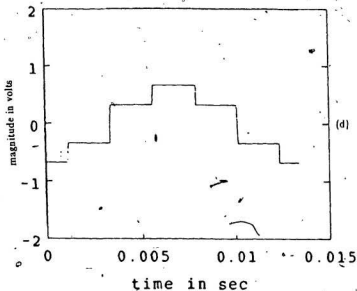
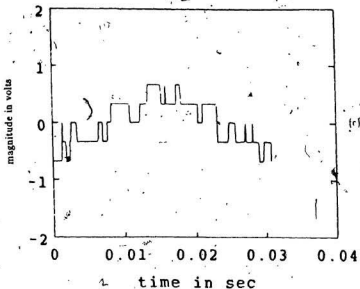


Fig. 4 10 Line to neutral voltage waveforms of a tuned rectangular wave delta modulated inverter.
 (a) at 10 Hz , control voltage = 2 volts.
 (b) at 10 Hz , control voltage = 3 volts
 (c) at 35 Hz , control voltage = 1 volt.
 (d) at 75 Hz , control voltage = 1 volt.

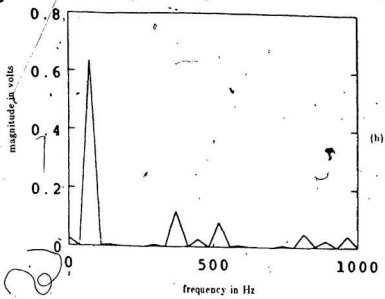
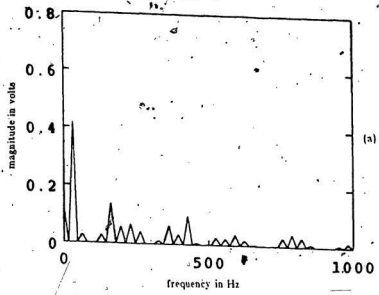


Fig 4.11 Spectra for inverter waveforms with constant control voltage but variable frequency.
(a) at 35 Hz, control voltage = 1 volt.
(b) at 75 Hz, control voltage = 1 volt.

$V_{an-w}(t)$ is the windowed waveform,

V_{an} is the line to neutral voltage of the inverter,

$w(t)$ is the window function.

The windowed waveforms of the inverter output of fig. 4-10(b) are shown in figs. 4-12, 4-13 and 4-14 for the Hamming, the Hanning and the Blackman windows respectively. Typical spectra for windowed waveforms of fig. 4-12 to 4-14 are shown in figs. 4-15 to 4-17 respectively.

The harmonic analyses of the three phase inverter waveforms were carried out to find the fundamental voltage availability and the low order harmonic contents of the output. It was evident from these studies that in three phase inverter output, the low order harmonics like 3rd, 5th, etc. are present, but in very small magnitude. The spectral plots obtained by the DFT are continuous spectra and the subharmonics of the inverter output voltages are detected as well. The information of these subharmonics is important in the frequency domain analyses of inverter fed motors.

4.5 Analytical Modeling of Inverter-Fed Submersible Motors:

In the past, the steady state and transient performances of inverter fed machines have been investigated by frequency domain analyses using the Fourier series and harmonic equivalent circuits of motors. It involves the determination

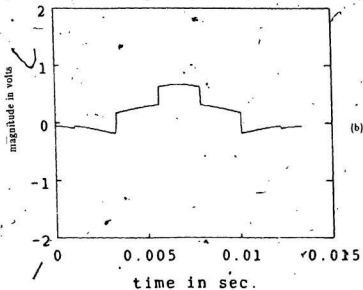
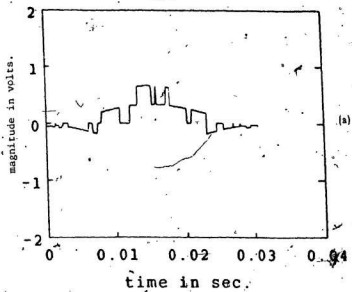


Fig. 4.12 Hamming windowed waveforms of a three phase tuned rectangular wave delta modulated inverter.

(a) at 35 Hz, control voltage = 1 volt.

(b) at 75 Hz, control voltage = 1 volt.

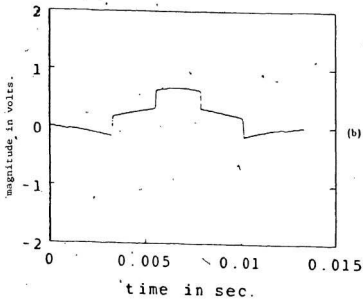
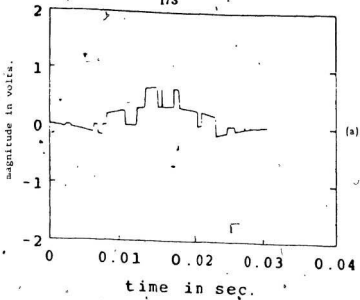


Fig. 4.13 Hanning windowed waveforms of a three phase tuned rectangular wave delta modulated inverter.
(a) at 35 Hz, control voltage = 1 volt.
(b) at 75 Hz, control voltage = 1 volt.

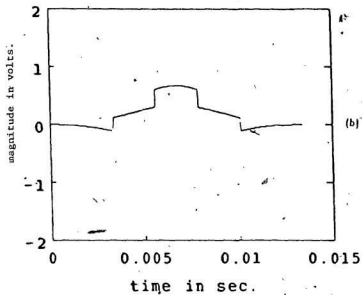
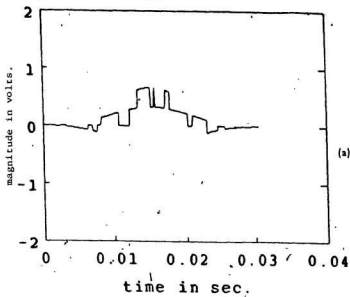


Fig. 4.14 Blackman windowed waveforms of a three phase tuned rectangular wave delta modulated inverter.
(a) at 35 Hz, control voltage = 1 volt.
(b) at 75 Hz, control voltage = 1 volt.

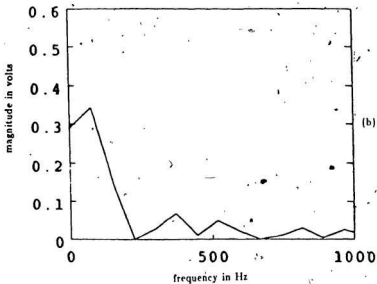
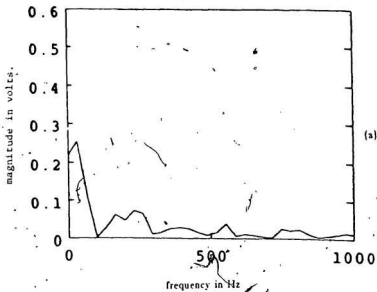


Fig. 4.15 Spectra of Hamming windowed waveforms of a three phase tuned rectangular wave delta modulated inverter.

(a) at 35 Hz, control voltage = 1 volt.

(b) at 75 Hz, control voltage = 1 volt.

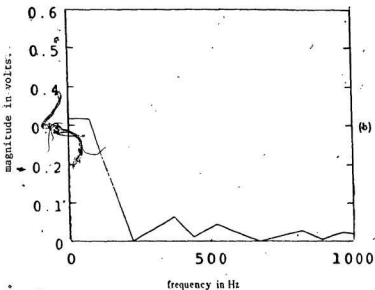
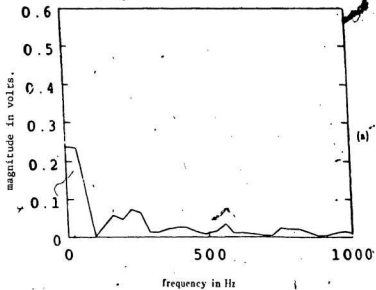


Fig. 4.18 Spectra of Hanning windowed waveforms of a three phase tuned rectangular wave delta modulated inverter.

(a) at 35 Hz, control voltage = 1 volt.

(b) at 75 Hz, control voltage = 1 volt.

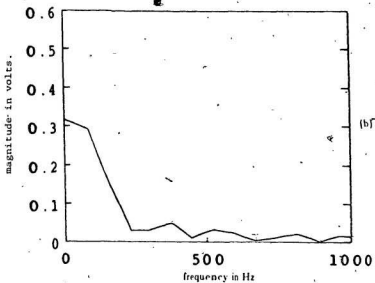
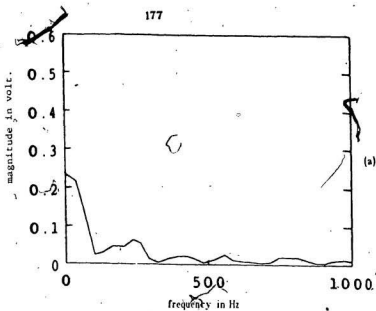


Fig. 4.17 Spectra of Blackman windowed waveforms of a three phase tuned rectangular wave delta modulated inverter.

(a) at 35 Hz, control voltage = 1 volt.

(b) at 75 Hz, control voltage = 1 volt.

of individual harmonic current and torque. The total current and the torque are obtained by superposition of the individual components. Motor losses and efficiency are also calculated from the harmonic motor equivalent circuits and the voltage harmonics of the inverter output. To obtain an accurate determination of the current and the torque by this method, it is necessary to include a large number of harmonics. For pulse width modulated inverters, it is necessary to include all significant sideband harmonics up to the fifth and the higher harmonics of the carrier frequency[130]. This implies that if the carrier frequency is eleven or thirteen times the frequency of the modulating wave, harmonics including 55 th or 65 th and higher of the inverter output waveform have to be considered for the solution of the motor equations. The process is, therefore, computationally long and tedious. Another factor that restricts the accuracy of this kind of analysis is the omission of subharmonic components of the voltage waveforms. Ordinary Fourier series analysis does not provide pertinent information about the subharmonic components of inverter output voltage. However, the pulse width modulated inverter output voltages contain subharmonic components due to the simultaneous presence of modulating and carrier wave frequencies. As a result, significant deviation from actual performance is obtained from this type of analysis.

These problems involving frequency domain analyses of inverter fed machines are not encountered in time domain analyses. In the time domain model the effects of all harmonics are accounted for in the definition of output

waveforms of the inverter. As a result, time domain analysis is considered, to be accurate and more efficient in finding the performances of inverter fed motors.

The analysis of the performance of an inverter fed motor in the time domain requires the formulation of the inverter output voltage and the system equations of the motor and the load. The basic three phase inverter voltage equations are developed in section 4.2. For motor equations standard d-q axis equations of reduced order are used. The system equations of the submersible pump load are formulated using the electrical analog circuit of the pump. The system equations are presented in sections 4.5.1 through 4.5.3. The solutions of the system equations of inverter output voltage, the motor and the load models give complete performance result of the submersible drive systems.

4.5.1 Inverter Output Waveforms:

Inverter output voltages for the analysis are based on the inverter voltage synthesis presented in section 4.2. In section 4.2 inverter line voltages are described as

$$\begin{bmatrix} V_{ab} \\ V_{bc} \\ V_{ca} \end{bmatrix} = \frac{1}{2} V_{dc} \begin{bmatrix} m(t) & m(t + \frac{T}{6}) \\ m(t - \frac{T}{6}) & -m(t + \frac{T}{6}) \\ -m(t) & -m(t - \frac{T}{6}) \end{bmatrix}$$

$$X \begin{bmatrix} G_1 u(t) & 0 & 0 \\ 0 & G_2 u(t) & 0 \\ 0 & 0 & G_3 u(t) \end{bmatrix} \quad (4-26)$$

The d-q axis voltages required for the analysis are given by

$$\begin{bmatrix} V_q \\ V_d \end{bmatrix} = \frac{V_{dr}}{3} \begin{bmatrix} 0 & \frac{\sqrt{3}}{2} & -\frac{\sqrt{3}}{2} \\ 1 & -\frac{1}{2} & -\frac{1}{2} \end{bmatrix} \begin{bmatrix} m(t) & m(t + \frac{T}{6}) \\ m(t - \frac{T}{6}) & -m(t + \frac{T}{6}) \\ -m(t) & -m(t - \frac{T}{6}) \end{bmatrix} \\ \times \begin{bmatrix} G_1 u(t) & 0 & 0 \\ 0 & G_2 u(t) & 0 \\ 0 & 0 & G_3 u(t) \end{bmatrix} \quad (4-27)$$

4.5.2 Motor Model:

The motor model used for the study of inverter fed submersible motors is based on the d-q axis motor equivalent circuits shown in fig. 4-18. A reduced order model in stationary axis can be obtained by assuming $V_{qr} = 0$ and $V_{dr} = 0$, and neglecting the derivatives of V_{qr} and V_{dr} (appendix-VI). The motor-model equations in matrix form are given as

$$\begin{bmatrix} V_{qs} \\ V_{ds} \\ 0 \\ 0 \end{bmatrix} = \begin{bmatrix} r_s & 0 & 0 & 0 \\ 0 & r_s & 0 & 0 \\ L_m p & -\omega_r L_m & r_r + L_r p & -\omega_r L_r \\ \omega_r L_m & L_m p & \omega_r L_r & r_r + L_r p \end{bmatrix} \begin{bmatrix} i_{qs} \\ i_{ds} \\ i_{qr} \\ i_{dr} \end{bmatrix} \quad (4-28)$$

where,

$$L_{1s} + L_m = L_s \quad (4-29)$$

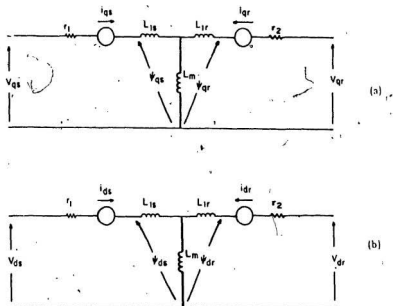


Fig 4.18 The induction machine models in d-q axes.

- (a) q - axis
 (b) d - axis

$$L_{lr} + L_r = L_r \quad (4-30)$$

$$\text{and } p = \frac{d}{dt}$$

In the above dynamic motor model each of the d-q axis voltage is dependent on two current variables. But if the current variables are replaced in equation (4-28) by flux variables, the voltages become dependent on the state variable of the flux. This makes computer solution of these equations easier. The following modification is carried out for the dynamic motor model.

Let,

$$\psi = [\psi_{qr} \ \psi_{dr} \ \psi_{qr} \ \psi_{dr}]^T \quad (4-31)$$

$$L = \begin{bmatrix} L_s & 0 & L_m & 0 \\ 0 & L_r & 0 & L_m \\ L_m & 0 & L_r & 0 \\ 0 & L_m & 0 & L_r \end{bmatrix} \quad (4-32)$$

$$L^{-1} = \frac{1}{L_s L_r - L_m^2} \begin{bmatrix} L_r & 0 & -L_m & 0 \\ 0 & L_r & 0 & -L_m \\ -L_m & 0 & L_s & 0 \\ 0 & -L_m & 0 & L_s \end{bmatrix} \quad (4-33)$$

$$i = L^{-1} \psi \quad (4-34)$$

substituting $L_s L_r - L_m^2 = F$, and equations (4-34) and (4-33) in equation (4-28), one obtains the required equations in flux variable as

$$\begin{bmatrix} V_{qs} \\ V_{ds} \\ 0 \\ 0 \end{bmatrix} = \begin{bmatrix} \frac{r_s L_m}{F} & 0 & -\frac{r_s L_m}{F} & 0 \\ 0 & \frac{r_s L_r}{F} & 0 & -\frac{r_s L_m}{F} \\ -\frac{r_r L_m}{F} & 0 & \frac{r_r L_s}{F} + p & -\omega_r \\ 0 & -\frac{r_r L_m}{F} & \omega_r & \frac{L_r r_r}{F} + p \end{bmatrix} \begin{bmatrix} \psi_{qs} \\ \psi_{ds} \\ \psi_{qr} \\ \psi_{dr} \end{bmatrix} \quad (4-35)$$

The simplified form of motor equations as shown in equation (4-35), and the voltage equations of inverter waveforms given in section 4.5.3 form the basis for the performance study of the inverter fed submersible motor. The solution of equation (4-35) allows one to obtain the flux information. This can also be used for solution of currents using equation (4-34). The equation used for finding the torque is

$$T_e = \frac{3}{2} \left(\frac{P}{2} \right) L_m (i_{qs} i_{dr} - i_{ds} i_{qr}) \quad (4-36)$$

where,

P is the number of poles.

4.5.3 Load Model:

The load used in the study is a submersible pump coupled to the submersible motor set. The motor pump set can be modeled as shown in fig 4-19. The equations governing this model can be derived from the electrical analog circuit as shown in fig. 4-19(b). These equations are given as

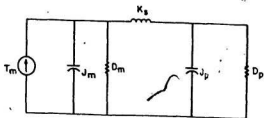
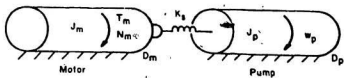


Fig. 4.19 The electrical analog model of a submersible pump.

(a) mechanical model (b) electrical model

$$\begin{bmatrix} T_m \\ 0 \end{bmatrix} = \begin{bmatrix} D_m + p J_m + \frac{1}{p K_s} & -\frac{1}{p K_s} \\ -\frac{1}{p K_s} & D + p J_p + \frac{1}{p K_s} \end{bmatrix} \begin{bmatrix} \omega_m \\ \omega_p \end{bmatrix} \quad (4-37)$$

where,

T_m is the motor torque,

J_m is the motor inertia constant,

ω_m is the motor angular speed,

K_s is the stiffness constant,

J_p is the pump inertia constant,

ω_p is the pump angular speed.

Equation (4-37) can be re-written as

$$\begin{bmatrix} \omega_m \\ \omega_p \end{bmatrix} = \begin{bmatrix} D_m + p J_m + \frac{1}{p K_s} & -\frac{1}{p K_s} \\ -\frac{1}{p K_s} & D + p J_p + \frac{1}{p K_s} \end{bmatrix}^{-1} \begin{bmatrix} T_m \\ 0 \end{bmatrix} \quad (4-38)$$

4.6 Steady State Performance of Submersible Motor Fed From RWDM

Inverter:

The models of the three phase inverter voltages, the motor and the load were used to study the steady state performance of the submersible motor fed from the rectangular wave delta modulated inverter. The study was done for a

230 V, 1.5 hp, 2 pole submersible motor. The motor parameters for the submersible motor are listed in the appendix-IV. The parameters of a 230 V, 1.5 hp, 2 pole conventional class-B induction motor are also included in the table. The steady state performances were studied for the submersible motor and the conventional induction motor. The parameters listed in appendix-IV show that, compared to the conventional class-B induction motor the submersible motor, has higher stator and rotor resistances and also has higher leakage reactances. These higher values of motor parameters of submersible motor obviously increase the motor losses during the steady state operation. These would also lead to higher input current in the submersible motor for the same load conditions.

The steady state performances of the motors were analytically carried out by solving the simultaneous differential equations formed by the motor input voltages and the motor equations. From the dynamic motor model of the equation (4-35), the flux waveforms were obtained by re-arranging the equation (4-30) as

$$\begin{bmatrix} \psi_{qs} \\ \psi_{ds} \\ \psi_{qr} \\ \psi_{dr} \end{bmatrix} = \begin{bmatrix} \frac{r_s L_r}{F} & 0 & \frac{r_s L_m}{F} & 0 \\ 0 & \frac{r_s L_r}{F} & 0 & \frac{r_s L_m}{F} \\ \frac{L_m r_r}{F} & 0 & \frac{r_r L_s}{F} + p & -\omega_r \\ 0 & \frac{L_m r_r}{F} & \omega_r & \frac{L_s r_r}{F} + p \end{bmatrix}^{-1} \begin{bmatrix} V_{qs} \\ V_{ds} \\ 0 \\ 0 \end{bmatrix} \quad (4-30)$$

Equation (4-30) shows that the flux relationships in a reduced order model are first order simultaneous differential equations. For steady state conditions,

these equations were solved using a standard technique (using IMSL subroutines in VAX/VMS system) for sinusoidal and rectangular wave delta modulated inverter fed motors. The d-q axis currents of the motor are related to the d-q axis flux by linear algebraic equations as in equation (4-40)

$$\begin{bmatrix} i_{qs} \\ i_{ds} \\ i_{qr} \\ i_{dr} \end{bmatrix} = \begin{bmatrix} \frac{L_r}{F} & 0 & \frac{L_m}{F} & 0 \\ 0 & \frac{L_r}{F} & 0 & -\frac{L_m}{F} \\ \frac{L_m}{F} & 0 & \frac{L_s}{F} & \frac{L_m}{F} \\ 0 & -\frac{L_m}{F} & 0 & \frac{L_s}{F} \end{bmatrix} \begin{bmatrix} \psi_{qs} \\ \psi_{ds} \\ \psi_{qr} \\ \psi_{dr} \end{bmatrix} \quad 4-40$$

Equation (4-40) shows that the d-q axis currents are the scaled combination of flux waveforms. Since the flux solution for the different inputs were calculated by solving the equation (4-39), calculation for current at steady state condition of the motors required simple algebraic summation of scaled d-q axis fluxes. The d-q axis currents were then used to obtain the line currents during the steady state operation. The steady state line currents thus obtained for the conventional motor and the submersible motor with sinusoidal input are shown in figs. 4-20 and 4-21. The line current for the submersible motor fed from the rectangular wave delta modulated inverter at 60 Hz operation is shown in fig. 4-22. The results show that the submersible motor, due to its higher motor constant than conventional induction motor, draws higher line currents from the supply under the same operating conditions. The current waveforms thus obtained were

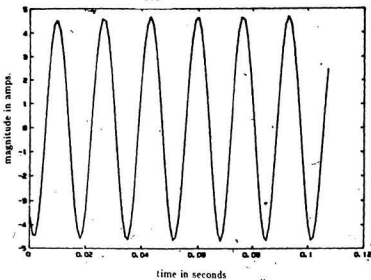


Fig. 4.20 The line current of the conventional induction motor with sinusoidal supply (1/4 full load).

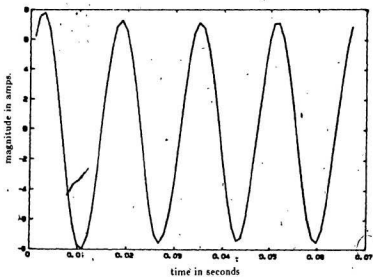


Fig. 4.21 The line current of the submersible induction motor with sinusoidal supply (1/4 full load).

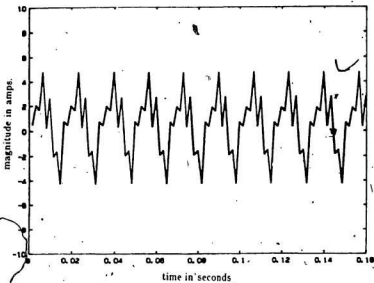


Fig. 4.22 The line current of the submersible motor with the rectangular wave delta modulated inverter supply at 60 Hz. (1/4 full load)

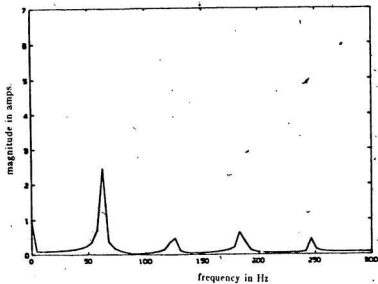


Fig. 4.23 The spectrum of the line current obtained by discrete Fourier transform at 60 Hz. (1/4 full load)

analyzed for the harmonic components. Typical spectrum obtained by ordinary discrete Fourier transform on a current wave at 60 Hz operation for $\frac{1}{4}$ full load is shown in fig. 4-23. The torque of the submersible motor obtained for the 60 Hz operation at $\frac{1}{4}$ load is shown in fig. 4-24. In variable frequency open loop operation, the slip of the induction motor changes with the change of load and the frequency. It is necessary to adapt a strategy that would change the frequency and the voltage of the supply in accordance with the variation of the load in such a manner that near constant slip operation is always ensured. This is necessary to maintain the motor efficiency consistently at its optimum.

4.7 Start-up Response of Submersible Motor Fed From RWDM Inverter:

The start up performance of the submersible motor and the conventional induction motor were studied theoretically for sinusoidal and RWDM inverter voltage inputs. Both on-line start with, and without the ramp frequency and voltage (RFV) variation of input voltages were considered. The method involved the solution of equation (4-35). The results are presented for no-load start up responses of the submersible motor and the conventional motor. The solutions were obtained by solving simultaneous differential equations and appropriate torque and position relationships using IMSL subroutines in VAX/VMS.

The starting current, torque and the speed characteristics of a conventional induction motor fed from sinusoidal line voltage are presented in figs. 4-25 to 4-

27. The current, torque and the speed characteristics of a submersible motor fed from sinusoidal voltage are shown in figs. 4-28 to 4-30. These characteristics were obtained for a derated motor voltage of 175 V line to line. The experiments were carried out with an inverter having a fundamental voltage limitation of 175 V. Thus the derating was necessary for the purpose of experimental verification. The on-line starting characteristics show that both the conventional and the submersible motors demonstrate a similar tendency. Without ramp frequency and voltage start, the starting currents of both motors are very high. It was almost 12 times the rated current for a conventional motor and 8 times the rated current for the submersible motor. The speed responses of both motors were also found to be extremely quick. The conventional motor reached its operating speed in 2.5 second whereas the submersible motor reached the operating speed in 0.5 seconds. The faster speed response of the submersible motor was due to its low inertia constant. Initial torque fluctuations of the motors were found to be high as well. The start up performance with a RWDM inverter supply without RFV showed that motors take longer times to reach steady state conditions. The results are shown in figs. 4-31 to 4-33. Since high starting current and the fast speed response are not desirable for submersible motors, it is necessary to extend the starting period of these motors with a gradual increase of voltage and frequency during start up. This would ensure longer life and more reliable operation of these motors. The ramp voltage and frequency characteristic of the rectangular wave delta modulated inverter was successfully used for providing soft start

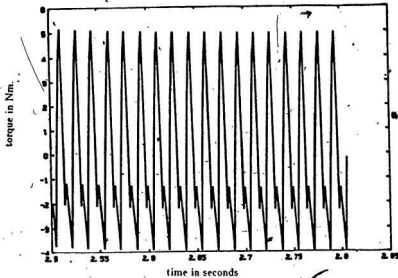


Fig. 4.24 The computed developed torque of the submersible motor with the rectangular wave delta modulated inverter supply. (load = 1/4 full load, where full load = 1.5 hp.)

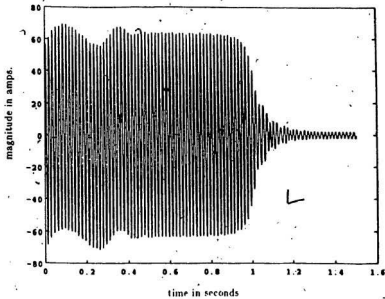


Fig. 4.25 The computed on-line starting current of the conventional induction motor with sinusoidal input.

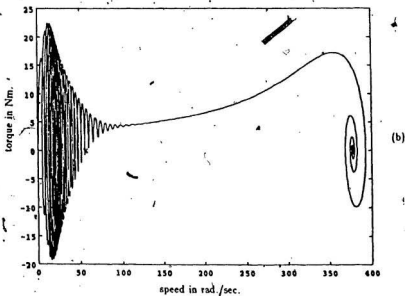
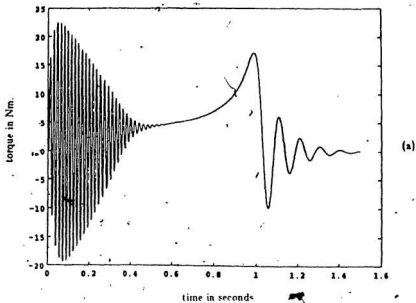


Fig. 4.26 Computed on-line developed torque characteristics of the conventional induction motor for a sinusoidal supply.
 (a) The torque versus time characteristic.
 (b) The torque versus speed characteristic.

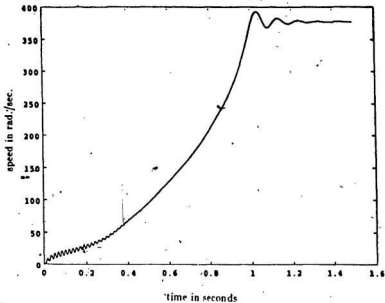


Fig. 4.27 The starting speed of the conventional induction motor with sinusoidal supply.

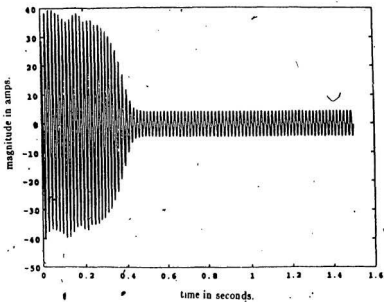


Fig. 4.28 The computed on-line starting current of the submersible induction motor with sinusoidal supply.

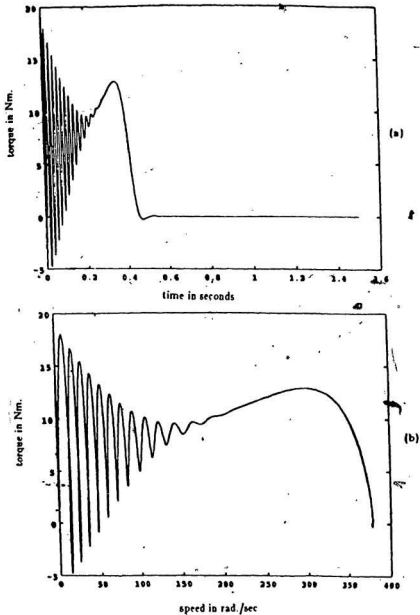


Fig. 4.29 Computed on-line developed torque characteristics of the submersible induction motor with sinusoidal supply.
 (a) The torque versus time characteristic.
 (b) The torque versus speed characteristic.

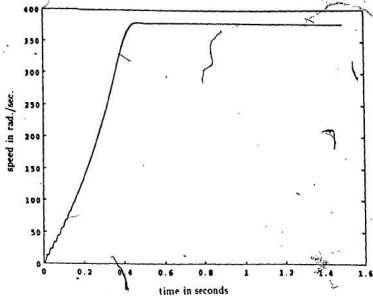


Fig. 4.30 The starting speed of the submersible induction motor with sinusoidal supply.

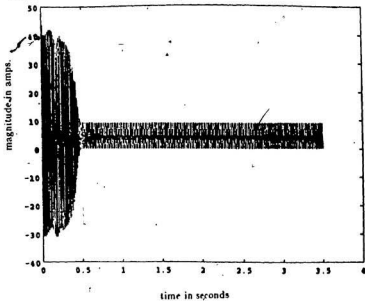


Fig. 4.31 The computed on-line starting current of the submersible induction motor with the rectangular wave delta modulated inverter supply without RFV.

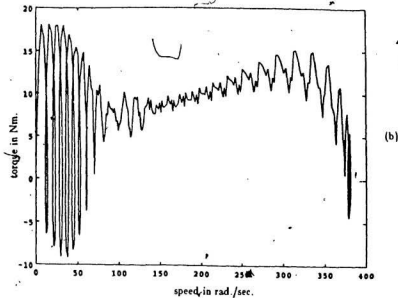
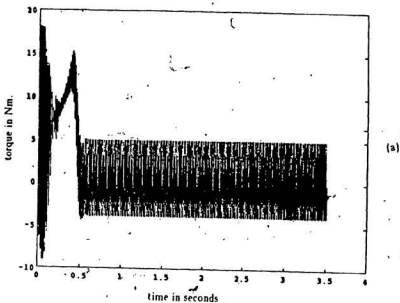


Fig. 4.32 Computed on-line developed torque characteristics of the submersible induction motor for a rectangular wave delta modulated inverter supply without RFV.

(a) The torque versus time characteristic.

(b) The torque versus speed characteristic.

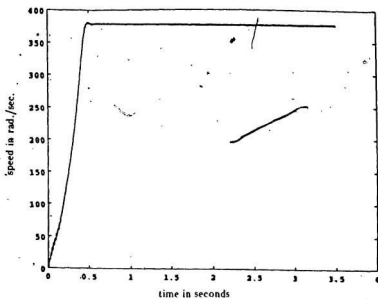


Fig. 4.33 The starting speed of the submersible induction motor with the rectangular wave delta modulated inverter supply without RFV.

characteristic of the the submersible motors. When the RFV characteristic of RWDM inverters was used, the starting current and speed responses showed gradual transition to the operating current and the speed. The start up responses of the submersible motor with a rectangular wave delta modulated inverter with the RFV characteristic at no-load are shown in figs. 4-34 to 4-36. A comparison of these results with those obtained for start up characteristics for on-line start without the RFV shows a significant reduction in transient torque and current from those obtained during start up with the RFV. The developed torque vs. time characteristics showed a smoother transition to the operating point rather than high oscillation as compared to those obtained for start up without the RFV. The current profile showed that the initial current is lower with RFV supply than the currents obtained during on-line start up with sinusoidal supply or RWDM inverter supply without RFV. The speed time characteristic has a smoother transition to the operating speed. It is, therefore, proved that the desired soft start characteristic of submersible motors can be obtained by the RFV characteristic of RWDM inverter supply.

4.8 Experimental Results:

The theoretical results obtained in sections 4.2 to 4.7 were verified experimentally. The experimental verifications were done on a 230 V, 1.5 hp submersible motor coupled to a $\frac{1}{2}$ horse power submersible pump. For inverter voltages, a transistorized three phase inverter rated at 175 V, 5 kW was designed and

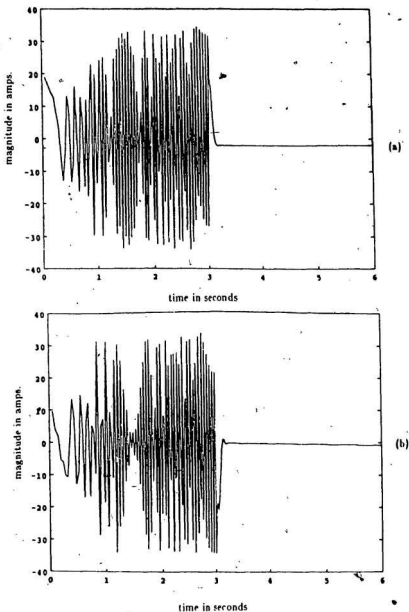


Fig. 4.34 The computed on-line starting current of the submersible induction motor with the rectangular wave delta modulated inverter supply with RFV.
(a) q - axis current.
(b) d - axis current.

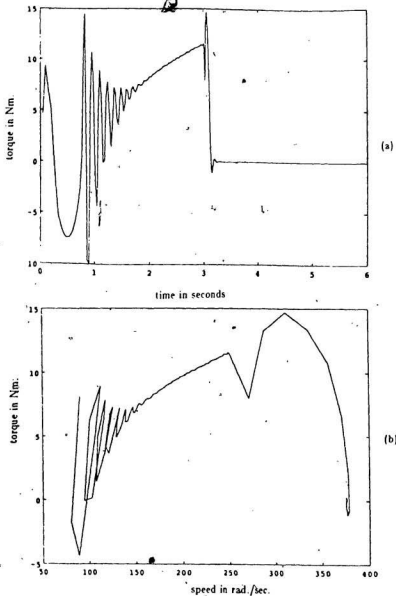


Fig. 4.35 Computed on-line developed torque characteristics of the submersible induction motor for a rectangular wave delta modulated inverter supply with RFV.

(a) The torque versus time characteristic.

(b) The torque versus speed characteristic.

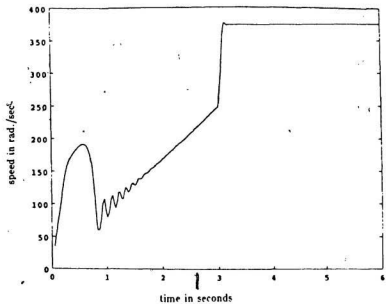


Fig. 4.36 The starting speed of the submersible induction motor with the rectangular wave delta modulated inverter supply with RFV.

constructed. The RWDM logic control circuit for switching the inverter is included in appendix I. A novel three phase sine wave generator was used for the reference signal generator of the delta modulators(appendix III).

The submersible motor was run from sinusoidal line voltage and the rectangular wave delta modulated inverter voltage.. The motor current was recorded. The line current waveform of the rectangular wave delta modulated inverter fed motor at $\frac{1}{4}$ full load and 60 Hz operation is shown in fig. 4-37. The line current shown in fig. 4-37 compares favorably with that obtained analytically. It is shown in fig. 4-22. The error between theoretical and the experimental results is within 5 percent. The start up response of the submersible motor was also experimentally determined for no load conditions. The current during the experimental start up of a submersible motor fed from sinusoidal line voltage is shown in fig. 4-38. A similar waveform for the motor start-up with RWDM inverter (without RFV) supply is shown in fig. 4-39. The line current and speed variations obtained for RWDM inverter supply (with RFV) for a no load condition is shown in fig. 4-40. It shows that the current fluctuation is reduced as predicted. In the study of start up response of the motor the errors found in calculated and experimental results are within 12 percent.

4.9 Conclusions:

An analysis of the submersible motor fed from RWDM inverter has been presented with the time domain modeling of the inverter output voltages, the

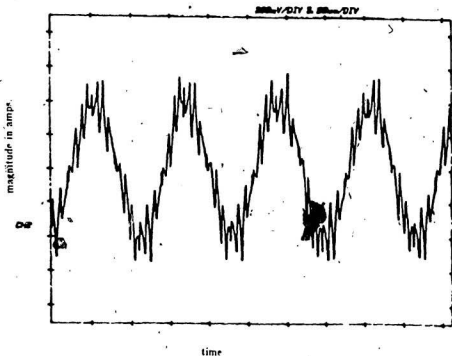


Fig. 4.37 The experimental line current of the submersible motor fed from the three phase rectangular wave delta modulated inverter at 60 Hz.

(load = 1/4 full load where full load = 1.5 hp.)

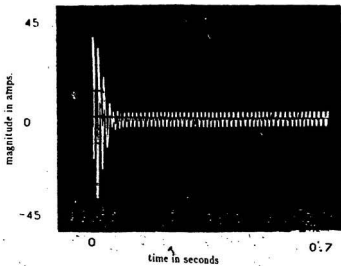


Fig. 4.38 The starting current of the submersible motor with sinusoidal supply (at no load).

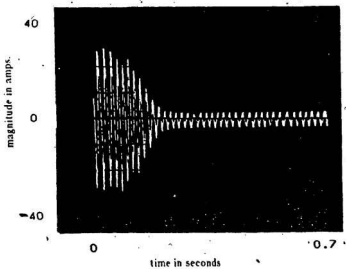


Fig. 4.39 The starting current of the submersible motor with the rectangular wave delta modulated inverter supply at no load.

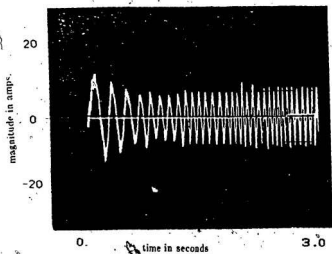


Fig. 4.40 The starting current of the submersible motor with the rectangular wave delta modulated inverter supply at no load (with RFV).

motor and the load. The conventional frequency domain analysis was avoided. To obtain accurate results by frequency domain analysis, it is necessary to include precise values of a large number of voltage harmonics. The time domain analysis is free from such limitations. It is computationally easier and faster as well. The steady state responses showed that the submersible motor has higher losses and lower efficiency than a conventional induction motor of the same size. These results were anticipated because of the higher leakage reactances and resistances of the motor. The start up performance showed that without the ramp frequency and voltage (RFV) control, the starting current of the motor was initially in the order of 8-10 times the full load current. The current and speed oscillations were also prominent. The use of the RFV during start up period limited the initial current to a low value of 2-3 times the full load current. It also reduced the torque and speed oscillations substantially. The inherent property of V/f of rectangular wave delta modulated inverter was used for RFV control in this study. This property would enhance the expected operating life of motors by providing soft starting characteristics of these units.

Chapter - 5

Variable Speed Operation of Submersible Motors

5.1 Introduction :

Variable speed operation of the submersible motor was studied with a pump as its load. The production of a submersible motor is determined by the intersection of the pump load line and the pump capacity curve. With the constant speed, the operating point in the head capacity curve moves with the change in production. The intersection of the load line and the capacity curve may occur outside the prescribed efficiency range. With the adjustable speed pumping, the operating point may be held within the desired range during the change in production. Where productivity is less than expected it is desired that the system be operated at a lower speed. Whereas, if the productivity is more than expected, the motor-pump should be operated at higher speed. Adjustable speed operations also provide a means to avoid throttling, pump-offs, gas lock conditions, solid settling and motor over heating etc.[21].

When submersible motors are used for pump operation, it is impractical to have a closed loop operation of the system with motor speed as the control parameter. This is due to the inaccessibility of the shaft of the sealed motor. The closed loop operation of these motors is therefore possible only with the speed estimation from measured quantities other than that measured at the shaft. This chapter outlines a semi-closed loop operation of submersible motors supplied from

delta modulated inverters. The semi-closed loop operation is suggested for the speed variability to match variable loads. The speed information of the submersible motor pump was obtained by an indirect method from the motor's input voltage, current and the power factor. This control technique ensured the constant slip operation of the motor, and maintained the motor efficiency at its optimum value at various loads.

5.2 Submersible Pump Performance:

The performance curves of a pump indicating total head versus capacity at rated speed are usually provided by the manufacturer. The curve for the pump used as the load in this study is shown in fig. 5-1. The performance curve can be shifted to give a new productivity curve at different speed of operation by observing the following conditions:

Flow rate is proportional to (speed),

Head is proportional to (speed)², and

torque is proportional to (speed)³.

Using the above proportionalities it is possible to duplicate the curves of other frequencies as follow

$$\frac{\text{New flow rate}}{\text{New speed}} = \frac{\text{old rate}}{\text{old speed}} \quad (5-1)$$

$$\frac{\text{New Head}}{\text{New speed}^2} = \frac{\text{old head}}{\text{old speed}^2} \quad (5-2)$$

The new pump performance curves at different operating frequencies as obtained by equations (5.1) and (5.2) are shown in fig. 5-2. The pump efficiency

140/8

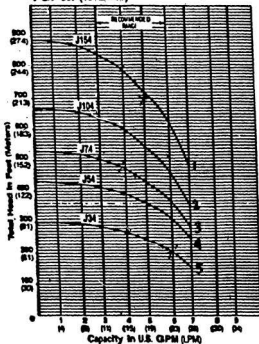
SJ PERFORMANCE CURVES**4 GPM (15 LPM)**

Fig. 5.1 The performance curve of the submersible pump (J54).
 (Performance curves were supplied on request by the
 pump division of F.E. Myers Co., Ashland, Ohio, U.S.A.)

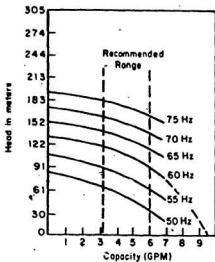


Fig. 5.2 Performance curves of the submersible pump at different operating frequencies.

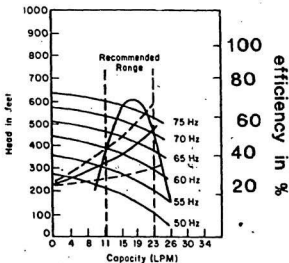


Fig. 5.3 Performance curves and the pump efficiency curve showing the range of maximum efficiency operation of the pump.

curve (also provided by the manufacturer) peaks at certain operating range as shown in fig. 5-3. As the operating point moves on a constant speed head capacity curve away from peak efficiency point, the pump operation becomes unbalanced. If, however, the working point is moved down the load line by adjustable speed operation, the balanced relationship between the flow and the lift can be maintained. The efficiency will remain practically unchanged in such a situation. The criterion, therefore, demands that the flow be reduced or increased in proportion to the speed and the head in proportion to the speed squared. The following relationships are thus required for such an operation:

$$Q = K N \quad (5-3)$$

$$H = K_1 N^2 \quad (5-4)$$

where,

Q is the flow rate in litre per minute,

H is the head lift in meter,

N is the speed in rpm,

K and K_1 is the constants of proportionality.

Based on the submersible pump performance, the control strategies adapted for the submersible motor drive with delta modulated inverter supply are discussed.

5.3 Control Strategy for Variable Speed Submersible Motor Drive

Basic requirements of the submersible pump operation with a submersible motor can be met in an open loop scalar control manner. The schematic diagram of such a control scheme is shown in fig. 5-4. In this open loop control, the increased or decreased load demand of the pump is matched with the proper speed selection of the motor by frequency command to the inverter. Since the delta modulation technique is used to control the inverter operation, the current control of the motor is achieved inherently by the modulation process. However, to provide the soft start characteristic of the whole system and to achieve an automatic control of the speed when a sudden change of load takes place, it is desirable to have a semi-closed loop operation with speed feedback. This type of control is necessary in order to obtain a constant slip operation of the motor because the efficiency of a motor depends on the slip. Since feedback using a tachometer or other devices for speed sensing is not permissible, a novel method has been developed to monitor the speed of the motor from the terminal quantities at the supply. The technique was used for the semi-closed loop operation of a submersible motor as shown in fig. 5-5. During the starting period, the speed reference signal was set to attain a predetermined speed. As the motor supply was turned ON, the speed feedback ensured a smooth linear speed up with time. During operation the speed command was changed to match the new production level according to the need of the increased or the decreased load. The changes in loading were sensed simultaneously by the current and the voltage sensors. The

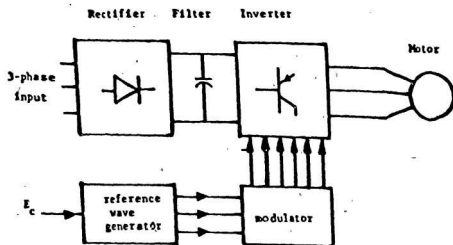


Fig. 5.4 The schematic diagram of the open loop control of a submersible motor fed from the delta modulated inverter supply.

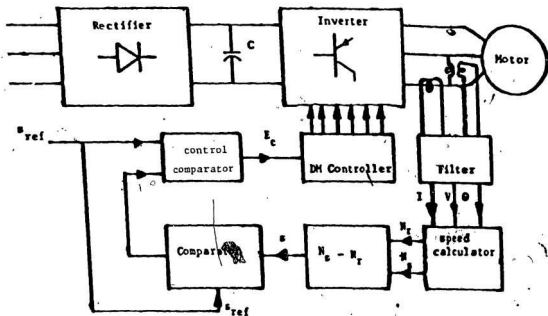


Fig. 5.5 The schematic diagram of the semi-closed loop control of a submersible motor fed from the delta modulated inverter supply.

operating speed was calculated, feedback to the comparator and was compared with the reference speed signal. A corrective signal to the inverter to change the frequency in order to maintain the constant slip operation was issued accordingly. It should be noted that the closed loop scheme has sensors in one phase of the supply to sense the required voltage and current for speed measurement. The sensors for the other two phases are not required for this purpose.

5.4 Determination of Operating Condition of Induction Motors From Terminal Quantities:

In many applications, maintaining the induction motor's operating conditions is important. When a closed loop operation is desired, quantities like speed, torque, rotor position, etc., are used as feedback signals. Usually these operating conditions are monitored by direct coupled sensors. In many adverse situations, it is not possible to monitor such operating conditions directly by sensors. The submersible motor is one such example, where the motor and its load operating conditions cannot be monitored by direct sensors. To overcome this problem an easy and effective way of finding motor operating conditions from terminal quantities has been developed.

In developing the method, the basic equivalent circuit of the induction motor of fig. 5-6 was used. With this method the motor's input voltage and current were used to determine the equivalent input impedance of motor.

The basic equations for the equivalent circuit shown in fig. 5-6 are.

$$V_1 = [r_1 + j(X_1 + X_m)]I_1 - jX_m I_2 \quad (5-5)$$

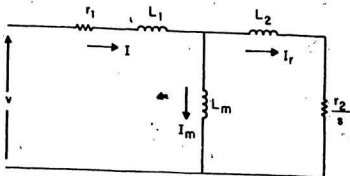


Fig 5.6 The basic equivalent circuit of an induction motor.

$$0 = -j X_m I_1 + \left[\frac{r_2}{s} + j (X_2 + X_m) \right] I_2 \quad (5-6)$$

where,

$$s = \frac{N_s - N_r}{N_s}$$

$$N_s = \frac{120 f}{P}$$

N_r = rotor speed

After simplifications the slip of the motor can be expressed as shown below

[appendix-III]

$$s = \frac{r_2 (L_e - L_1 - L_m)}{(R_e - r_1) (L_2 + L_m)} \quad (5-7)$$

since

$$N_r = N_s (1 - s) \quad (5-8)$$

$$N_r = \frac{120 f}{P} \left[1 + \frac{r_2 (L_e - L_1 - L_m)}{(R_e - r_1) (L_2 + L_m)} \right] \quad (5-9)$$

From the equation (5-9), it is evident that the motor speed N_r can be calculated from motor constants r_2 , L_1 , L_2 , L_m and the measured motor equivalent resistance R_e , and inductance L_e , R_e and L_e can be found by measuring the motor voltage and current as

$$R_e = \operatorname{Re} [Z_e] = Z_e \cos \theta_1 = \frac{V_1}{I_1} \cos \theta_1 \quad (5-10)$$

$$L_e = \operatorname{Im} \left[\frac{Z_e}{\omega} \right] = \frac{Z_e}{\omega} \sin \theta_1 = \frac{V_1}{\omega I_1} \sin \theta_1 \quad (5-11)$$

The equations (5-9) to (5-11) were used for continuous speed monitoring of submersible motor for semi-closed loop operation as shown in fig. 5. The same

relationships can further be used in estimating torque, temperature and other operating conditions of the motor pump in practical applications.

5.4.1 Speed Measurement Using a Practical Circuit:

The speed monitoring technique discussed in the preceding section has been investigated both theoretically and experimentally to verify the accuracy of the proposed technique. The method has been extensively tested for several motors with fixed and variable frequency supply with load. The theoretical speeds determined by this method for a 230V, 3-phase, 1/4 hp motor with variable frequency PWM supply and variable loads are shown in figs. 5-7 and 5-8. The motor speed at the same operating conditions were measured by conventional speed measuring device (tachometer) and are presented in figures 5-7 and 5-8. The results were obtained for the PWM inverter fed motor so as to test the validity of the method in inverter-fed motors. The maximum variation of the measured values of speeds calculated by this method from the actual speeds were observed to be only 0.5 percent. Also, it was observed that the maximum variation took place during the light load and the overload operations of the motor. This might be due to the saturation effect that changed the motor constants. However, since the error was found to be negligible, it is considered to be fairly accurate method when employed for the speed feedback in the submersible motor operation with inverter supply. For experimental purpose, and for the use in the semi-closed loop operation, a proto-type speed measuring device was designed and built. The block diagram of the device is shown in fig. 5-9. The device received voltage and

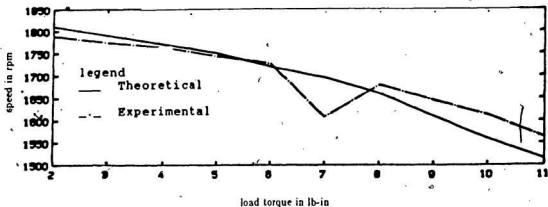


Fig. 5.7 The computed and the measured speed obtained by the proposed speed estimation method at 63 Hz. operation of the motor.

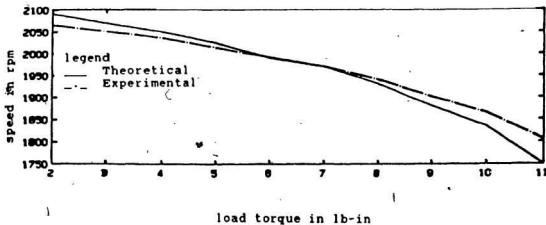


Fig. 5.8 The computed and the measured speed obtained by the proposed speed estimation method at 73 Hz. operation of the motor.

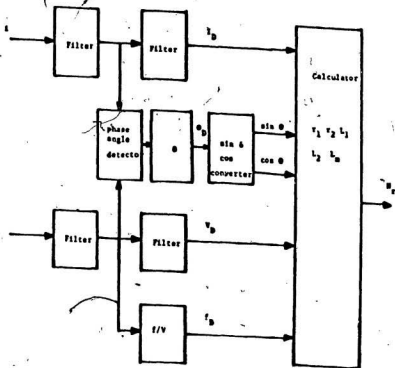


Fig. 5.9 The block diagram of the speed sensor.

current waveforms through a potential transformer (PT) and a noninductive current shunt connected to the line with the motor. Fundamental waveforms of the current and voltage were extracted by low pass filters. The phase difference between the two waveforms was detected by the comparator and was then converted to a dc signal θ_D in the phase angle detector. The current and voltage waveforms were used for getting the dc voltage F_D proportional to the frequency of the supply by a frequency to voltage (f/V) converter. A calculator was built to calculate the speed N_D of the motor from θ_D , V_{ID} , I_{ID} , F_D and the motor constants. N_D is a dc voltage proportional to the speed N_r in equation (5-9). The details of the device are given in appendix II. The speed measured by this device for the submersible motor at various operating frequency at no load is shown in fig. 5-10. The device is used for the semi-closed loop control of submersible motors fed from a delta modulated inverter.

5.5 Semi-Closed Loop Operation of Submersible Motor Pump Fed From DM Inverter:

The semi closed loop control of a submersible motor pump is obtained with the delta modulated inverter and the speed estimator described in the previous section. The open loop control of the motor pump to match the varying loads has been mentioned previously. With the delta modulation scheme the required capacity curve matching of the pump is met by varying the frequency of the inverter. The motor requirements of V/f for constant flux operation is met inherently by the modulation process. This requirement of the induction motor is needed by the

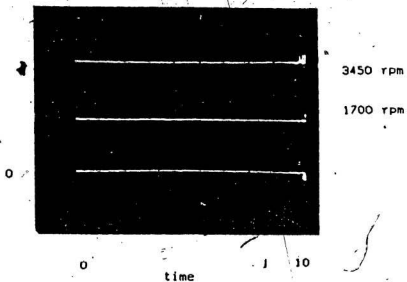


Fig. 5.10 The speed of the submersible motor at no load measured by the proposed speed sensor.

following torque relationships of the motor

$$T = 3 \frac{V_g^2}{\left(\frac{r_2}{s}\right)^2 + \omega^2 L_2^2} \frac{r_2}{s} \quad (5-12)$$

$$T = 3 \frac{\phi_m^2 \omega}{\frac{r_2}{s \omega} + \frac{s \omega}{r_2} L_2^2} \quad (5-13)$$

where:

$$\frac{V_g}{\omega} = \phi_m$$

Matching of the load by increasing or decreasing the frequency of the inverter ensures near optimum efficiency operation of the pump. However, to ensure the maximum efficiency and the constant torque operation of the motor, it must be operated at a constant slip from a supply having $V/f = \text{constant}$ characteristic. In this study the feedback is obtained by the speed estimation from terminal quantities of the motor by the relationship given in equation (5-9). With this speed feedback, the constant slip operation of the motor is ensured. This feedback is also required for stable operation within certain limits during a sudden change in pump operating condition. The same control can also be obtained in scalar control schemes with voltage and current as the control parameter (fig. 5-5) [109].

In terms of motor current, the torque equation can be written as

$$T = 3 \frac{\omega^2 L_m^2 I^2}{\left(\frac{r_2}{s}\right)^2 + \omega^2 (L_2 + L_m)^2} \frac{r_2}{s} \quad (5-14)$$

Which can be rearranged as

$$T = 3 \frac{\omega L_m^2 I^2}{\frac{r_2}{s} \omega + \frac{s \omega}{r_2} (L_2 + L_m)^2} \quad (5-15)$$

The motor current is given as

$$I = \frac{V_g}{j \omega L_m} + \frac{V_g}{\frac{r_2}{s} + j \omega L_2} \quad (5-16)$$

Which can be replaced as

$$I = \frac{-j V_g}{\omega L_m} + \frac{V_g \left(\frac{r_2}{s} - j \omega L_2 \right)}{\left(\frac{r_2}{s} \right)^2 - \omega^2 L_2^2} \quad (5-17)$$

Since,

$$\left(\frac{r_2}{s} \right)^2 \gg \omega^2 L_2^2 \quad (5-18)$$

$$I \approx \frac{-j V_g}{\omega L_m} + \frac{V_g \left(\frac{r_2}{s} - j \omega L_2 \right)}{\left(\frac{r_2}{s} \right)^2} \quad (5-19)$$

Replacing I from equation (5-19) in the following motor voltage expression

$$V = V_g + [r_1 + \omega L_1] I \quad (5-20)$$

The following expression can be obtained

$$V = V_g \left[1 + \frac{r_1 s}{r_2} + \frac{\omega L_1}{\omega L_m} + \frac{\omega^2 L_2 L_1 s^2}{r_2^2} \right] \quad (5-21)$$

$$j V_g \left[-\frac{r_1}{\omega L_m} + \frac{s \omega L_1}{r_2} - \frac{\omega r_1 L_2 s^2}{r_2^2} \right]$$

Since $\omega \gg s\omega$ and $L_1 \ll L_m$, the third and fourth terms in the real part of the above expression can be neglected. Also with negligible error the imaginary part of the above expression can be neglected to obtain the following:

$$V \approx V_g \left[1 + \frac{r_1 s}{r_2} \right] \quad (5-22)$$

$$V \approx \phi \omega \left[1 + \frac{r_1 s}{r_2} \right] \quad (5-23)$$

The above equations can be used for the scalar control and the constant slip operation.

Usually it is difficult to measure ϕ . An expression is derived from alternate terminal voltage estimation as follows:

Substituting equation (5-22) in (5-13) one obtains,

$$T \approx \frac{3}{\omega} \frac{V^2}{\left(1 + \frac{r_1 s}{r_2} \right)^2 \left(\frac{r_2}{s\omega} + \frac{s\omega}{r_2} L_2^2 \right)} \quad (5-24)$$

Since,

$$\frac{r_2}{\omega s} \gg L_2^2 \frac{\omega s}{r_2}$$

One can write

$$T \approx \frac{3 V^2}{\frac{r_2}{s} \left(1 + \frac{r_1 s}{r_2} \right)^2} \quad (5-25)$$

For small perturbation [109]

$$\Delta T = \frac{\delta T}{\delta s} \Delta s + \frac{\delta T}{\delta V} \Delta V \quad (5-26)$$

$$\Delta T = \frac{\delta T}{\delta s} \Delta s + \frac{\delta T}{\delta I} \Delta I \quad (5-27)$$

From equations (5-12), (5-23) and (5-24), the following relationship can be obtained

$$\frac{\Delta s}{s} = \frac{2}{1+k_v} \left(\frac{\Delta I}{I} - \frac{\Delta V}{V} \right) \quad (5-28)$$

where,

$$k_v = \frac{r_2 - s r_1}{r_1 + s r_1} = 1 \quad (5-29)$$

$$k_i = \frac{s^2 \omega^2 (k L_2 + L_m) - r_2^2}{s^2 \omega^2 (L_2 + L_m) + r_2^2} = 1 \quad (5-30)$$

$$\frac{\Delta s}{s} = \left(\frac{\Delta I}{I} - \frac{\Delta V}{V} \right) \quad (5-31)$$

Integrating one obtains

$$\ln s = \ln I - \ln V \quad (5-32)$$

From equation (5-32), the following relationship can be obtained

$$s = \frac{I}{V} \quad (5-33)$$

Equation (5-33) shows that $\left(\frac{I}{V} \right)$ is a good approximation of actual slip.

The constant slip operation of a motor can thus be obtained by maintaining $\frac{I}{V}$ = constant, either by voltage control or by current control. However, in principle this type of control can be expected to have large overshoots in voltage for any sudden increase in load [109]. The overshoot would be even higher with current control. This will happen even though the controller with a $\left(\frac{I}{V} \right)$ constant principle was found to be stable one [109].

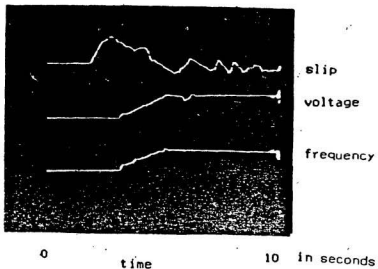


Fig. 5.11 Variation of slip, frequency and fundamental voltage of the motor for a sudden increase in load.

5.6 Experimental Results:

The two methods described for scalar control are different in nature. The first method uses a frequency variation of the supply to obtain the constant slip operation. The second method uses either the voltage or the current variation to maintain the constant slip operation at a fixed frequency of the supply. In the applications of submersible motor pumps the speed variation method is the desired technique. The reason is that pump production and efficiency are dependent on the speed of the pump. The block diagram of the control mechanism based on the first method is shown in fig. 5-5. The operational characteristic of the overall system is shown in fig. 5-11 for 60 Hz. In this figure the variation of inverter frequency and motor slip are shown for sudden change of load. When the load to the motor is suddenly increased it can be observed from fig. 5.11, that the slip of the motor is increased. The inverter responded to this slow down with an increase of operating frequency. As a result, the slip of the motor started to decrease and eventually after the initial oscillations settled to a constant value.

5.7 Conclusions:

Two different scalar control methods have been described in this chapter. The first method uses the speed information deduced from motor terminal quantities to maintain a constant slip operation. The second method uses a constant current to voltage ratio (I/V) operation to maintain the constant slip operation. The first method is suitable for the submersible motor application to drive pumps because it allows the pump to operate at different speed at different loads. This

method would also be better in terms of the overshoots and the oscillations associated with sudden load changes.

Chapter-6**Summary and Conclusions**

The objectives established to investigate the use of the delta modulation technique in inverters to operate submersible motors were satisfactorily realized during this research. The requirements of a submersible motor during its start and operation were met by the delta modulated inverter in a simple and reliable way. The performances of three delta modulators were examined and the rectangular wave delta modulator was selected for inverter switching. A novel method of on-line optimization of pulse width modulated waveforms using tuned rectangular wave delta modulation has been proposed. Analyses of the modulator waveforms were done using discrete Fourier transform (DFT). Spectral leakages in DFT of modulated waveforms were reduced by proper windowing. The waveforms of the modulator and the inverter were studied by discrete Fourier transform on the sampled windowed waveforms. The performance of the submersible motor fed from a delta modulated inverter was studied employing time domain analyses. Studies were done for the motor fed from supply voltages with, and without ramp frequency and voltage (RFV) characteristic. The performance of the submersible motor thus obtained was compared to that of the motor fed from the fixed voltage and the fixed frequency supply. Substantial improvements in the starting and operating characteristics of the motor were observed. A simple and effective method has been developed to determine the speed of induction

motors. The method was developed due to the requirement of the motor to operate at near constant slip so that the desired maximum efficiency operation can be achieved. The new speed measurement technique was used with the delta modulated inverter to obtain a constant slip operation of the submersible motor.

Major contributions and achievements of this work towards inverter fed submersible motors are summarized as follows:

1. The rectangular wave delta modulation (RWDM) technique was successfully used in an inverter-fed submersible drive. The severe starting current characteristic of the submersible motor was reduced by the inherent V/f characteristic of the RWDM inverter. The variable load demand of the submersible motor was met by the change of frequency in the inverter. Variable speed operation enabled the motor and its load to operate within the maximum efficiency range consistently. Further, the use of the rectangular wave delta modulator provides a current limiting process by its inherent signal tracking capability and the hysteresis comparator in the modulator.
2. An on-line optimization of inverter waveforms is proposed and implemented. This optimization method uses the tuned rectangular wave delta modulation technique. Unlike conventional inverter waveform optimization techniques, this method is suitable for easy on-line hardware implementation. Furthermore, the tuned RWDM modulator allowed the optimization criteria for inverter waveforms to be changed easily.

3. The RWDM and the tuned RWDM waveforms were analyzed using discrete Fourier transform. This method was found to be simple and capable of calculating the sub-harmonics of the modulator and the inverter waveforms. The discrete Fourier transform method can also be used for on-line calculation of harmonics of the inverter output voltages and the input currents. The spectral leakage associated with discrete Fourier transform on the sampled truncated waveforms introduces errors in the spectra. To reduce these spectral leakages windowed sampled waveforms were considered for the analysis. Windowing of the PWM modulator and the inverter waveforms was examined and it was found to be useful in smoothing the spectra considerably.
4. Analyses of the steady state and the start up performances of the delta modulated inverter fed submersible motor was carried out using the time domain solution of the motor d-q axis, and the inverter output voltage equations. Accurate determination of the motor performance using conventional frequency domain analysis requires a large number of harmonic components. Frequency domain analysis is computationally difficult and time consuming. Time domain analysis on the other hand was found to be an easier and accurate method for determining the performance of the motor. The analysis was done for the RWDM inverter fed motor, with and without RFV characteristic. The starting characteristics of the motor improved with RFV supply.

5. A semi-closed loop operation of the submersible motor with a delta modulated inverter supply has been proposed. With constant slip operation of the motor, speed feedback from the shaft of the motor was avoided. The speed information was obtained from the terminal quantities and motor constants. This technique can be used in all types of induction motor applications where speed feedback from the rotor side is not available.
7. The overall performance of the submersible motor fed from a delta modulated inverter compares reasonably well with any closed loop scalar and vector controlled motor.

Future Work:

The delta modulation technique has been employed in various power converter applications such as inverters, controlled rectifiers and voltage controllers. The use of this technique has been reported for drives and for uninterruptible power supplies. Efforts are underway to implement this technique for various converters with computer generated switching waveforms. The use of the DM technique for operating a single phase inverter by micro-computer has already been reported [131,132]. Micro-computer generation of three phase switching waveforms for various power converters can be undertaken in future works. In the waveform optimization by delta modulation technique, only the slope variation of the carrier wave has been examined. There are several other parameters in

the modulator which can be controlled on-line for optimization of waveforms. One of these is the window width of the hysteresis band. It was found that window width variation plays a major part in determining the harmonics at the output of the modulator. Optimization using simultaneous variation of the slope of the carrier wave and the window width can be examined and implemented. Also, the possibility of using switched-capacitors filter in the modulators can be explored in the future works.

In the submersible motor area, the possibility of using permanent magnet synchronous motors can be explored. Permanent magnet motors are more energy efficient than induction motors and are of smaller size than the conventional synchronous motors. These motors have shown promise in various areas of applications. The starting characteristics of these motors are severe under line voltage start. However, similar to the submersible motors of the induction type, the use of delta modulated inverter for their start would limit the severity of starting current of these motors [133,134,135].

Extensive field tests will require modifications and additions in the the inverter logic to provide various fault protections.

Further work can be done to find the effects of harmonics and sub-harmonics on the motor performance e.g. losses, pulsating torque, noise, etc. The stability study of the motor fed by the delta modulated inverter should also be carried out.

Reference

- 1 Legg, L.V., ' Submersible pump selection, part-1', Oil and Gas Journal, July 9, 1970, pp. 127 - 131
- 2 Legg, L.V., ' Submersible pump selection, part-2 ', Oil and Gas Journal, July 23, 1970, pp. 60-63
- 3 Legg, L.V., ' Submersible pump selection, part-3 ', Oil and Gas journal, August 6, 1970, pp. 95-102
- 4 Legg, L.V., ' Submersible pump selection, part-4 ', Oil and Gas Journal, August 27, 1970, pp. 105-110
- 5 Hoestenbach, R.D., ' Large volume high horsepower submersible pumping problems in water source well. ', Journal of Petroleum Technology (JPT), October, 1982, pp. 2397 - 2400
- 6 Anderson, H.H., and Crawford, L., ' Submersible pumping plant. ', Proc. IEE, November 1959, pp. 127-140
- 7 Anderson, H.H., ' Modern developments in the use of large single entry centrifugal pump. ', Proc. IMC, 1955, vol. 169, pp. 141-152
- 8 Coltharp, E.D., ' Submersible electrical centrifugal pumps. ', JPT, April 1984, pp. 645 -652
- 9 Yaucey, F.R. and Khanis, A.G., ' Submersible pumping Long Beach unit of East Wilmington fields. - a 17 year review. ', JPT, August, 1984, pp. 1321-1325

- 10 Way, A.R. and Hewett, M.A., ' Engineers evaluate the North Sea field ', Petroleum Engineers International, July, 1982, pp. 92-112
- 11 Motierman, S.J., ' Accelerated development planned for the Beatrice. ', Petroleum Engineers International, January, 1979, pp. 66-69
- 12 Kilvington, L.J. and Gallivan, J.D., ' Beatrice Field: Electrical submersible pump and reservoir performance, 1981-1983. ', JPT, November, 1984 pp. 1934-1942
- 13 Ryall, M.L. and Grant, A.A., ' Development of new high reliability down hole pumping system for large horsepower', JPT, November, 1983, pp. 1709-1718
- 14 Kuntz, G., ' The technical advantage of submersible motor pumps in deep sea technology and the delivery of manganese nodules. ', Ocean Technology Conference (OTC) record, 1979, pp. 85-91
- 15 Kuntz, G., ' Advantage of submersible motor pumps in deep sea mining' - JPT, December, 1980, pp. 2241-2246
- 16 Ogawa, Kitno, S., and Takahashi, M., ' Commutatorless propulsion for deep sea submersible research vessels ', Report on the commutatorless propulsion motors of ocean engineering R and D division, Kawasaki Heavy Metal Industries Ltd, Japan, 1979
- 17 Smith, J.R., Stronach, A.F. and Goodman, K.A., ' Prediction of dynamic response of marine systems incorporating induction motor propulsion drives',

- Proc. IEE, vol. 127, pt. B, no. 5, September, 1980, pp. 308-315
- 18 Kuntz, G., ' Submersible motor pumps, a modern solution for offshore and on-shore technology. ', paper C-129/76, pump and compressor for offshore oil and gas conference, University of Aberdeen, June 29- July 1, 1976
 - 19 Alcock, D.N., ' The equipment for the economics of variable flow well pumping ', IEEE trans. on Industrial Applications (IA), vol. IA-16, no. 1, Jan./Feb., 1980, pp. 144-153
 - 20 Alcock, D.N., ' Application of variable frequency drives to deep well submersible pumps', Petroleum Engineers International, March 15, 1980, pp. 37-44
 - 21 Alcock, D.N., ' Production operation of submersible pump with closed loop adjustable speed control', IEEE trans. on IA, vol. IA-17, no. 5, Sept./Oct., 1981, pp. 481 -489
 - 22 McClung, W.J., and Johnson, J.A., ' Electric submersible pump applications and operation in small open-hole completion ', JPT, November, 1983, pp. 1719 - 1720
 - 23 Baily, M.C., ' ESP - electrical submersible pumps, part-1', Petroleum Engineers International, August/1982, pp. 98 - 103
 - 24 Baily, M.G., ' ESP - electrical submersible pumps, part-2', Petroleum Engineers International, September, 1982, pp. 128-132
 - 25 Baily, M.G., 'ESP - electrical submersible pumps, part-3', Petroleum

Engineers International, November, 1982, pp. 33-40

- 26 Devine, D.L., ' Variable speed submersible pump find wider applications', Oil and Gas Journal, June 11, 1979, pp. 55-66
- 27 Dickinson, W.D., ' Microcomputer control of variable frequency drives using submersible motor as an instrument ', IEEE trans. on IA, vol. IA -18, no. 4, July/August, 1982, pp. 373-381
- 28 Brown, K.E., ' Overview of artificial lift systems ', JPT, Oct., 1982, pp. 2384 -2406
- 29 Cetrilift Huges Inc, ' Submersible pump handbook ', 1978
- 30 Bose, B. K., ' Adjustable speed ac drive systems ', - IEEE press, 1981, pp. 1-23
- 31 Bozdzer, A. and Bose, B.K., 'Three phase ac power control using power transistor', IEEE trans. on IA, vol.IA-12, September/October, 1976, pp. 490-505
- 32 Mungenast, J., ' Design and application of a solid state ac motor starter', IEEE/IAS conference record, 1974, pp. 861-866
- 33 Paice, D.A., ' Induction motor speed control by stator voltage control', IEEE trans. on power apparatus and systems (PAS), vol. PAS 87, February/1968, pp. 585-590
- 34 Foote, L.R., ' Adjustable speed control of ac motors ', Electrical Engg., vol. 78, August, 1959, pp. 840 -843

- 35 McMurray, W., ' A comparative study of symmetrical three phase circuits for phase controlled ac motor drives ', - IEEE trans. on IA, vol. IA-10, May/June, 1974, pp. 403-411
- 36 Lipo, T.A., ' The analysis of induction motors with voltage control by symmetrically triggered thyristors ', IEEE trans. on PAS, vol. PAS-90, April /May, 1971, pp. 515-525
- 37 Locke, R., ' Design and application of industrial solid state contractors ', IEEE/IAS conference record, 1981, pp. 501 -505. 17
- 38 Dubey, S., ' Classification of commutation methods ', IEEE/IAS conference record, 1981, pp. 895-909
- 39 Mapham, N.W., ' The classification of SCR inverter circuits ', IEEE international convention record, part 4, 1984, pp. 99-105
- 40 Bird, B.M. and King, K.G. ' An introduction to power electronics ', Wiley, 1983
- 41 Gyo, C. and Park, S. B., ' Novel six step and twelve stepped CSI with dc side commutation and energy rebound ', IEEE trans. on IA, trans, September/October, 1981 pp. 524 - 530
- 42 Bose, B.K., ' Adjustable speed ac drives : A technological status review ', Proc. IEEE, vol. 70, no.2 , February, 1982, pp. 116-135
- 43 Kliman, G.B., ' Harmonic effects in PWM inverter induction motor drives ', IEEE/IAS conference record , 1972, PP. 783 - 790

- 44 Klingbrin, E.A. and Jordan, H.E., ' Polyphase induction motor performance and losses on non-sinusoidal voltage source ', IEEE trans. on PAS, PAS-87, no.3 March/1968, pp. 624-631
- 45 Robertson, S.T.D. and Heiber, K.M., ' Torque pulsation in induction motors with inverter drives ', IEEE trans. on IA, March/April, 1971, pp. 318-323
- 46 Krause, P.C. and Thomas, C.H., ' Simulation of symmetrical induction machinery ', IEEE trans. on PAS, vol. PAS-84, 1965, pp. 1038-1053
- 47 Krause, P.C., and Lipo, T.A., ' Analysis and simplified representation of a rectifier inverter induction motor drive ', IEEE trans. on PAS, vol - PAS, no. 88, May, 1969, pp. 588-596
- 48 King, K.G., ' Variable frequency thyristor inverters for induction motor speed control ', Direct Current, February, 1965, pp. 125-132
- 49 Kinnick, A. and Heinrick, ' Static inverters with neutralization of harmonics ', AIEE transactions, vol.81, May, 1962, pp.58-68
- 50 Turnbull, F.G., ' Selected harmonic reduction in static dc-ac inverters ', AIEE transactions, vol. 83, July, 1964, pp. 374-378
- 51 Schonung, A. and Steinmiller, H., ' Static frequency changer with sub-harmonic control in conjunction with variable speed ac drives ', Brown Boveri Review, August/September, 1964, pp. 555-577
- 52 Nonaka, S. and Okada, H., ' Methods to control pulse width of three pulse inverters ', Journal of IEE, Japan, vol.86, July, 1972, pp. 71-79

- 53 Mokrytzki, B., ' Pulse width modulated inverters for ac motor drives ', IEEE trans. on IA, vol. IGA-3, November/December, 1967, pp. 493-503
- 54 Grant, D.A. and Seinder, R., ' Ratio changing in pulse width modulated inverters ', Proc. IEE, vol 128, pt. B, no. 5, Sept., 1981, pp. 243-248
- 55 Bowes, S.R., ' New sinusoidal pulse width modulated inverters ', Proc. IEE, vol 122, pt. B, no. 11, 1975, pp. 1279-1285
- 56 Bowes, S.R. and Mount, M.J., ' Microprocessor control of PWM inverters ', Proc. IEE, vol 128, pt. B, 1981, pp. 293-305
- 57 Bowes, S.R. and Clements, S.R., ' Microprocessor based PWM inverters ', Proc. IEE, vol 129, pt. B, no. 1, January, 1982, pp. 1-17
- 58 Bowes, S.R. and Clare, J.C., ' PWM inverter drives. ', Proc. IEE, vol. 130, pt. B, no. 4, July, 1983, pp. 229-240
- 59 Zubeck, J., Abbodanti, A. and Nordby, C.J., ' Pulse width modulated inverter motor drives with improved modulation ', IEEE trans. on IA, IA-11, no. 6, 1975, pp. 695-703
- 60 Buja, G.S. and Indri, G.B., ' Optimal pulse width modulation for feeding ac motors ', IEEE trans. on IA, vol. IA-13, 1977, pp. 38-39
- 61 Green, R.M. and Boys, J.T., ' Implementation of pulse width modulated inverter strategies ', IEEE trans. on IA, vol. IA-18, no. 2, March/April, 1982, pp. 138-145
- 62 Buck, F.D., Gistellinck, P., and Backer, D.D., ' Optimized PWM inverter

- driven induction motor losses', Proc. IEE, vol 130, pt. B, no. 5, 1983, pp. 310-320
- 63 Pollman, A., 'A digital pulse width modulator employing advanced modulation technique', IEEE conference record on IA, 1982, pp. 116-121
- 64 McMurray, W., 'Modulation of chopping frequency of dc chopper and PWM inverters having hysteresis comparator', IEEE Power Electronics Specialist Conference (PESC) record, 1983, pp. 295-299
- 65 Palaniappan, R.G. and Vithayathil, J., 'A control strategy for reference wave adaptive current generation', IEEE trans. Industrial Electronics (IE), vol IECE -27, no.2, May, 1980, pp. 92-96
- 66 Menzis, R. W. and Mahmoud, A.M.A., 'Comparison of optimal PWM techniques with bang bang reference current controller for voltage source inverter fed induction motor drives', IEEE conference record on IA, 1985, pp. 1205-1212
- 67 Kawamura, A., and Hoft, R., 'Instantaneous feedback controlled PWM inverter with adaptive hysteresis', IPEC conference record, Tokyo, March, 1983, pp. 851-857
- 68 Ziogas, P.D., 'The delta modulation technique in static PWM inverters', IEEE trans. on IA, no. 17, 1981, pp. 199-204
- 69 Esmail, A.D., Rahman, M.A., Quaicoe, J.E. and Choudhury, M.A., 'High performance three phase rectifier using delta PWM technique', International

- symposium on Electronic devices, circuits and systems, IIT, Kharagpur, India, 1987, pp. 578-580
- 70 Rahman, M.A., Quaicoe, J.E., Esmail, A.R.D., and Choudhury, M.A., 'Delta Modulated Inverter for UPS', IEEE Intelec conference record 1986, pp.445-450
- 71 Huang, I.B. and Lin, W., ' Harmonic reduction in inverters by the use of sinusoidal pulse width modulator ', IEEE tran. on control instrumentation, vol. IECI-27, no. 3, August, 1982, pp. 201-207
- 72 Bowes, S.R. and Bird, B.M., ' Novel approach of analysis of modulation process in power converters ', Proc. IEEE, vol 122, no.5, May, 1975, pp. 507-513
- 73 Ziogas, P.D. and Photiadis, P.N.D., ' An exact input current analysis of ideal static PWM inverters ', IEEE trans. on IA, vol. IA-19, no. 2 , March/April, 1983, pp. 281-295
- 74 Dewan S.B. and Forsythe, S. B., ' Harmonic analysis of synchronized pulse width modulated three phase inverters ', IEEE trans on IA, vol. IA-10 January/February, 1974, pp. 117-122
- 75 Lawrenson, P. and Stephenson, J.M., ' Note on induction machine performance with variable frequency supply', Proc. IEE, 1965, no.112(10), pp. 1917-1925
- 76 Campbell, S.J., ' Solid state ac motor controls ', Marcel Dekker, Inc., 1987

- 77 Bose, B.K., 'Power electronics and ac drives', Prentice Hall, 1987
- 78 Dewan, S.B., Slemon, G.R. and Straughen, A., 'Power semiconductor drives', Wiley Interscience, 1984
- 79 Lipo, T.A., 'Recent progress in the developments of solid state ac motor drives', IEEE trans. on power electronics, vol.3, no.2, April, 1988, pp. 105-117
- 80 Rahman, M.A., Quaicoe, J.E. and Choudhury, M.A., 'A comparative study of delta sine PWM inverters', First European conference on Power Electronics and Applications, Brussels, 1985, pp. 1.163-1.168
- 81 Rahman, M.A., Quaicoe, J.E. and Choudhury, M.A., 'An optimum delta modulation strategy for inverter operation', IEEE PESC conference record, 1986, pp. 410-416
- 82 Rahman, M.A., Quaicoe, J.E., and Choudhury, M.A., 'Harmonic minimization in delta modulated inverters using tuned filters', IEEE PESC conference record, 1988, pp. 462-468
- 83 Rahman, M.A., Quaicoe, J.E., Newman, R.W.L. and Choudhury, M.A., 'Spectral Analysis of PWM Converters using Discrete Fourier Transform', Canadian conference on Electrical and Computer engineering, Vancouver, B.C, Canada, 1988, pp 11-14.
- 84 Rahman, M.A., Quaicoe, J.E., Esmail, A.D. and Choudhury, M.A., 'Spectral Analysis of delta modulated inverter waveforms using discrete Fourier

- Transform', IEEE IECON'88 conference record, vol. II, Singapore, 1988, pp. 338-343.
- 85 Rabiner, L.R. and Rader, C.M., 'Digital signal processing', IEEE press, N.Y, 1972, pp. 150-151, pp. 228-259
- 86 Steele, R., 'Delta modulation systems', Halsted Press, Hohn Wiley and Sons, 1975
- 87 De Jager, F., 'Delta modulation - a new method of pcm transmission using the 1 unit code.', Philips research report, no.7, Dec., 1952, pp. 442-446.
- 88 Vande weg, N., 'Quantization noise of a single integration delta modulation system with an N - digit code.', Philips research report, Oct., 1953, pp. 367-385.
- 89 Schindler, H.R., 'Delta modulation.', IEEE Spectrum, Oct., 1970, pp. 69-78.
- 90 Greefkes, J.A. and De Jager, F., 'Continuous delta modulation.', Philips research report, no. 23, 1968, pp. 233-246.
- 91 Goodman, D.J., 'The application of delta modulation.', Philips research report, no. 23, 1969, pp. 321-342.
- 92 Steele, R. and Thomas, M.W.S., 'Two transistor delta modulator.', Electronic Engineering, no. 40, 1968, pp. 513-516.
- 93 Steele, R., 'Pulse delta modulators - inferior performance but simpler circuitry.', Electronic Engineering, no. 42, 1970, pp. 55-70.
- 94 Nielson, P.T., 'On the stability of double integrator delta modulation.',

IEEE trans. on communication technology, June, 1971, pp. 384-386.

- 95 Johnson, F.B., 'Calculating delta modulator performance.', IEEE trans. on AU, vol. AU-16, 1968, pp. 122-129.
- 96 Slepain, D., 'On delta modulation.', Bell system technical journal, vol. 51, Dec., 1971, no. 10, pp. 2101-2137.
- 97 Jayant, N.S. and Noll, P., 'Digital coding of waveforms.', Prentice Hall, 1984, pp. 399-415.
- 98 Abate, J.E., 'Linear and adaptive delta modulation.', Proc. IEEE, vol. 55, no.3, March, 1967, pp. 298-307.
- 99 Cartmatt, A.A. and Steele, R., 'Calculating the performance of syllabically companded delta-sigma modulators.', Proc. IEE, 1970, pp. 1915-1921.
- 100 Sharma, P.D., 'Characteristics of asynchronous delta modulation and binary slope quantization pcm systems.', Electronic Engineering, Jan., 1968, pp. 32-37.
- 101 Sharma, P.D., 'Signal characteristics of rectangular wave modulation.', Electronic Engineering, vol. 40, Feb., 1968, pp. 103-107.
- 102 Das, J. and Sharma, P.D., 'Some asynchronous-pulse modulation systems.', Electronic Letters, vol. 3, no. 6, June, 1967, pp. 75-79.
- 103 Steele, R. and Stevens, P., 'An automatic digital trace encoder for polaroid photographs', Electronic Engineering, September, 1973, pp. 80-85
- 104 Dempster, I.A. and Steele, R., 'Delta sigma wattmeter', Electronics letters,

- 7, no-18, September 9, 1971, pp. 519-520
- 105 Kikkert, C. J., 'Digital techniques in delta modulation', IEEE trans. on com. Tech., vol-19, August, 1971, pp. 570-573
- 106 Lockhart, G.B., ' Digital encoding and filtering using delta modulation ', Radio and Electronic Engineering, vol. 42, no-12, December, 1972, pp. 547-551
- 107 Creighton, G.K. and Steele, R., ' Source frequency adjustment controls motor speed', Electronic Engineering, May, 1973 pp. 70-71
108. Bose,B.K., 'Introduction to ac drives', IEEE press ,1981,pp. 1-16
- 109 Boys, J.T. and Walton, S.J.' Scalar control: an alternative ac drive philosophy', Proc. IEE , vol. 135, pt. B, no. 3, May, 1988, pp. 151-158
- 110 Takahashi, I. and Nogouchi,T., ' A new quick response and high efficiency control strategy for an induction motor', IEEE trans. on IA, vol-22, no 5, September/October, 1986, pp. 820-834
- 111 Takahashi, I. and Ohmori, Y., ' High performance direct control of an induction motor', IEEE IAS conference record, part-1, 1987, pp. 163-169
- 112 Bowes, S.R. and Buluagh, R.I., 'Harmonic minimization in microprocessor controlled current fed PWM inverter drives', Proc. IEE , vol. 134, pt. B, no. 1, January, 1987, pp. 25-41
- 113 Adams,R.D. and Fox,R., ' Several modulation techniques for PWM inverters' IEEE trans. on IA,vol. IA-3, no. 5, Sept./Oct., 1982, pp. 636-643

- 114 Cook, B.J., Cantoni and Evans, 'A microprocessor based three phase pulse width modulator', IEEE/IAS conference record, 1982, pp. 375-383
- 115 Rahman, M.A., Quisicoe, J.E., and Choudhury, M.A., ' Performance analysis of delta modulated inverters ', IEEE trans. on Power Electronics, July, 1987, pp. 227-233
- 116 Atherton, D.P., ' Nonlinear control engineering', Van Nostrand Reinhold company, 1975, pp. 75-235
- 117 Gelb, A. and Vander Velde, W.E., ' Multiple input describing functions and non-linear system design', Mc-Graw Hill, 1968
- 118 Gibson, J.E., ' Nonlinear automatic control', Mc-Graw Hill, 1963
- 119 Takahashi, Y., Rabins, M.J., and Auslander, D.M., ' Control and dynamic systems', Addison Wesley, 1970
- 120 Nagrath, I.J. and Gopal, M., ' Control system engineering', John Wiley and Sons, 1975, pp. 439
- 121 Choudhury, M.A., ' An analysis of delta PWM inverters ', - M.Engg thesis, Faculty of Engg. and Applied Science, Memorial University of Newfoundland, St. John's, Canada, 1984
- 122 Patel, H. and Hoft, R., ' Generalized technique of harmonic elimination and voltage control of thyristor inverters , part-1 ' IEEE trans. on IA , vol. IA-9, 1973, pp. 310 - 317
- 123 Capoling, G.A., ' Survey of PWM techniques for single phase transistor

- inverters', Proceedings of the First European conference on Power Electronics and Applications, vol. 1, Brussels, October, 1985, pp. 2.93-2.98
- 124 Divan, D.M., 'Optimum PWM waveform synthesis - A filtering approach.', IEEE trans. on IA, September / October, 1985, pp. 1199 - 1205.
- 125 Wang, Y.J. and OH, W.E., 'Function circuits', McGraw Hill, 1976, pp. 264
- 126 Bowes, S.R., and Bird, B.M., 'Novel approach to the analysis and synthesis of modulation processes in power converters', Proc. IEE, vol. 122, pt. B, no. 5, 1975, pp. 507-513
- 127 Savino, M., and Trotta, A., 'Analysis and measurement of PWM waveforms', Proceedings of the Second European conference on Power Electronics and Applications, Grenoble, France, 1987, vol. 2, pp. 725-731
- 128 Stanley, W.D., Dougherty, G.R. and Dougherty, R., 'Digital signal processing', Reston publishing company Inc., 2nd Ed., 1984, pp. 245-250
- 129 Harris, F.J., 'On the use of windows for harmonic analysis with discrete Fourier transform', Proc. IEEE, 66, no. 1/1978, pp. 51-83
- 130 Bowes, S.R. and Clare, J., 'Steady state performance of PWM inverter drives', Proc. IEE, vol. 130, pt. B, no. 4, July 1983, pp. 229-244
- 131 Rahman, M.A., Srivastava.R.K., Quaicoe, J.E. and Choudhury, M.A., 'Micro-computer implementation of delta modulation technique for inverter operation' -IEEE/IAS conference record, part 1, 1987, pp. 856-862
- 132 Rahman, M.A. and Choudhury M.A., 'Delta Modulated Inverter Fed P.M

Motors,

- International Drive Motors and Controller (DMC) conference record, London, U.K., 1985, pp. 59-65
- 133 Rahman, M.A., Srivastava, R.K., Quicoe, J.E. and Choudhury, M.A., 'Software control of delta modulated inverters', IEEE IECON'88 conference record, vol.-III, Singapore, 1988 pp. 836-862.
- 134 Rahman, M.A., Quicoe, J.E., Choudhury, M.A. and Slemon, G.R., 'Steady state performance of P.M synchronous motors fed from delta modulated inverters', IEEE IAS conference record, 1984, pp. 1359-1363
- 135 Rahman, M.A. and Choudhury, M.A., 'Performance Analysis of Samarium Cobalt P.M synchronous motor fed from PWM inverter', Conference record of International conference on Rare Earth developments and applications, Beijing, China, 1985, pp. 1009-1028
- 136 Rahman, M.A., Quicoe, J.E., Srivastava, R.K. and Choudhury, M.A., 'A Simple variable frequency three phase reference sine wave generator', Conference record of International Symposium on Electronic devices, circuits and systems, IIT Kharagpur, India, 1987, pp. 460-471
- 137 Ramamurthi, V.P. and Bellamkunda, 'A novel three phase reference sine wave generator for PWM inverters', IEEE trans. on IE, vol IE-29, no. 3, Aug/1982, pp.235-240
- 138 Pavithran, K. and Ramallelgan, R., 'A novel polyphase reference sine wave

generator using multiplexing technique', IEEE Trans. on IE, vol. IE-33, no.

3, August 1986, pp. 342-344

139 Krause, P.C., 'Analysis of Electric Machinery', Mc-Graw Hill, 1986

Appendix-I

Three Phase Delta Modulator circuits and The Logic circuits

A three phase delta modulated inverter requires the same modulating circuit as the modulating circuit for a single phase inverter. For the three phase implementation of delta modulated logic, one needs a three phase reference sine wave generator, three single phase delta modulators and the logic circuits for producing the gating signals of transistors, SCRs or other switching devices of an inverter. The three phase sine wave generator used in this research is discussed at length in appendix-III. The actual RWDM modulator to produce the modulated waveform is shown in fig. A1.1. The logic circuit for producing the gating signals of one pair of SCRs of the inverter is shown in fig: A1.2. The main gating signals are high frequency modulated for SCR gating. The switching signals for the transistorized inverter can be tapped from the same circuit before high frequency modulation. For the tuned RWDM, the modulated signal to the logic circuit is supplied from a tuned modulator. The modulator circuits in both cases have provisions for resetting the capacitor through two bi-directional static switches S_1 and S_2 . At the start of each half cycle of the reference sine wave, the switches are simultaneously closed for a short period to allow the capacitor in the integrator circuit to discharge. This ensures that the modulators will start performing at the beginning of each half cycle.

The modulators were used for both SCR and transistorized inverters. The

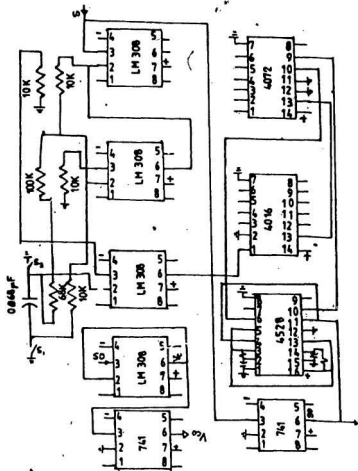


Fig. A11 Practical delta modulator

basic diagrams of the inverter, individual snubber, the base drive circuit and the power supplies for the base drive circuits are shown in figs. A1-3.

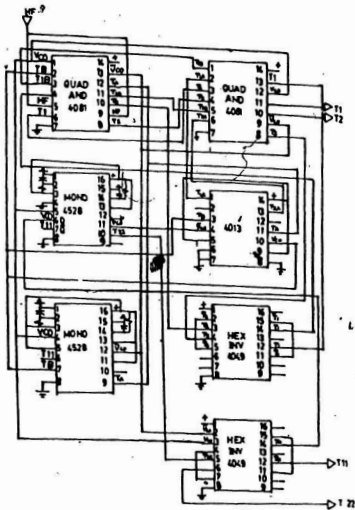


Fig. A1.2 The logic circuit for generating gate signals of two SCRs or transistors of a three phase inverter.

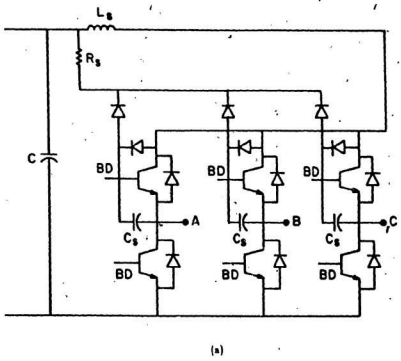
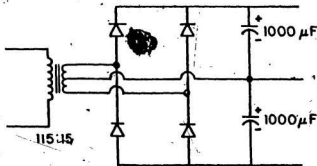
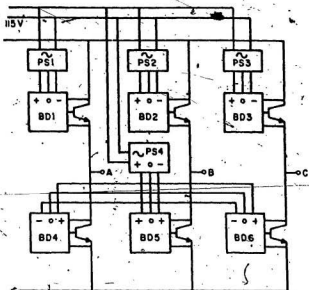


Fig. A1.3 The transistorized inverter (continued)



(b)

Fig. A1.3 The transistorized inverter (continued)

Appendix-II

Design and Construction of The Speed Sensor

Researchers are constantly striving to find a way to estimate or derive induction motor's operating conditions from terminal quantities by various methods. The submersible motor is one area of applications where a motor and its operating conditions cannot be monitored from the shaft by a physical sensor. To overcome this problem, an easy but effective way of finding motor speed from terminal quantities has been developed.

In developing the method, the basic equivalent circuit of the induction motor shown in fig. 4.6 is used. With this method the motor's input voltage and current are used to determine the equivalent input impedance of motor as follows,

Let,

V_1 = fundamental input voltage to the motor,

I_1 = fundamental input current to the motor,

θ_1 = fundamental input power factor,

Z_e = motor equivalent input impedance,

$$= \frac{V_1}{I_1} = R_e + jX_e$$

R_e = equivalent resistance of motor = $Z_e \cos \theta_1$, and

X_e = equivalent motor reactance = $Z_e \sin \theta_1$.

Defining,

$$X_1 = \omega L_1,$$

$$X_2 = \omega L_2,$$

$$X_m = \omega L_m,$$

$$\omega = 2\pi f,$$

$$s = \frac{N_s - N_r}{N_r} = \text{slip of the motor,}$$

$$N_s = \frac{120 f}{P} = \text{synchronous speed, and}$$

P = number of poles of the motor;

The basic loop equations for the motor circuit shown in fig. 4.6 are

$$V_1 = [r_1 + j(X_1 + X_m)] I_1 - j X_m I_2 \quad (\text{A2-1})$$

$$0 = -j X_m I_1 + \left[\frac{r_2}{s} + j(X_2 + X_m) \right] I_2 \quad (\text{A2-2})$$

From equation (A2-2) one can obtain I_2 as

$$I_2 = \frac{j X_m I_1}{\left[\frac{r_2}{s} + j(X_2 + X_m) \right]} \quad (\text{A2-3})$$

Substituting equation (A2-2) into (A2-1), the following expressions can be obtained

$$V_1 = [r_1 + j(X_1 + X_m)] I_1 - j X_m \frac{j X_m I_1}{\left[\frac{r_2}{s} + j(X_2 + X_m) \right]} \quad (\text{A2-4})$$

Solving for input impedance one obtains

$$\frac{V_1}{I_1} = Z_s = R_s + j X_s \quad (\text{A2-5})$$

$$\begin{aligned}
 & -r_1 + j(X_1 + X_m) + \frac{X_m^2}{\left[\frac{r_2}{s} + j(X_2 + X_m) \right]} \\
 & = \frac{r_1 \left[\frac{r_2^2}{s^2} + (X_2 + X_m)^2 \right] + \frac{r_2 X_m^2}{s}}{\frac{r_2^2}{s^2} + (X_2 + X_m)^2} \\
 & + j \left[\frac{(X_1 + X_m) \left[\frac{r_2^2}{s^2} + (X_2 + X_m)^2 \right] - (X_2 + X_m) X_m^2}{\frac{r_2^2}{s^2} + (X_2 + X_m)^2} \right]
 \end{aligned}$$

Equating real and imaginary parts of (A2-5) the following relationships can be obtained

$$R_s = \frac{r_1 \left[\frac{r_2^2}{s^2} + (X_2 + X_m)^2 \right] + \frac{r_2 X_m^2}{s}}{\frac{r_2^2}{s^2} + (X_2 + X_m)^2} \quad (\text{A2-6})$$

$$X_s = \frac{(X_1 + X_m) \left[\frac{r_2^2}{s^2} + (X_2 + X_m)^2 \right] - (X_2 + X_m) X_m^2}{\frac{r_2^2}{s^2} + (X_2 + X_m)^2} \quad (\text{A2-7})$$

Equation (A2-6) can be re-arranged as

$$R_s - r_1 = \frac{r_2 X_m^2 s}{r_2^2 + s^2 (X_2 + X_m)^2} \quad (\text{A2-8})$$

Equation (A2-7) can be re-arranged as

$$X_s - X_1 - X_m = \frac{(X_2 + X_m) X_m^2 s^2}{r_2^2 + s^2 (X_2 + X_m)^2} \quad (\text{A2-9})$$

Dividing equation (A2-8) by (A2-9), we get

$$\frac{R_s - r_1}{X_s - X_1 - X_m} = \frac{-r_2}{s} \quad (\text{A2-10})$$

From (A2-10), the motor slip s can be written as

$$s = \frac{r_2 (X_e - X_1 - X_m)}{(R_e - r_1)(X_2 + X_m)} \quad (\text{A2-11})$$

$$s = \frac{r_2 (L_e - L_1 - L_m)}{(R_e - r_1)(L_2 + L_m)} \quad (\text{A2-12})$$

The motor speed in terms of equivalent resistance, inductance and the motor constants can be found as

$$N_r = N_s (1 - s) \quad (\text{A2-13})$$

$$N_r = N_s \left[1 + \frac{r_2 (L_e - L_1 - L_m)}{(R_e - r_1)(L_2 + L_m)} \right] \quad (\text{A2-14})$$

$$N_r = \frac{120f}{P} \left[1 + \frac{r_2 (L_e - L_1 - L_m)}{(R_e - r_1)(L_2 + L_m)} \right] \quad (\text{A2-15})$$

where,

$$R_e = \text{Re} [Z_e] = Z_e \cos \theta_1 = \frac{V_1}{I_1} \cos \theta_1 \quad (\text{A2-16})$$

$$L_e = \text{Im} \left[\frac{Z_e}{\omega} \right] = \frac{Z_e}{\omega} \sin \theta_1 = \frac{V_1}{\omega I_1} \sin \theta_1 \quad (\text{A2-17})$$

The equations (A2-16) to (A2-17) have been used for continuous speed monitoring of the submersible motor for the semi-closed loop operation.

A practical speed sensor using the developed equations was built. The basic block diagram of the speed sensor is shown in fig. A2-1. The speed sensor consists of a voltage sensor, a current sensor, a phase angle detector and a frequency to voltage converter. The sensor quantities are all converted to dc signals for calculation purposes. The voltage, the current, the frequency and the phase angle sensors are shown in figs. A2-2 to A2-5. The circuit diagrams of motor's speed measuring device are shown in fig. A2-6.

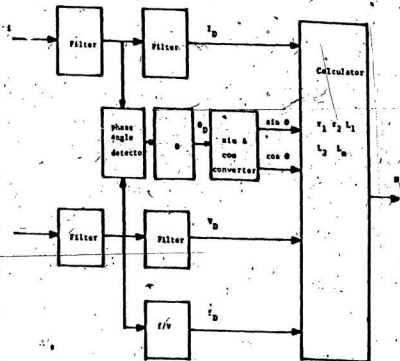


Fig. A2.1 The block diagram of the speed sensor.

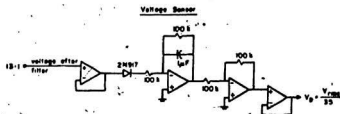


Fig. A2.2 The voltage conditioning circuit used in the speed calculator.

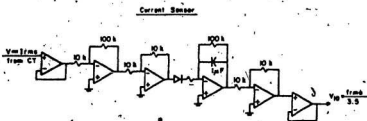


Fig. A2.3 The current conditioning circuit-used in the speed calculator.

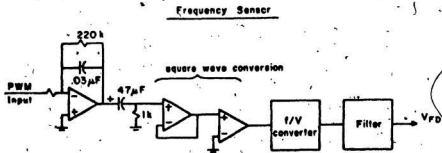


Fig. A2.4 The frequency conditioning circuit used in the speed calculator.

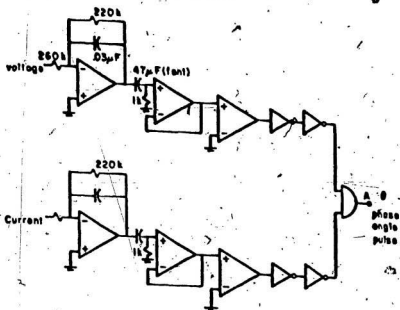
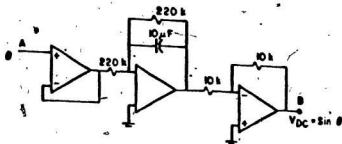
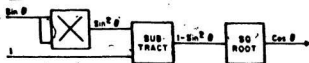
phase angle sensorphase angle conversion to sine θ 

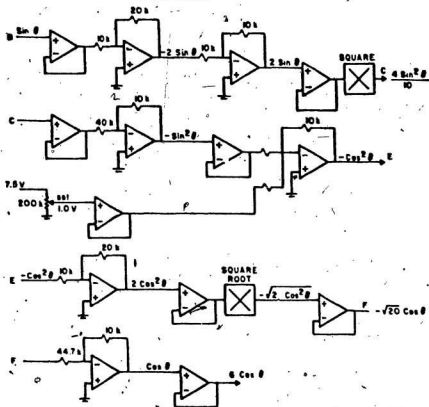
Fig. A2.5 The phase angle measurement circuit of the speed calculator.
(continued)

conversion of $\sin \theta$ to $\cos \theta$

Schematic



Actual Circuit



(b)

Fig. A2.5 The phase angle measurement circuit of the speed calculator.
 (a) phase angle sensor. (b) conversion to sin and cosine.

Speed Measurement

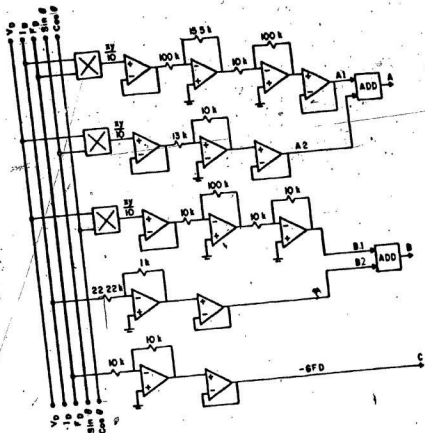


Fig. A2.6 The speed calculator. (continued)

Speed Measurement (continued)

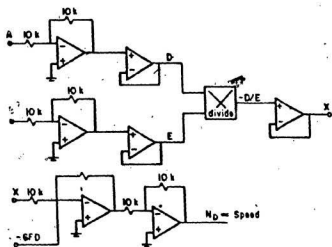


Fig. A2.6 The speed calculator.

Appendix III

A Novel Variable Frequency Three Phase Sine Wave Generator

A simple variable frequency three phase reference sine wave generator was used for reference signals of the delta modulators in this study [136]. Apart from simplicity this new sine wave generator generates virtually distortionless sine waves and the method can easily be extended to any number of polyphase sine wave generation. Three phase variable frequency reference waveform of 5-200 Hz are usually used in ac motor controls. The low power variable frequency sinusoidal signals are used as reference signals for control circuitry of cycloconverters and pulse width modulated inverters. A number of techniques have been reported in literatures in the past. These methods are described and compared in reference [137,138]. The methods were either complicated or failed to generate completely distortionless sine waves. For the use of delta modulation technique in inverters it is necessary to obtain distortionless sine waves. It is important because, without distortionless reference waveforms, the modulated signals in the three controllers will be different and will result in mal-operation of the inverter. The new method is based on the phasor addition of sine and cosine waves. In this method pure sine and cosine waves are generated initially by voltage controlled oscillators and then converted to three phase waveforms by phasor addition of sine and cosine waves.

A3.1 Scheme:

Fig A3-1 shows the phasor diagram of the generation of three phase variable frequency sine wave. V_o and V_x are the phasor representation of the original sine and cosine waves, which are generated by voltage controlled quadrature oscillator (VCO). The oscillator output V_o is doubled in magnitude and added with V_x to produce phase A waveform. The oscillator voltage V_o is then reversed, amplified and added to V_x to give phase B waveform. To obtain phase C, the voltage V_x is reversed and amplified to have equal magnitude as the other phases.

A3.2 Three Phase Sine Wave Generator:

The sine and cosine waveforms are generated by a voltage controlled quadrature oscillator. The block diagram of the oscillator is shown in fig A3-2 (b). The quadrature oscillator is a variation of universal filter [136]. Typical waveforms obtained from this circuit are shown in fig A3-2(c). Fig A3-3(a) is the block diagram of the three phase sine reference wave generator. The oscillator output voltages are added by phasor addition to obtain the three phase waveforms. The circuit implementation is shown in fig A3-3(b) and the output waveforms of the circuit is shown in fig A3-3(c). The distortion of the generated sine waves were within 0.5 percent error below 30 Hz operation and within 0.25 percent above 30 Hz operation. The distortion is due to the amplitude limiting circuit used.

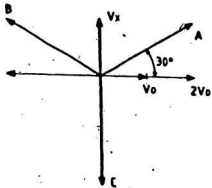


Fig. A3.1 Phasor diagram of generating the three phase variable frequency sine wave.

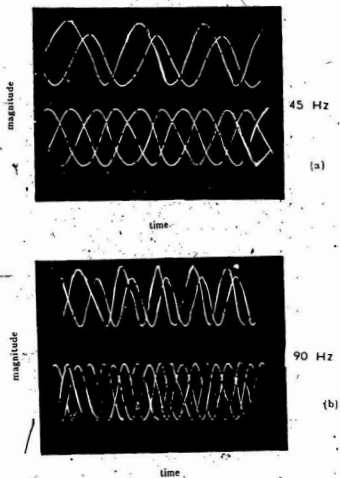


Fig. A3.2 The output of a quadrature oscillator.
(a) at 45 Hz operation. (b) at 90 Hz operation.

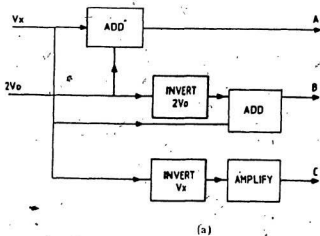
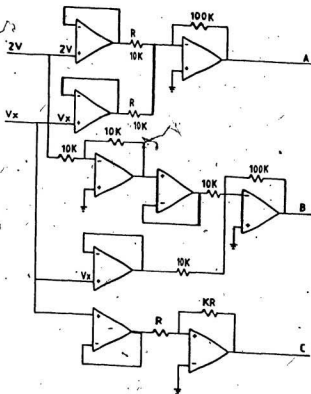


Fig. A3.3 Three phase sine wave generator and its output (continued)



(b)

Fig. A3.3 Three phase sine wave generator and its output. (continued)

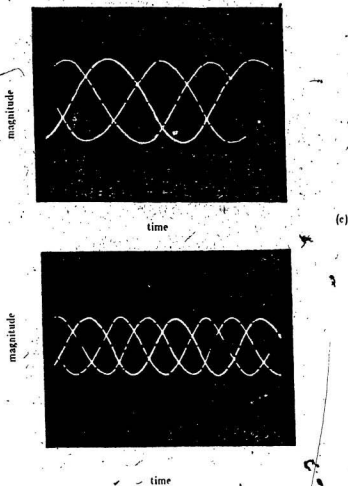


Fig. A3.3 Three phase sine wave generator and its output.
(a) schematic of three phase sine wave generator.
(b) circuit implementation.
(c) output.

APPENDIX-IV
Motor Ratings

1. Type Three phase submersible induction motor

Volts: 230V (L-L)

HP : 1.5 hp

Hz. : 60 Hz.

Number of poles:

2

rpm : 3450 rpm

L_2 : 0.13 h/phase

R_1 : 127 ohm/phase

R_1 : 1.8 ohm/phase (cold resistance)

R_1 : 2.3 ohm/phase (hot resistance)

R_2 : 1.2 ohm/phase (hot resistance)

L_1 : 0.0084 h/phase

L_2 : 0.0084 h/phase

Motor parametrs at various frequencies

From Open Circuit Tests:

	L_2 /phase in henry	r_1 /phase in ohms
70 Hz.	0.141	334
60 Hz.	0.141	280
50 Hz.	0.139	242
40 Hz.	0.153	182
30 Hz.	0.143	127
20 Hz.	0.149	39

From Blocked Rotor Tests:

	r_b /phase in ohms	Z_b /phase in ohms
75 Hz.	3.2	8.565
70 Hz.	3.11	7.22
60 Hz.	3.04	7.06
50 Hz.	2.96	6.02
40 Hz.	2.866	5.226
30 Hz.	2.81	4.22
20 Hz.	2.76	3.90

2. Three Phase Normal Induction Motor

Volts: 230 V (L-L)

HP : 1.5 hp

Hz: 60 Hz.

No. of
poles: 2

rpm : 3475 rpm

F.L efficiency : 76 %

power factor : 0.80

 L_m : .200 h/phase r_i : .164 ohm/phase r_1 : .32 ohm/phase r_2 : .21 ohm/phase L_1 : 0.005 h/phase L_2 : 0.005 h/phase

(data for normal induction machine has been taken from
 'Theory and Design of Small Induction Motors', By: Cyril G.
 Veinott, McGraw-Hill, 1959)

Appendix-V

Motor Equations of d-q Axis

The motor model used for the analysis of the performance of inverter-fed submersible motors is based on the d-q axis motor equivalent circuit shown in fig.

3.18. Based on these models the motor equations are

In synchronously rotating axis

Stator side:

$$V_{qs} = R_s i_{qs} + \frac{d\psi_{qs}}{dt} + \omega_s \psi_{ds} \quad (A5-1)$$

$$V_{ds} = R_s i_{ds} + \frac{d\psi_{ds}}{dt} - \omega_s \psi_{qs} \quad (A5-2)$$

Rotor Side:

$$V_{qr} = R_r i_{qr} + \frac{d\psi_{qr}}{dt} + (\omega_s - \omega_r) \psi_{dr} \quad (A5-3)$$

$$V_{dr} = R_r i_{dr} + \frac{d\psi_{dr}}{dt} - (\omega_s - \omega_r) \psi_{qr} \quad (A5-4)$$

Also from the motor d-q axis model, one obtains the following expressions

$$\psi_{qs} = L_{ls} i_{qs} + L_m (i_{qs} + i_{qr}) \quad (A5-5)$$

$$\psi_{qr} = L_{lr} i_{qr} + L_m (i_{qs} + i_{qr}) \quad (A5-6)$$

$$\psi_{ds} = L_{ls} i_{ds} + L_m (i_{ds} + i_{dr}) \quad (A5-7)$$

$$\psi_{dr} = L_{lr} i_{dr} + L_m (i_{ds} + i_{dr}) \quad (A5-8)$$

Replacing equations (A5-5) to (A5-8) in equations (A5-1) to (A5-4) and also substituting

$$L_{ls} + L_m = L_l \quad (A5-9)$$

$$L_{lr} + L_m = L_r \quad \text{and} \quad p = \frac{d}{dt} \quad (A5-10)$$

One obtains the following dynamic model of the motor for analysis

$$\begin{bmatrix} V_{\varphi} \\ V_{ds} \\ V_{qr} \\ V_{dr} \end{bmatrix} = \begin{bmatrix} r_s + L_s p & \omega_e L_m & L_m p & \omega_e L_m \\ -\omega_e L_r & r_s + L_s p & -\omega_e L_m & L_m p \\ L_m p & (\omega_e - \omega_r) L_m & r_r + L_r p & (\omega_e - \omega_r) L_r \\ -(\omega_e - \omega_r) L_m & L_m p & -(\omega_e - \omega_r) L_r & r_r + L_r p \end{bmatrix} \begin{bmatrix} i_{\varphi} \\ i_{ds} \\ i_{qr} \\ i_{dr} \end{bmatrix} \quad (\text{A5-11})$$

In the stationary axis $\omega_e = 0$. Therefore, the equation in stationary frame can be written as

$$\begin{bmatrix} V_{\varphi} \\ V_{ds} \\ V_{qr} \\ V_{dr} \end{bmatrix} = \begin{bmatrix} r_s + L_s p & 0 & L_m p & 0 \\ 0 & r_s + L_s p & 0 & L_m p \\ L_m p & -\omega_r L_m & r_r + L_r p & -\omega_r L_r \\ \omega_r L_m & L_m p & \omega_r L_r & r_r + L_r p \end{bmatrix} \begin{bmatrix} i_{\varphi} \\ i_{ds} \\ i_{qr} \\ i_{dr} \end{bmatrix} \quad (\text{A5-12})$$

Assuming $V_{qr} = 0$ and $V_{dr} = 0$, the model can be further modified as

$$\begin{bmatrix} V_{\varphi} \\ V_{ds} \\ 0 \\ 0 \end{bmatrix} = \begin{bmatrix} r_s + L_s p & 0 & L_m p & 0 \\ 0 & r_s + L_s p & 0 & L_m p \\ L_m p & -\omega_r L_m & r_r + L_r p & -\omega_r L_r \\ \omega_r L_m & L_m p & \omega_r L_r & r_r + L_r p \end{bmatrix} \begin{bmatrix} i_{\varphi} \\ i_{ds} \\ i_{qr} \\ i_{dr} \end{bmatrix} \quad (\text{A5-13})$$

According to reference [139], all the derivatives in V_{φ} and V_{ds} voltage equations can be neglected for further simplification of equation to obtain a reduced order model

$$\begin{bmatrix} V_{\varphi} \\ V_{ds} \\ 0 \\ 0 \end{bmatrix} = \begin{bmatrix} r_s & 0 & 0 & 0 \\ 0 & r_s & 0 & 0 \\ L_m p & -\omega_r L_m & r_r + L_r p & -\omega_r L_r \\ \omega_r L_m & L_m p & \omega_r L_r & r_r + L_r p \end{bmatrix} \begin{bmatrix} i_{\varphi} \\ i_{ds} \\ i_{qr} \\ i_{dr} \end{bmatrix} \quad (\text{A5-14})$$

In the above dynamic motor model, each of the d-q axis voltage is dependent on two current variables. But if the current variables in equation (A5-14) are

replaced by flux variables, the voltages become dependent on one state variable of flux only, and the computer solution becomes easier. For this convenience, the following modification is carried out for the dynamic motor model

$$\psi = [\psi_{qr} \ \psi_{dr} \ \psi_{\sigma r} \ \psi_{\sigma d}]^T \quad (A5-15)$$

$$L = \begin{bmatrix} L_s & 0 & L_m & 0 \\ 0 & L_s & 0 & L_m \\ L_m & 0 & L_r & 0 \\ 0 & L_m & 0 & L_r \end{bmatrix} \quad (A5-16)$$

$$L^{-1} = \frac{1}{L_s L_r - L_m^2} \begin{bmatrix} L_r & 0 & -L_m & 0 \\ 0 & L_r & 0 & -L_m \\ -L_m & 0 & L_s & 0 \\ 0 & -L_m & 0 & L_s \end{bmatrix} \quad (A5-17)$$

$$i = L^{-1} \psi \quad (A5-18)$$

substituting $L_s L_r - L_m^2 = F$, and (A5-15) and (A5-18) in equation (A5-14), one obtains the required equations in flux variable as

$$\begin{bmatrix} V_{qr} \\ V_{dr} \\ 0 \\ 0 \end{bmatrix} = \begin{bmatrix} \frac{r_s L_r}{F} & 0 & \frac{-r_s L_m}{F} & 0 \\ 0 & \frac{r_s L_r}{F} & 0 & \frac{-r_s L_m}{F} \\ \frac{-L_m r_r}{F} & 0 & \frac{r_r L_s}{F} + p & -\omega_r \\ 0 & \frac{-L_m r_r}{F} & \omega_r & \frac{L_s r_r}{F} + p \end{bmatrix} \begin{bmatrix} \psi_{qr} \\ \psi_{dr} \\ \psi_{\sigma r} \\ \psi_{\sigma d} \end{bmatrix} \quad (A5-19)$$

The dynamic motor equations in simplified form as shown in equation (A5-19), together with voltage equations of RWDM inverter waveforms given in 3.5.3, constitute the basis of the steady state and start up performance study of the inverter-fed submersible motor in this thesis. The solution of equation (A5-19)

allows one to obtain the flux information which in turn can be used for solution of currents from the following equation

$$\begin{bmatrix} i_{qs} \\ i_{ds} \\ i_{qr} \\ i_{dr} \end{bmatrix} = \begin{bmatrix} \frac{L_r}{F} & 0 & -\frac{L_m}{F} & 0 \\ 0 & \frac{L_r}{F} & 0 & -\frac{L_m}{F} \\ -\frac{L_m}{F} & 0 & \frac{L_r}{F} & 0 \\ 0 & -\frac{L_m}{F} & 0 & \frac{L_r}{F} \end{bmatrix} \begin{bmatrix} \psi_{qs} \\ \psi_{ds} \\ \psi_{qr} \\ \psi_{dr} \end{bmatrix} \quad (\text{A5-20})$$

The equation used for calculation of torque is

$$T_e = \frac{3}{2} \left(\frac{P}{2} \right) L_m (i_{qs} i_{dr} - i_{ds} i_{qr}) \quad (\text{A5-21})$$

where P is number of poles of the motor

The flux is obtained from (A5-10) as

$$\begin{bmatrix} \psi_{qs} \\ \psi_{ds} \\ \psi_{qr} \\ \psi_{dr} \end{bmatrix} = \begin{bmatrix} \frac{r_s L_r}{F} & 0 & -\frac{r_s L_m}{F} & 0 \\ 0 & \frac{r_s L_r}{F} & 0 & -\frac{r_s L_m}{F} \\ -\frac{L_m r_r}{F} & 0 & \frac{r_s L_s}{F} + p & -\omega_r \\ 0 & -\frac{L_m L_r}{F} & \omega_r & \frac{L_s r_r}{F} + p \end{bmatrix}^{-1} \begin{bmatrix} V_{qs} \\ V_{ds} \\ 0 \\ 0 \end{bmatrix} \quad (\text{A5-22})$$

Speed is obtained from the following expression

$$\left[T_e - T_L \right] = \frac{2}{p} j \frac{d\omega_r}{dt} \quad (\text{A5-23})$$

$$\frac{P}{2J} \left[T_e - T_L \right] = \frac{d\omega_r}{dt} \quad (\text{A5-24})$$



